Comparison of methane combustion mechanisms using shock tube and rapid compression machine ignition delay time measurements

Peng Zhang †, István Gy. Zsély *, †, Viktor Samu †, Tibor Nagy ‡, Tamás Turányi †

† Institute of Chemistry, ELTE Eötvös Loránd University, Budapest, Hungary
‡ Institute of Materials and Environmental Chemistry (IMEC), Research Centre for Natural Sciences (RCNS), Eötvös Loránd Research Network, Budapest, Hungary

Supplementary

All experimental data used in the present study were stored in RKD-format (ReSpecTh Kinetics Data format) version 2.3 files in the ReSpecTh database (http://respecth.hu/)[1]. Each dataset has a unique file identifier. In Tables A and B of Section 1, the basic properties of the datasets are listed in rows for shock tube and rapid compression machine experiments, respectively. Datasets generated from the same publication are shown in the same block headed by the name of the first author, year of publication, reference of the publication and the definition of ignition delay as used in the experiment. Each line in the block contains the unique identifier of a dataset (which is also the name of the .xml file), number of data points (N_i) in the dataset, estimated experimental standard deviation (σ), diluent gas (*e.g.* Ar/N_2), equivalence ratio (φ), experimental pressure and temperature ranges, and a comment. This comment refers to the location of the data in the original article, initial composition, diluent ratio, and occasionally the key values or species used in the definition of ignition delay.

Grey shading of the first cell in a row indicates that none of the investigated mechanisms can predict the corresponding experimental results within an error limit of 3σ (*i.e.* $E_i \leq 9$). Green shading indicates that the corresponding dataset was not used for testing the mechanisms because the measurement is identical to an adjacent measurement while the IDT definition used is different. As discussed in the main article, in this case we added all the IDT data with the identical measurement but different IDT definitions to the Respecth database, but only one was used for mechanism comparison. This means that to each row with a green shaded first cell there is another row with either no shading or grey shading. Yellow shading in the first cell means that helium was used as diluent and these datasets were not used for mechanism comparison. Orange shading means that the dataset was not used in the comparison study, because the effect of vibration relaxation during CO production was not considered.

The lines of Tables A and B show the covered ranges of experimental conditions for each dataset. This information is summarized in Fig. S1, which contains the bivariate distributions of the collected experimental data as functions of temperature, pressure, equivalence ratio and diluent ratio.

In most cases, the standard deviation of the experimental error of a data set was estimated based on both the statistical scatter of the data ($\sigma_{\mathrm{stat},i}$) and the reported experimental uncertainty ($\sigma_{\mathrm{exp},i}$) as discussed in the main text. If the authors of the original article did not provide any information on the experimental uncertainty, then the estimation of the standard deviation of a data set was based on the statistical scatter of the data only. Standard deviations belonging to whole data sets are given in the 3rd columns of Tables A and B. If the third cell of a row contains an interval of uncertainties, it indicates that uncertainties of the measured pressure and temperature (but not those of the IDTs) were provided in the original article and the uncertainties of IDTs were calculated from them using the method described in Part 2 of the Supplementary. This approach provided a different experimental error for each data point, which are listed in another supplementary material. The uncertainty interval indicates the highest and lowest standard deviation values of the data points belonging to the data set.

Part 3 presents the comparison of the performance of several excited OH sub-mechanisms, which were published as parts of methane combustion mechanisms. Part 4 indicates the performance of all mechanisms at low-temperature conditions and investigates the IDT reproducing ability of the mechanisms for experimental IDTs of various orders of magnitude. Part 5 presents the mean signed deviations calculated from the mechanisms at a series of condition intervals, which correspond to Figs. 5 to 8 in the main article. Part 6 gives an overview of the origin of the Arrhenius parameter values of reaction $CH_3 + O_2 = CH_2O + OH$ (R2) in the various mechanisms, and compares the frequencies of the sensitivity coefficients of reactions R7 to R12. Also, performance of the four best mechanisms with respect to IDT and their scaled normalized sensitive coefficients are compared in various intervals of temperature, pressure, equivalence ratio and diluent ratio.

Part 1: Overview of collected experimental data

Table A. Ignition delay time measurements of methane combustion in shock tubes

ID[.xml]	***Ni***	***σ***	**Diluents**	***φ***	***p* / atm**	***T* / K**	**Comment**
Seery and Bowman (1970)[2]; ignition criterion: time of maximum of the d*p*/d*t* profile							
x10004001	6	0.100	Ar	0.20	3.04 - 4.07	1463 - 1705	Table 2, $CH_4/O_2/Ar$, dilution: 78.4%
x10004002	29	0.390	Ar	0.50	1.56 - 4.83	1348 - 1881	Table 2, $CH_4/O_2/Ar$, dilution: 76.1%
x10004003	12	0.159	Ar	1.00	1.60 - 2.41	1428 - 1772	Table 2, $CH_4/O_2/Ar$, dilution: 72.7%
x10004004	10	0.136	Ar	2.00	1.76 - 1.90	1560 - 1721	Table 2, $CH_4/O_2/Ar$, dilution: 66.6%
x10004005	12	0.100	Ar	5.01	3.67 - 4.29	1510 - 1735	Table 2, $CH_4/O_2/Ar$, dilution: 53.4%
Spadaccini and Colket III (1994)[3]; ignition criterion: time of maximum of the d*p*/d*t* profile							
x10004006	9	0.405 - 0.457	Ar	1.00	3.77 - 8.28	1516 - 1918	Table 5, $CH_4/O_2/Ar$, dilution: 89.5%
x10004007	10	0.365 - 0.434	Ar	0.45	3.63 - 8.53	1336 - 1679	Table 5, $CH_4/O_2/Ar$, dilution: 81.29%
x10004008	10	0.433 - 0.469	Ar	0.75	3.40 - 8.81	1479 - 1759	Table 5, $CH_4/O_2/Ar$, dilution: 87.2%
x10004009	11	0.569 - 0.621	Ar	1.25	2.99 - 14.95	1461 - 2025	Table 5, $CH_4/O_2/Ar$, dilution: 90.9%
x10004010	5	0.312 - 0.336	Ar	1.00	5.45 - 10.94	1464 - 1708	Table 5, $CH_4/O_2/Ar$, dilution: 82%
Brabbs and Robertson (1986)[4]; ignition criterion: time of maximum of d *Signal*/dt profile							
x10004011	17	0.100	Ar	0.5	2.61 - 3.46	1499 - 1778	Table II, $CH_4/O_2/Ar$, dilution: 90%; *Signal*: pressure
x10004012	17	0.100	Ar	0.5	2.61 - 3.46	1499 - 1778	Table II, $CH_4/O_2/Ar$, dilution: 90%; *Signal*: [CHEX]
x10004013	18	0.100	Ar	1.0	2.76 - 3.68	1593 - 1915	Table II, $CH_4/O_2/Ar$, dilution: 94%; *Signal*: pressure
x10004014	18	0.100	Ar	1.0	2.76 - 3.68	1593 - 1915	Table II, $CH_4/O_2/Ar$, dilution: 94%; *Signal*: [CHEX]
x10004015	15	0.100	Ar	2.0	2.98 - 4.01	1602 - 1922	Table II, $CH_4/O_2/Ar$, dilution: 92%; *Signal*: pressure
x10004016	15	0.100	Ar	2.0	2.98 - 4.01	1602 - 1922	Table II, $CH_4/O_2/Ar$, dilution: 92%; *Signal*: [CHEX]
Lamoureux et al. (2002)[5]; ignition criterion: time of reaching *A*×the maximum value in [OHEX] profile							
x10004017	5	0.550	Ar	2	3.60 - 9.02	1778 - 1983	Table 4, $CH_4/O_2/Ar$, dilution: 97%; *A:* 0.1
x10004018	5	0.455	Ar	2	3.60 - 9.02	1778 - 1983	Table 4, $CH_4/O_2/Ar$, dilution: 97%; *A:* 0.5
x10004019	3	0.394	Ar	2	9.52 - 11.08	1704 - 1896	Table 4, $CH_4/O_2/Ar$, dilution: 96%; *A:* 0.1
x10004020	3	0.394	Ar	2	9.52 - 11.08	1704 - 1896	Table 4, $CH_4/O_2/Ar$, dilution: 96%; *A:* 0.5
x10004021	5	0.354	Ar	1	5.96 - 15.25	1571 - 1749	Table 4, $CH_4/O_2/Ar$, dilution: 89%; *A:* 0.1
x10004022	5	0.376	Ar	1	5.96 - 15.25	1571 - 1749	Table 4, $CH_4/O_2/Ar$, dilution: 89%; *A:* 0.5
x10004023	6	0.330	Ar	1	4.71 - 17.56	1641 - 1870	Table 4, $CH_4/O_2/Ar$, dilution: 97%; *A:* 0.1
x10004024	6	0.358	Ar	1	4.71 - 17.56	1641 - 1870	Table 4, $CH_4/O_2/Ar$, dilution: 97%; *A:* 0.5
x10004025	4	0.519	Ar	4	4.42 - 9.70	1730 - 1804	Table 4, $CH_4/O_2/Ar$, dilution: 95%; *A:* 0.1
x10004026	4	0.421	Ar	4	4.42 - 9.70	1730 - 1804	Table 4, $CH_4/O_2/Ar$, dilution: 95%; *A:* 0.5
x10004027	4	0.260	Ar	4	8.33 - 10.43	1526 - 1748	Table 4, $CH_4/O_2/Ar$, dilution: 90%; *A:* 0.1
x10004028	4	0.294	Ar	4	8.33 - 10.43	1526 - 1748	Table 4, $CH_4/O_2/Ar$, dilution: 90%; *A:* 0.5
Beerer and McDonell (2011)[6]; ignition criterion: time of maximum of d[CHEX]/d*t* profile							

ID[.xml]	*Ni*	σ	Diluents	φ	*p* / atm	*T* / K	Comment
x10004029	97	0.130 - 0.146	Ar	0.6	9	862 - 935	Suppl. Table S2 and Table S3, $CH_4/O_2/Ar$, dilution: 74.4%
Christopher et al. (2013)[7]; ignition criterion: time of maximum of the d*p*/d*t* profile							
x10004030	16	0.100 - 0.112	Ar	1.0	1.13 - 1.44	1686 - 2248	Suppl. Table A-2, Mixture 4, $CH_4/O_2/Ar$, dilution: 98%
x10004031	6	0.100 - 0.111	Ar	0.5	0.76 - 0.88	1543 - 1802	Suppl. Table A-2, Mixture 8, $CH_4/O_2/Ar$, dilution: 75%
x10004032	8	0.123 - 0.143	Ar	2.0	26.75 - 29.00	1470 - 1775	Suppl. Table A-4, Mixture 16, $CH_4/O_2/Ar$, dilution: 95%
x10004033	5	0.177 - 0.196	Ar	1.0	13.33 - 14.52	1336 - 1728	Suppl. Table A-4, Mixture 20, $CH_4/O_2/Ar$, dilution: 85%
Zhang et al. (2011)[8]; ignition criterion: time of maximum of d[OHEX]/d*t* profile							
x10004034	27	0.171 - 0.230	N_2	2	3.45 - 4.05	1529 - 1804	Table 3, Mixture 1, $CH_4/O_2/N_2$, dilution: 95%
x10004035	24	0.180 - 0.237	N_2	2	3.45 - 3.95	1505 - 1815	Table 3, Mixture 2, $CH_4/H_2/O_2/N_2$, dilution: 95.13%
x10004036	18	0.126 - 0.200	N_2	2	2.96 - 3.85	1464 - 1877	Table 3, Mixture 3, $CH_4/H_2/O_2/N_2$, dilution: 95.26%
x10004037	13	0.136 - 0.190	N_2	2	3.16 - 3.85	1422 - 1831	Table 3, Mixture 4, $CH_4/H_2/O_2/N_2$, dilution: 95.54%
Zhang et al. (2012)[9] - with PRR; ignition criterion: time of maximum of d[OHEX]/d*t* profile							
x10004038	10	0.154 - 0.292	Ar	0.5	4.93	1457 - 2030	Fig 4, Mixture 1, $CH_4/O_2/Ar$, dilution: 95.01%
x10004039	12	0.176 - 0.312	Ar	0.5	9.87	1412 - 1988	Fig 4, Mixture 1, $CH_4/O_2/Ar$, dilution: 95.01%
x10004040	9	0.282 - 0.380	Ar	0.5	19.74	1283 - 1728	Fig 4, Mixture 1, $CH_4/O_2/Ar$, dilution: 95.01%
x10004041	10	0.154 - 0.268	Ar	0.5	4.93	1340 - 1842	Fig 5, Mixture 2, $CH_4/H_2/O_2/Ar$, dilution: 95.11%
x10004042	14	0.203 - 0.324	Ar	0.5	9.87	1294 - 1809	Fig 5, Mixture 2, $CH_4/H_2/O_2/Ar$, dilution: 95.11%
x10004043	8	0.317 - 0.440	Ar	0.5	19.74	1215 - 1785	Fig 5, Mixture 2, $CH_4/H_2/O_2/Ar$, dilution: 95.11%
x10004044	10	0.179 - 0.311	Ar	0.5	4.93	1220 - 1863	Fig 6, Mixture 3, $CH_4/H_2/O_2/Ar$, dilution: 95.25%
x10004045	14	0.180 - 0.351	Ar	0.5	9.87	1154 - 1778	Fig 6, Mixture 3, $CH_4/H_2/O_2/Ar$, dilution: 95.25%
x10004046	11	0.268 - 0.437	Ar	0.5	19.74	1139 - 1626	Fig 6, Mixture 3, $CH_4/H_2/O_2/Ar$, dilution: 95.25%
x10004047	8	0.280 - 0.410	Ar	0.5	4.93	1117 - 1390	Fig 7, Mixture 4, $CH_4/H_2/O_2/Ar$, dilution: 95.47%
x10004048	11	0.267 - 0.398	Ar	0.5	9.87	1076 - 1398	Fig 7, Mixture 4, $CH_4/H_2/O_2/Ar$, dilution: 95.47%
x10004049	10	0.314 - 0.499	Ar	0.5	19.74	1074 - 1553	Fig 7, Mixture 4, $CH_4/H_2/O_2/Ar$, dilution: 95.47%
x10004050	7	0.356 - 0.495	Ar	0.5	4.93	1055 - 1299	Fig 8, Mixture 5, $CH_4/H_2/O_2/Ar$, dilution: 95.83%
x10004051	10	0.451 - 0.624	Ar	0.5	9.87	1059 - 1275	Fig 8, Mixture 5, $CH_4/H_2/O_2/Ar$, dilution: 95.83%
x10004052	8	0.441 - 0.637	Ar	0.5	19.74	1020 - 1488	Fig 8, Mixture 5, $CH_4/H_2/O_2/Ar$, dilution: 95.83%
Krishnan and Ravikumar (1980)[10]; ignition criterion: root of the tangent line at the first inflection point of the [CHEX] profile							
x10004071	11	0.100	Ar	0.2	3	1599 - 1972	Fig 1A, Mixture 1, $CH_4/O_2/Ar$, dilution: 95.05%
x10004072	11	0.100	Ar	0.5	3	1614 - 2004	Fig 1A, Mixture 2, $CH_4/O_2/Ar$, dilution: 95%
x10004073	13	0.100	Ar	1.0	3	1602 - 2109	Fig 1A, Mixture 3, $CH_4/O_2/Ar$, dilution: 95.01%
x10004074	13	0.100	Ar	2.0	3	1692 - 2132	Fig 1A, Mixture 4, $CH_4/O_2/Ar$, dilution: 95%
x10004075	9	0.100	Ar	4.0	3	1794 - 2195	Fig 1A, Mixture 5, $CH_4/O_2/Ar$, dilution: 95.05%
x10004076	11	0.100	Ar	0.2	6	1566 - 1852	Fig 1B, Mixture 1, $CH_4/O_2/Ar$, dilution: 95.05%

ID[.xml]	*Ni*	*σ*	Diluents	*φ*	*p* / atm	*T* / K	Comment
x10004077	11	0.100	Ar	0.5	6	1603 - 1982	Fig 1B, Mixture 2, $CH_4/O_2/Ar$, dilution: 95%
x10004078	12	0.100	Ar	1.0	6	1582 - 2011	Fig 1B, Mixture 3, $CH_4/O_2/Ar$, dilution: 95.01%
x10004079	11	0.106	Ar	2.0	6	1633 - 2046	Fig 1B, Mixture 4, $CH_4/O_2/Ar$, dilution: 95%
x10004080	10	0.100	Ar	4.0	6	1717 - 2119	Fig 1B, Mixture 5, $CH_4/O_2/Ar$, dilution: 95.05%
Asaba et al. (1963)[11]; ignition criterion: root of the tangent line at the inflection point of *p*(t)							
x10004081	16	0.648	-	3.00	7	1359 - 1794	Fig 7, CH_4/O_2, dilution: 0%
x10004082	18	0.645	-	2.00	7	1108 - 1749	Fig 7, CH_4/O_2, dilution: 0%
x10004083	5	0.384	N_2	2.38	10	1562 - 1771	Fig 7, $CH_4/O_2/N_2$, dilution: 63.2%
x10004084	4	0.292	N_2	1.68	10	1670 - 1766	Fig 7, $CH_4/O_2/N_2$, dilution: 67.15%
x10004085	4	0.100	N_2	1.06	10	1612 - 1854	Fig 7, $CH_4/O_2/N_2$, dilution: 71.1%
x10004086	3	0.300	Ar	1.64	10	1631 - 1886	Fig 7, $CH_4/O_2/Ar$, dilution: 80%
x10004087	1	0.300	Ar	6.00	10	1685	Fig 7, $CH_4/O_2/Ar$, dilution: 80%
x10004088	10	0.280	-	1.33	7	916 - 1350	Fig 8, CH_4/O_2, dilution: 0%
x10004089	14	0.364	-	0.86	7	905 - 1323	Fig 8, CH_4/O_2, dilution: 0%
x10004090	9	0.291	-	0.50	7	922 - 1229	Fig 8, CH_4/O_2, dilution: 0%
x10004091	7	0.419	-	0.22	7	972 - 1206	Fig 8, CH_4/O_2, dilution: 0%
Burcat et al. (1971)[12]; ignition criterion: time of maximum of the d*p*/d*t* profile							
x10004092	13	0.163	Ar	1	13.18	1501 - 1895	Fig 1. A, $CH_4/O_2/Ar$, dilution: 76.9%
Cooke and Williams (1971)[13]; ignition criterion: time of reaching 0.05×the maximum value in [OHEX] profile							
x10004093	12	0.100	Ar	2.0	0.33	1728 - 2327	Fig 2, $CH_4/O_2/Ar$, dilution: 90%
x10004094	24	0.103	Ar	1.0	0.33	1688 - 2176	Fig 2, $CH_4/O_2/Ar$, dilution: 90%
x10004095	9	0.100	Ar	0.5	0.33	1829 - 2026	Fig 2, $CH_4/O_2/Ar$, dilution: 90%
Cooke and Williams (1975)[14]; ignition criterion: root of the tangent line at the first inflection point of the *Signal* profile, unless otherwise noted							
x10004096	7	0.289	Ar	0.5	0.33	1885 - 2107	Fig 3, $CH_4/O_2/Ar$, dilution: 90%; *Signal*: [CO_2]
x10004097	8	0.295	Ar	0.5	0.33	1876 - 2107	Fig 3, $CH_4/O_2/Ar$, dilution: 90%; ignition criterion: time of maximum of the d*p*/d*t* profile
x10004098	22	0.226	Ar	0.5	0.33	1717 - 2110	Fig 3, $CH_4/O_2/Ar$, dilution: 90%; *Signal*: [OHEX]
x10004099	6	0.222	Ar	1.0	0.33	1809 - 1975	Fig 3, $CH_4/O_2/Ar$, dilution: 90%; *Signal*: [CO_2]
x10004100	6	0.239	Ar	1.0	0.33	1763 - 2017	Fig 3, $CH_4/O_2/Ar$, dilution: 90%; ignition criterion: time of maximum of the d*p*/d*t* profile
x10004101	17	0.263	Ar	1.0	0.33	1736 - 2016	Fig 3, $CH_4/O_2/Ar$, dilution: 90%; *Signal*: [OHEX]
x10004102	6	0.291	Ar	2.0	0.33	1765 - 2148	Fig 3, $CH_4/O_2/Ar$, dilution: 90%; *Signal*: [CO_2]
x10004103	5	0.376	Ar	2.0	0.33	1739. - 1960	Fig 3, $CH_4/O_2/Ar$, dilution: 90%; ignition criterion: time of maximum of the d*p*/d*t* profile
x10004104	9	0.367	Ar	2.0	0.33	1769 - 2143	Fig 3, $CH_4/O_2/Ar$, dilution: 90%; *Signal*: [OHEX]
x10004105	5	0.237	Ar	0.5	0.33	1845 - 2052	Fig 3, $CH_4/O_2/Ar$, dilution: 95%; *Signal*: [CO_2]
x10004106	10	0.255	Ar	0.5	0.33	1695 - 2040	Fig 3, $CH_4/O_2/Ar$, dilution: 95%; ignition criterion: time of maximum of the d*p*/d*t* profile

ID[.xml]	*Ni*	σ	Diluents	φ	*p* / atm	*T* / K	Comment
x10004107	20	0.223	Ar	0.5	0.33	1693 - 2106	Fig 3, $CH_4/O_2/Ar$, dilution: 95%; *Signal*: [OHEX]
x10004108	5	0.236	Ar	1.0	0.33	1870 - 2001	Fig 3, $CH_4/O_2/Ar$, dilution: 95%; *Signal*: [CO_2]
x10004109	10	0.254	Ar	1.0	0.33	1760 - 2016	Fig 3, $CH_4/O_2/Ar$, dilution: 95%; *Signal*: [OHEX]
x10004110	6	0.206	Ar	2.0	0.33	1768 - 2037	Fig 3, $CH_4/O_2/Ar$, dilution: 95%; *Signal*: [CO_2]
x10004111	12	0.215	Ar	2.0	0.33	1719 - 2037	Fig 3, $CH_4/O_2/Ar$, dilution: 95%; *Signal*: [OHEX]
Dabora (1975)[15]; ignition criterion: time of maximum of the d*p*/d*t* profile							
x10004112	7	0.209	N_2	1.02	14	1427 - 1647	Fig 1, Mixture A, $CH_4/O_2/N_2$, dilution: 71.32%
Vries and Petersen (2007)[16]; ignition criterion: root of the tangent line at the first inflection point of the [CHEX] profile							
x10004113	2	0.200	Ar	0.05	10.2 - 20.1	849 - 1107	Table 2, Mixture 1, $CH_4/O_2/Ar$, dilution: 75.1%
x10004114	3	0.160 - 0.164	N_2	0.05	24.9 - 27.5	1007 - 1099	Table 2, Mixture 1a, $CH_4/O_2/N_2$, dilution: 75.1%
x10004115	1	0.150	Ar	0.04	20.7	816	Table 2, Mixture 6, $CH_4/H_2/O_2/Ar$, dilution: 74.21%
x10004116	1	0.150	Ar	0.03	20.1	803	Table 2, Mixture 21, $CH_4/H_2/O_2/Ar$, dilution: 72.90%
x10004117	10	0.157 - 0.183	Ar	0.05	20.0	850 - 1464	Fig 4, $CH_4/O_2/Ar$, dilution: 75.06%
Donohoe et al. (2014)[17] - with PRR; ignition criterion: root of the tangent line at the first inflection point of the [OHEX] profile							
x10004118	10	0.185	Ar	0.3	1.51 - 1.67	1283 - 1722	Fig 6, Mixture 1, $CH_4/H_2/O_2/Ar$, dilution: 90.49%
x10004119	10	0.175	Ar	0.5	9.77 - 10.49	1116 - 1317	Fig 6, Mixture 2, $CH_4/H_2/O_2/Ar$, dilution: 91.88%
x10004120	9	0.159	Ar	1.0	29.52 - 32.54	1110 - 1220	Fig 6, Mixture 3, $CH_4/H_2/O_2/Ar$, dilution: 94.44%
Eubank et al. (1981)[18]; ignition criterion: root of the tangent line at the inflection point of the [CH_4] profile							
x10004121	11	0.117	N_2	0.19	3.54 - 4.17	1441 - 1733	Fig 2, $CH_4/O_2/N_2$, dilution: 77.42%
x10004122	15	0.118	Ar	0.20	3.59 - 4.58	1458 - 1861	Fig 2, $CH_4/O_2/Ar$, dilution: 78%
x10004123	4	0.100	N_2	0.40	3.83 - 4.15	1558 - 1686	Fig 3, $CH_4/O_2/N_2$, dilution: 75.84%
x10004124	15	0.310	N_2	0.10	3.31 - 4.25	1347 - 1725	Fig 3, $CH_4/O_2/N_2$, dilution: 78.21%
Frenklach and Bornside (1984)[19]; ignition criterion: time of maximum of the d*p*/d*t* profile							
x10004125	15	0.173	Ar	1	2.54 - 2.90	1405 - 1604	Fig 3, $CH_4/O_2/Ar$, dilution: 71.5%
x30004126	14	0.254	Ar	1	2.54 - 2.89	1405 - 1603	Fig 3, $CH_4/O_2/Ar$, dilution: 71.5%
Higgin and Williams (1969)[20]; ignition criterion: time of reaching 0.05×the maximum value in [OHEX] profile							
x10004127	11	0.139 - 0.216	Ar	2.00	0.33	1901 - 2632	Fig 2, $CH_4/O_2/Ar$, dilution: 90%
x10004128	15	0.115 - 0.166	Ar	1.00	0.33	1828 - 2278	Fig 2, $CH_4/O_2/Ar$, dilution: 90%
x10004129	15	0.119 - 0.183	Ar	0.50	0.33	1825 - 2577	Fig 2, $CH_4/O_2/Ar$, dilution: 90%
x10004130	15	0.144 - 0.207	Ar	0.25	0.33	1783 - 2481	Fig 2, $CH_4/O_2/Ar$, dilution: 90%
Huang et al. (2004)[21]; ignition criterion: root of the tangent line at the inflection point of *p*(t)							
x10004132_1	13	0.380	N_2	0.99	36.5 - 41.6	1024 - 1295	Table 3, Mixture 1, $CH_4/O_2/N_2$, dilution: 71.36%
x10004132_2	7	0.380	N_2	0.99	29.6 - 31.4	1035 - 1296	Table 3, Mixture 1, $CH_4/O_2/N_2$, dilution: 71.36%
x10004132_3	9	0.380	N_2	0.99	20.9 - 26.1	1032 - 1309	Table 3, Mixture 1, $CH_4/O_2/N_2$, dilution: 71.36%
x10004132_4	11	0.380	N_2	0.99	14.1 - 17.9	1038 - 1348	Table 3, Mixture 1, $CH_4/O_2/N_2$, dilution: 71.36%
x10004133_1	9	0.321	N_2	0.69	37.6 - 39.1	1004 - 1370	Table 3, Mixture 2, $CH_4/O_2/N_2$, dilution: 73.6%

ID[.xml]	*Ni*	σ	Diluents	φ	*p* / atm	*T* / K	Comment
x10004133_2	9	0.321	N_2	0.69	30.4 - 32.3	1059 - 1286	Table 3, Mixture 2, $CH_4/O_2/N_2$, dilution: 73.6%
x10004133_3	5	0.321	N_2	0.69	14.9 - 16.8	1143 - 1304	Table 3, Mixture 2, $CH_4/O_2/N_2$, dilution: 73.6%
x10004134	6	0.288	N_2	1.30	36.0 - 39.4	1068 - 1290	Table 3, Mixture 3, $CH_4/O_2/N_2$, dilution: 69.43%
Krishnan et al. (1983)[22]; ignition criterion: root of the tangent line at the first inflection point of the [CHEX] profile							
x10004135	23	0.100	Ar	1	0.99	1585 - 1977	Fig 1, Mixture 1, $CH_4/O_2/Ar$, dilution: 90.09%
Lifshitz et al. (1971)[23]; ignition criterion: time of maximum of the d*p*/d*t* profile							
x10004136	9	0.132 - 0.170	Ar	1.00	10.43	1715 - 2020	Fig 1, Group 1A, $CH_4/O_2/Ar$, dilution: 97%
x10004137	9	0.242 - 0.284	Ar	1.00	3.04	1600 - 2144	Fig 1, Group 1B, $CH_4/O_2/Ar$, dilution: 89.5%
x10004138	11	0.174 - 0.230	Ar	1.00	10.45	1522 - 1870	Fig 1, Group 1C, $CH_4/O_2/Ar$, dilution: 89.5%
x10004139	10	0.150 - 0.193	Ar	2.00	9.42	1681 - 2027	Fig 2, Group 2A, $CH_4/O_2/Ar$, dilution: 95.76%
x10004140	12	0.159 - 0.202	Ar	0.50	9.21	1620 - 1887	Fig 2, Group 2B, $CH_4/O_2/Ar$, dilution: 90%
x10004141	11	0.146 - 0.188	Ar	2.00	11.81	1608 - 1921	Fig 2, Group 2C, $CH_4/O_2/Ar$, dilution: 86.6%
x10004142	7	0.194 - 0.218	Ar	1.01	10.39	1631 - 1804	Fig 4, Group 4A, $CH_4/H_2/O_2/Ar$, dilution: 89.5%
x10004143	9	0.207 - 0.227	Ar	1.04	10.36	1596 - 1734	Fig 4, Group 4B, $CH_4/H_2/O_2/Ar$, dilution: 89.5%
Slack and Grillo (1981)[24]; ignition criterion: time of maximum of d[OHEX]/d*t* profile							
x10004144	11	0.147 - 0.215	N_2	0.5	1.8	1499 - 1877	Fig 2, Mixture A, $CH_4/O_2/N_2$, dilution: 76%
Tang et al. (2012)[25]; ignition criterion: root of the tangent line at the first inflection point of the [CHEX] profile							
x10004145	9	0.145	Ar	1	0.99	1701 - 2107	Fig 4(a) Mixture 1-M100, $CH_4/O_2/Ar$, dilution: 94.3%
x10004146	9	0.121	Ar	1	4.93	1519 - 1800	Fig 4(a) Mixture 1-M100, $CH_4/O_2/Ar$, dilution: 94.3%
x10004147	7	0.127	Ar	1	9.87	1392 - 1749	Fig 4(a) Mixture 1-M100, $CH_4/O_2/Ar$, dilution: 94.3%
Tsuboi and Wagner (1974)[26]; ignition criterion: root of the tangent line at the first inflection point of the *Signal* profile							
x10004148	10	0.157	Ar	0.2	3.35 - 4.07	1703 - 2069	Fig 2, $CH_4/O_2/Ar$, dilution: 97.8%; *Signal*: [CH_4]
x10004149	9	0.109	Ar	0.2	6.82 - 7.68	1663 - 1872	Fig 2, $CH_4/O_2/Ar$, dilution: 97.8%; *Signal*: [CH_4]
x10004150	13	0.100	Ar	0.2	7.53 - 8.85	1610 - 1891	Fig 2, $CH_4/O_2/Ar$, dilution: 97.8%; *Signal*: [CH_4]
x10004151	9	0.139	Ar	0.2	11.70 - 13.11	1585 - 1775	Fig 2, $CH_4/O_2/Ar$, dilution: 97.8%; *Signal*: [CH_4]
x10004152	19	0.158	Ar	0.2	22.29 - 29.72	1430 - 1906	Fig 2, $CH_4/O_2/Ar$, dilution: 97.8%; *Signal*: [CH_4]
x10004153	6	0.100	Ar	0.2	33.87 - 40.02	1474 - 1742	Fig 2, $CH_4/O_2/Ar$, dilution: 97.8%; *Signal*: [CH_4]
x10004154	5	0.100	Ar	0.2	89.97 - 104.33	1371 - 1589	Fig 2, $CH_4/O_2/Ar$, dilution: 97.8%; *Signal*: [CH_4]
x10004155	5	0.100	Ar	0.2	213.82 - 245.96	1448 - 1665	Fig 2, $CH_4/O_2/Ar$, dilution: 97.8%; *Signal*: [CH_4]
x10004156	3	0.100	Ar	0.2	2.88 - 3.38	1528 - 1789	Fig 4, $CH_4/O_2/Ar$, dilution: 89.0%; *Signal*: pressure
x10004157	4	0.100	Ar	1.0	3.08 - 3.64	1635 - 1927	Fig 4, $CH_4/O_2/Ar$, dilution: 97%; *Signal*: pressure
x10004158	5	0.140	Ar	0.2	2.76 - 3.91	1461 - 2074	Fig 4, $CH_4/O_2/Ar$, dilution: 89%; *Signal*: pressure
x10004159	3	0.100	Ar	0.2	3.25 - 3.86	1725 - 2047	Fig 4, $CH_4/O_2/Ar$, dilution: 97.8%; *Signal*: pressure
x10004160	4	0.100	Ar	0.2	3.14 - 3.19	1663 - 1692	Fig 4, $CH_4/O_2/Ar$, dilution: 97.8%; *Signal*: pressure

ID[.xml]	*Ni*	*σ*	Diluents	*φ*	*p* / atm	*T* / K	Comment
x10004161	3	0.100	Ar	0.2	2.98 - 3.25	1579 - 1724	Fig 4, $CH_4/O_2/Ar$, dilution: 99.5%; *Signal*: pressure
x10004162	2	0.100	Ar	2.0	2.69 - 3.12	1426 - 1654	Fig 4, $CH_4/O_2/Ar$, dilution: 96.0%; *Signal*: pressure
x10004163	1	0.100	Ar	1.0	2.75	1460	Fig 4, $CH_4/O_2/Ar$, dilution: 97.0%; *Signal*: pressure
Tsuboi and Katoh (1985)[27]; ignition criterion: root of the tangent line at the inflection point of the [CH_4] profile							
x10004164	5	0.153	Ar	1.0	0.96 - 1.17	1671 - 2038	Fig 2, Mixture 6, $CH_4/O_2/Ar$, dilution: 85%
x10004165	5	0.386	Ar	1.0	1.32 - 1.61	1605 - 1969	Fig 2, Mixture 6, $CH_4/O_2/Ar$, dilution: 85%
x10004166	5	0.100	Ar	1.0	3.60 - 4.55	1464 - 1851	Fig 2, Mixture 6, $CH_4/O_2/Ar$, dilution: 85%
x10004167	4	0.325	Ar	1.0	6.07 - 7.48	1479 - 1824	Fig 2, Mixture 6, $CH_4/O_2/Ar$, dilution: 85%
x10004168	5	0.100	Ar	1.0	11.33 - 13.06	1381 - 1592	Fig 2, Mixture 6, $CH_4/O_2/Ar$, dilution: 85%
x10004169	3	0.100	Ar	0.2	1.17 - 4.00	1700	Fig 3a, Mixture 3, $CH_4/O_2/Ar$, dilution: 45%
x10004170	5	0.233	Ar	0.2	1.32 - 13.94	1700	Fig 3a, Mixture 2, $CH_4/O_2/Ar$, dilution: 78%
x10004171	5	0.264	Ar	0.2	1.35 - 16.92	1700	Fig 3a, Mixture 1, $CH_4/O_2/Ar$, dilution: 89%
x10004172	5	0.109	Ar	1.0	1.22 - 18.95	1700	Fig 3b, Mixture 6, $CH_4/O_2/Ar$, dilution: 85%
x10004173	5	0.100	Ar	1.0	1.40 - 16.91	1700	Fig 3b, Mixture 5, $CH_4/O_2/Ar$, dilution: 94%
x10004174	4	0.100	Ar	1.0	2.78 - 17.79	1700	Fig 3b, Mixture 4, $CH_4/O_2/Ar$, dilution: 97%
Zhang et al. (2012)[28] - with PRR; ignition criterion: time of maximum of [OHEX] profile							
x10004175	9	0.235 - 0.276	Ar	2.00	17.76	1398 - 1964	Fig 3a, $CH_4/O_2/Ar$, dilution: 93.06%
x10004176	8	0.223 - 0.244	Ar	1.00	17.76	1376 - 1677	Fig 3a, $CH_4/O_2/Ar$, dilution: 94.3%
x10004177	9	0.223 - 0.249	Ar	0.50	17.76	1288 - 1729	Fig 3a, $CH_4/O_2/Ar$, dilution: 95.01%
x10004178	8	0.224 - 0.253	Ar	2.00	17.76	1300 - 1866	Fig 3b, $CH_4/H_2/O_2/Ar$, dilution: 93.46%
x10004179	10	0.224 - 0.256	Ar	1.00	17.76	1177 - 1813	Fig 3b, $CH_4/H_2/O_2/Ar$, dilution: 94.5%
x10004180	8	0.215 - 0.235	Ar	0.50	17.76	1216 - 1616	Fig 3b, $CH_4/H_2/O_2/Ar$, dilution: 95.11%
x10004181	8	0.268 - 0.287	Ar	2.00	17.76	1227 - 1719	Fig 3c, $CH_4/H_2/O_2/Ar$, dilution: 94%
x10004182	10	0.229 - 0.250	Ar	1.00	17.76	1099 - 1615	Fig 3c, $CH_4/H_2/O_2/Ar$, dilution: 94.78%
x10004183	7	0.190 - 0.209	Ar	0.50	17.76	1131 - 1467	Fig 3c, $CH_4/H_2/O_2/Ar$, dilution: 95.26%
x10004184	7	0.166 - 0.176	Ar	1.84	17.76	1096 - 1378	Fig 4, $CH_4/H_2/O_2/Ar$, dilution: 94.49%
x10004185	9	0.247 - 0.263	Ar	1.00	17.76	1077 - 1377	Fig 4, $CH_4/H_2/O_2/Ar$, dilution: 95.19%
x10004186	10	0.234 - 0.259	Ar	0.50	17.76	1086 - 1503	Fig 4, $CH_4/H_2/O_2/Ar$, dilution: 95.47%
x10004187	8	0.266 - 0.274	Ar	2.00	17.76	1028 - 1298	Fig 5a, $CH_4/H_2/O_2/Ar$, dilution: 95.87%
x10004188	8	0.292 - 0.309	Ar	1.00	17.76	1020 - 1361	Fig 5a, $CH_4/H_2/O_2/Ar$, dilution: 95.84%
x10004189	8	0.485 - 0.498	Ar	0.50	17.76	1023 - 1489	Fig 5a, $CH_4/H_2/O_2/Ar$, dilution: 95.82%
Zhukov et al. (2003)[29]; ignition criterion: time of maximum of d[OHEX]/d*t* profile							
x10004190	15	0.220 - 0.258	N_2	0.5	2.75	1409 - 1715	Table 1, $CH_4/O_2/N_2$, dilution: 75.07%
x10004191	13	0.288 - 0.344	N_2	0.5	2.75	1347 - 1722	Table 1, $CH_4/O_2/N_2$, dilution: 75.07%

ID[.xml]	*Ni*	σ	Diluents	φ	*p* / atm	*T* / K	Comment
x10004192	4	0.239 - 0.252	N_2	0.5	2.75	1422 - 1504	Table 1, $CH_4/O_2/N_2$, dilution: 75.07%
x10004193	3	0.247 - 0.270	N_2	0.5	2.75	1351 - 1580	Table 1, $CH_4/O_2/N_2$, dilution: 75.07%
x10004194	10	0.292 - 0.334	N_2	0.5	2.75	1369 - 1659	Table 1, $CH_4/O_2/N_2$, dilution: 75.07%
x10004195	7	0.300 - 0.336	N_2	0.5	2.75	1209 - 1507	Table 1, $CH_4/O_2/N_2$, dilution: 75.07%
x10004196	4	0.167 - 0.193	N_2	0.5	2.75	1196 - 1379	Table 1, $CH_4/O_2/N_2$, dilution: 75.07%
Bowman (1975)[30]; ignition criterion: time of maximum of [O] profile							
x10004197	8	0.388 - 0.521	Ar	4.0	2.69 - 3.22	1905 - 2240	Table 2, Mixture 1, $CH_4/O_2/Ar$, dilution: 91%
x10004198	8	0.308 - 0.408	Ar	4.5	2.79 - 3.36	1920 - 2265	Table 2, Mixture 2, $CH_4/CO/O_2/Ar$, dilution: 91%
x10004199	8	0.412 - 0.508	Ar	2.0	3.36 - 3.57	1875 - 2100	Table 2, Mixture 3, $CH_4/O_2/Ar$, dilution: 94%
x10004200	8	0.439 - 0.533	Ar	2.5	3.20 - 3.55	1895 - 2110	Table 2, Mixture 4, $CH_4/CO/O_2/Ar$, dilution: 94%
x10004201	6	0.271 - 0.348	Ar	1.0	3.21 - 3.50	1870 - 2135	Table 2, Mixture 5, $CH_4/O_2/Ar$, dilution: 95.5%
x10004202	6	0.298 - 0.370	Ar	1.5	3.31 - 3.62	1865 - 2130	Table 2, Mixture 6, $CH_4/CO/O_2/Ar$, dilution: 95.5%
Cheng and Oppenheim (1984)[31]; ignition criterion: time of maximum of the d*p*/d*t* profile							
x10004203	31	0.125 - 0.178	Ar	0.99	2	1685 - 2141	Fig 3, Mixture 2, $CH_4/O_2/Ar$, dilution: 90%
x10004204	48	0.157 - 0.226	Ar	0.50	2	1688 - 2159	Fig 3, Mixture 2, $CH_4/O_2/Ar$, dilution: 90%
x10004205	48	0.146 - 0.507	Ar	1.13	2	1574 - 2236	Fig 5, Mixture 3, $CH_4/H_2/O_2/Ar$, dilution: 91.43%
x10004206	31	0.124 - 0.442	Ar	0.56	2	1551 - 2100	Fig 5, Mixture 4, $CH_4/H_2/O_2/Ar$, dilution: 90.91%
x10004207	25	0.154 - 0.216	Ar	1.25	2	1604 - 2121	Fig 6, Mixture 5, $CH_4/H_2/O_2/Ar$, dilution: 92.5%
x10004208	37	0.108 - 0.274	Ar	0.63	2	1421 - 2339	Fig 6, Mixture 6, $CH_4/H_2/O_2/Ar$, dilution: 91.66%
x10004209	43	0.145 - 0.210	Ar	1.50	2	1366 - 1896	Fig 7, Mixture 7, $CH_4/H_2/O_2/Ar$, dilution: 94%
x10004210	22	0.159 - 0.223	Ar	1.00	2	1305 - 1836	Fig 7, Mixture 8, $CH_4/H_2/O_2/Ar$, dilution: 95%
x10004211	40	0.148 - 0.359	Ar	0.75	2	1358 - 2182	Fig 7, Mixture 9, $CH_4/H_2/O_2/Ar$, dilution: 92.85%
Hidaka et al. (1999)[32]; ignition criterion: root of the tangent line at the first inflection point of the *Signal* profile							
x10004212	12	0.241 - 0.270	Ar	2.0	3	1840 - 2233	Fig 18, Mixture D, $CH_4/O_2/Ar$, dilution: 98%; *Signal*: [CO_2]
x10004213	7	0.245 - 0.276	Ar	1.0	3	1668 - 2147	Fig 18, Mixture E, $CH_4/O_2/Ar$, dilution: 97%; *Signal*: [CO_2]
x10004214	9	0.195 - 0.224	Ar	0.5	3	1669 - 2007	Fig 18, Mixture F, $CH_4/O_2/Ar$, dilution: 95%; *Signal*: [CO_2]
x10004215	14	0.266 - 0.287	Ar	2.0	3	1922 - 2365	Fig 18, Mixture G, $CH_4/O_2/Ar$, dilution: 99.6%; *Signal*: [CO_2]
x10004216	14	0.171 - 0.208	Ar	0.5	3	1763 - 2325	Fig 18, Mixture H, $CH_4/O_2/Ar$, dilution: 99%; *Signal*: [CO_2]
x10004217	8	0.102 - 0.125	Ar	1.3	2.9	1462 - 1869	Fig 3, $CH_4/H_2/O_2/Ar$, dilution: 98.6%; *Signal*: [H_2O]
x10004218	6	0.100	Ar	0.7	2.9	1338 - 1772	Fig 3, $CH_4/H_2/O_2/Ar$, dilution: 98.9%; *Signal*: [H_2O]
Bowman (1970)[33]; ignition criterion: time of reaching 0.90×the maximum value in *Signal* profile							
x10004219	6	0.245 - 0.345	Ar	4.01	2.6	1982 - 2356	Fig 2, $CH_4/O_2/Ar$, dilution: 90%; *Signal*: [CO]
x10004220	9	0.418 - 0.554	Ar	2.00	2.6	1754 - 2062	Fig 2, $CH_4/O_2/Ar$, dilution: 90%; *Signal*: [CO]
x10004221	2	0.100	Ar	2.00	2.6	2061 - 2064	Fig 2, $CH_4/O_2/Ar$, dilution: 95%; *Signal*: [CO_2]

ID[.xml]	*Ni*	σ	Diluents	φ	*p* / atm	*T* / K	Comment
x10004222	6	0.255 - 0.323	Ar	2.00	2.6	1950 - 2222	Fig 2, CH_4/O_2/Ar, dilution: 98%; *Signal*: [CO_2]
x10004223	6	0.265 - 0.420	Ar	4.00	2.6	1877 - 2543	Fig 2, CH_4/O_2/Ar, dilution: 97%; *Signal*: [CO_2]
x10004224	5	0.306 - 0.358	Ar	4.01	1.3	1944 - 2252	Fig 2, CH_4/O_2/Ar, dilution: 90%; *Signal*: [CO_2]
x10004225	12	0.355 - 0.524	Ar	2.00	1.3	1799 - 2307	Fig 2, CH_4/O_2/Ar, dilution: 90%; *Signal*: [CO_2]
x10004226	10	0.291 - 0.437	Ar	4.01	2.6	1877 - 2441	Fig 2, CH_4/O_2/Ar, dilution: 90%; *Signal*: [CO_2]
x10004227	8	0.392 - 0.521	Ar	2.00	2.6	1755 - 2087	Fig 2, CH_4/O_2/Ar, dilution: 90%; *Signal*: [CO_2]
x10004228	6	0.341 - 0.433	Ar	4.01	2.6	1887 - 2245	Fig 2, CH_4/O_2/Ar, dilution: 90%; *Signal*: [H_2O]
x10004229	8	0.433 - 0.551	Ar	2.00	2.6	1777 - 2072	Fig 2, CH_4/O_2/Ar, dilution: 90%; *Signal*: [H_2O]
Bozhenkov et al. (2003)[34]; ignition criterion: root of the tangent line at the first inflection point of the [OHEX] profile							
x10004230	14	0.328 - 0.426	N_2/Ar	0.5	1.67 - 2.21	1610 - 2075	Table 4, $CH_4/O_2/Ar/N_2$, dilution: 95%
Burke et al. (2015)[35] - with PRR; ignition criterion: root of the tangent line at the inflection point of *p*(t)							
x10004231	5	0.115 - 0.142	N_2	0.3	25	1302 - 1459	Fig 5a, Mixture 1, $CH_4/O_2/N_2$, dilution: 76.58%
x10004232	5	0.162 - 0.183	N_2	2.0	10	1461 - 1649	Fig 5d, Mixture 4, $CH_4/O_2/N_2$, dilution: 65.28%
x10004233	5	0.123 - 0.141	N_2	2.0	25	1441 - 1584	Fig 5d, Mixture 4, $CH_4/O_2/N_2$, dilution: 65.28%
x10004234	4	0.100	N_2	0.3	25	1207 - 1309	Fig 5a, Mixture 1, $CH_4/O_2/N_2$, dilution: 76.58%
x10004235	4	0.106 - 0.124	N_2	0.3	44	1289 - 1399	Fig 5a, Mixture 1, $CH_4/O_2/N_2$, dilution: 76.58%
x10004236	4	0.100	N_2	0.3	44	1193 - 1317	Fig 5a, Mixture 1, $CH_4/O_2/N_2$, dilution: 76.58%
x10004237	5	0.166 - 0.187	N_2	0.5	10	1419 - 1640	Fig 5b, Mixture 2, $CH_4/O_2/N_2$, dilution: 75.05%
x10004238	8	0.100 - 0.122	N_2	0.5	25	1315 - 1551	Fig 5b, Mixture 2, $CH_4/O_2/N_2$, dilution: 75.05%
x10004239	4	0.101 - 0.129	N_2	0.5	44	1323 - 1499	Fig 5b, Mixture 2, $CH_4/O_2/N_2$, dilution: 75.05%
x10004240	5	0.122 - 0.153	N_2	1.0	10	1346 - 1514	Fig 5c, Mixture 3, $CH_4/O_2/N_2$, dilution: 71.48%
x10004241	7	0.133 - 0.154	N_2	1.0	25	1327 - 1463	Fig 5c, Mixture 3, $CH_4/O_2/N_2$, dilution: 71.48%
Hu et al. (2015)[36]; ignition criterion: root of the tangent line at the first inflection point of the [CHEX] profile							
x10004242	11	0.146 - 0.227	N_2	0.5	1	1492 - 1897	Fig 8a, $CH_4/O_2/N_2$, dilution: 75.06%
x10004243	7	0.212 - 0.285	N_2	2.0	3	1461 - 1730	Fig 8c, $CH_4/O_2/N_2$, dilution: 65.29%
x10004244	8	0.196 - 0.276	N_2	2.0	5	1413 - 1768	Fig 8c, $CH_4/O_2/N_2$, dilution: 65.29%
x10004245	6	0.224 - 0.306	N_2	2.0	10	1367 - 1664	Fig 8c, $CH_4/O_2/N_2$, dilution: 65.29%
x10004246	9	0.204 - 0.299	N_2	0.5	3	1388 - 1748	Fig 8a, $CH_4/O_2/N_2$, dilution: 75.06%
x10004247	8	0.175 - 0.276	N_2	0.5	5	1408 - 1822	Fig 8a, $CH_4/O_2/N_2$, dilution: 75.06%
x10004248	7	0.216 - 0.305	N_2	0.5	10	1335 - 1662	Fig 8a, $CH_4/O_2/N_2$, dilution: 75.06%
x10004249	21	0.165 - 0.244	N_2	1.0	1	1513 - 1925	Fig 8b, $CH_4/O_2/N_2$, dilution: 71.49%
x10004250	9	0.165 - 0.254	N_2	1.0	3	1459 - 1821	Fig 8b, $CH_4/O_2/N_2$, dilution: 71.49%
x10004251	8	0.180 - 0.262	N_2	1.0	5	1443 - 1758	Fig 8b, $CH_4/O_2/N_2$, dilution: 71.49%
x10004252	8	0.184 - 0.285	N_2	1.0	10	1350 - 1720	Fig 8b, $CH_4/O_2/N_2$, dilution: 71.49%
x10004253	9	0.172 - 0.233	N_2	2.0	1	1557 - 1831	Fig 8c, $CH_4/O_2/N_2$, dilution: 65.29%

ID[.xml]	*Ni*	*σ*	Diluents	*φ*	*p* / atm	*T* / K	Comment
Jachimowski (1974)[37]; ignition criterion: time of maximum of [O]×[CO] profile							
x10004254	11	0.167	Ar	1.5	1.43 - 1.73	2195 - 2584	Table 3, Mixture A, $CH_4/CO/O_2/Ar$, dilution: 97%
x10004255	9	0.161	Ar	2.5	1.16 - 1.73	1790 - 2525	Table 3, Mixture B, $CH_4/CO/O_2/Ar$, dilution: 97%
x10004256	12	0.175	Ar	1.8	1.45 - 1.70	2230 - 2550	Table 3, Mixture C, $CH_4/CO/O_2/Ar$, dilution: 97.33%
x10004257	12	0.207	Ar	1.2	1.44 - 1.69	2200 - 2535	Table 3, Mixture D, $CH_4/CO/O_2/Ar$, dilution: 96.5%
x10004258	11	0.186	Ar	1.4	1.45 - 1.71	2195 - 2545	Table 3, Mixture E, $CH_4/CO/H_2/O_2/Ar$, dilution: 96.5%
Kistiakowsky and Richards (1962)[38]; ignition criterion: root of the tangent line at the first inflection point of the [CHEX] profile							
x10004259	1	0.400	Ar	0.80	0.2	1829	Fig 6, $CH_4/O_2/Ar$, dilution: 95%
x10004260	5	0.286	Ar	0.44	0.17 - 0.24	1755 - 2565	Fig 6, $CH_4/O_2/Ar$, dilution: 95%
x10004261	3	0.400	Ar	1.33	0.24 - 0.25	1888 - 1946	Fig 6, $CH_4/O_2/Ar$, dilution: 95%
x10004262	1	0.400	Ar	4.10	0.51	2180	Fig 6, $CH_4/O_2/Ar$, dilution: 95%
x10004263	5	0.397	Ar	0.80	0.07 - 0.09	1911 - 2556	Fig 6, $CH_4/O_2/Ar$, dilution: 95%
x10004264	14	0.485	Ar	1.33	0.08 - 0.12	1878 - 2800	Fig 6, $CH_4/O_2/Ar$, dilution: 95%
x10004265	2	0.400	Ar	4.10	0.18 - 0.20	2326 - 2547	Fig 6, $CH_4/O_2/Ar$, dilution: 95%
Levy et al. (2006)[39]; ignition criterion: root of the tangent line at the inflection point of *p*(t)							
x10004266	18	0.169 - 0.239	Ar	1.00	6.49 - 9.44	1500 - 1873	Appendix, Mixture 1, $CH_4/O_2/Ar$, dilution: 89.05%
x10004267	16	0.149 - 0.165	N_2/CO_2	0.30	6.78 - 9.14	1387 - 1616	Appendix, Mixture 10, $CH_4/O_2/N_2/CO_2$, dilution: 82.59%
x10004268	11	0.112 - 0.125	N_2/CO_2	0.32	7.04 - 9.05	1434 - 1633	Appendix, Mixture 11, $CH_4/O_2/N_2/CO_2$, dilution: 85.54%
x10004269	17	0.135 - 0.141	$N_2/H_2O/CO_2$	0.31	6.55 - 8.99	1353 - 1586	Appendix, Mixture 12, $CH_4/O_2/N_2/H_2O/CO_2$, dilution: 82.17%
x10004270	22	0.225 - 0.255	$N_2/H_2O/CO_2$	0.29	6.85 - 8.88	1365 - 1560	Appendix, Mixture 13, $CH_4/O_2/N_2/H_2O/CO_2$, dilution: 82.3%
x10004271	12	0.173 - 0.229	N_2/Ar	1.02	6.23 - 9.03	1583 - 1922	Appendix, Mixture 2, $CH_4/O_2/N_2/Ar$, dilution: 93.05%
x10004272	29	0.304 - 0.330	N_2/Ar	0.29	5.27 - 9.71	1394 - 1691	Appendix, Mixture 3, $CH_4/O_2/N_2/Ar$, dilution: 82.37%
x10004273	8	0.186 - 0.206	N_2	1.01	7.56 - 8.38	1503 - 1585	Appendix, Mixture 4, $CH_4/O_2/N_2$, dilution: 89.48%
x10004274	18	0.121 - 0.127	N_2	0.29	6.23 - 9.41	1376 - 1694	Appendix, Mixture 5, $CH_4/O_2/N_2$, dilution: 82.28%
x10004275	19	0.208 - 0.282	N_2	0.32	6.22 - 9.29	1377 - 1695	Appendix, Mixture 6, $CH_4/O_2/N_2$, dilution: 85.55%
x10004276	23	0.162 - 0.193	N_2	1.33	6.35 - 8.28	1521 - 1764	Appendix, Mixture 7, $CH_4/O_2/N_2$, dilution: 90%
x10004277	24	0.194 - 0.227	N_2	0.40	6.66 - 9.71	1344 - 1520	Appendix, Mixture 8, $CH_4/O_2/N_2$, dilution: 82.01%
x10004278	25	0.336 - 0.362	$N_2/Ar/CO_2$	0.29	6.87 - 10.10	1413 - 1705	Appendix, Mixture 9, $CH_4/O_2/N_2/Ar/CO_2$, dilution: 82.36%
Mathieu et al. (2015)[40]; ignition criterion: root of the tangent line at the first inflection point of the *Signal* profile							
x10004279	7	0.161	Ar	0.50	0.88 - 0.97	1523 - 1939	Fig 3a, $CH_4/O_2/Ar$, dilution: 97.5%; *Signal*: [OHEX]
x10004280	5	0.101	N_2	0.50	9.0 - 11.8	1335 - 1616	Fig 11b, $CH_4/O_2/N_2$, dilution: 75%; *Signal*: pressure
x10004281	5	0.109	N_2	1.01	1.21 - 1.55	1487 - 1705	Fig 12a, $CH_4/O_2/N_2$, dilution: 71.58%; *Signal*: pressure
x10004282	5	0.119	N_2	1.01	9.3 - 12.3	1312 - 1571	Fig 12b, $CH_4/O_2/N_2$, dilution: 71.58%; *Signal*: pressure

ID[.xml]	*Ni*	*σ*	Diluents	*φ*	*p* / atm	*T* / K	Comment
x10004283	5	0.120	N_2	2.00	7.2 - 10.1	1358 - 1633	Fig 13a, $CH_4/O_2/N_2$, dilution: 65.37%; *Signal*: pressure
x10004284	11	0.129	Ar	0.50	9.9 - 10.8	1529 - 1862	Fig 3b, CH_4/O_2/Ar, dilution: 97.5%; *Signal*: [OHEX]
x10004285	7	0.125	Ar	0.50	1.23 - 1.37	1669 - 2032	Fig 3c, CH_4/O_2/Ar, dilution: 97.5%; *Signal*: [OHEX]
x10004286	7	0.125	Ar	0.50	25.6 - 26.5	1436 - 1834	Fig 3d, CH_4/O_2/Ar, dilution: 97.5%; *Signal*: [OHEX]
x10004287	6	0.186	Ar	0.99	1.22 - 1.40	1669 - 2069	Fig 4a, CH_4/O_2/Ar, dilution: 97.5%; *Signal*: [OHEX]
x10004288	7	0.186	Ar	0.99	10.9 - 11.5	1536 - 1979	Fig 4b, CH_4/O_2/Ar, dilution: 97.5%; *Signal*: [OHEX]
x10004289	5	0.127	Ar	2.00	1.23 - 1.34	1728 - 2062	Fig 5a, CH_4/O_2/Ar, dilution: 97.5%; *Signal*: [OHEX]
x10004290	5	0.176	Ar	2.00	10.6 - 11.5	1603 - 1864	Fig 5b, CH_4/O_2/Ar, dilution: 97.5%; *Signal*: [OHEX]
x10004291	5	0.117	N_2	0.50	1.34 - 1.71	1467 - 1682	Fig 11a, $CH_4/O_2/N_2$, dilution: 75%; *Signal*: pressure
Petersen et al. (1999)[41]; ignition criterion: root of the tangent line at the inflection point of *p*(t)							
x10004296	6	0.141 - 0.174	Ar	3.01	85	1166 - 1420	Fig 5, Mixture 2, CH_4/O_2/Ar, dilution: 66.7%
x10004297	3	0.100 - 0.109	Ar	3.01	170	1208 - 1374	Fig 5, Mixture 2, CH_4/O_2/Ar, dilution: 66.7%
x10004298	10	0.138 - 0.165	N_2	3.01	40	1360 - 1511	Fig 5, Mixture 3, $CH_4/O_2/N_2$, dilution: 66.7%
x10004299	5	0.171 - 0.203	Ar	3.01	40	1327 - 1537	Fig 5, Mixture 2, CH_4/O_2/Ar, dilution: 66.7%
x10004300	3	0.100	Ar	3.01	260	1177 - 1302	Fig 6, Mixture 2, CH_4/O_2/Ar, dilution: 66.7%
x10004301	4	0.100 - 0.119	N_2	3.01	115	1151 - 1324	Fig 6, Mixture 3, $CH_4/O_2/N_2$, dilution: 66.7%
x10004302	3	0.109 - 0.133	Ar	3.00	65	1217 - 1347	Fig 7, Mixture 4, CH_4/O_2/Ar, dilution: 54.5%
x10004303	4	0.100	N_2	3.00	180	1152 - 1269	Fig 7, Mixture 5, $CH_4/O_2/N_2$, dilution: 54.5%
x10004304	7	0.100 - 0.128	N_2	3.00	130	1040 - 1327	Fig 7, Mixture 5, $CH_4/O_2/N_2$, dilution: 54.5%
x10004305	2	0.100	He	5.99	50	1458 - 1549	Fig 8, Mixture 6, CH_4/O_2/He, dilution: 33.3%
x10004306	3	0.100	He	5.99	90	1130 - 1292	Fig 8, Mixture 6, CH_4/O_2/He, dilution: 33.3%
x10004307	8	0.108 - 0.152	Ar	0.40	100	1137 - 1360	Fig 9, Mixture 1, CH_4/O_2/Ar, dilution: 77%
x10004308	6	0.119 - 0.146	Ar	0.40	50	1203 - 1360	Fig 9, Mixture 1, CH_4/O_2/Ar, dilution: 77%
x10004309	2	0.115 - 0.125	Ar	0.40	150	1198 - 1250	Fig 9, Mixture 1, CH_4/O_2/Ar, dilution: 77%
Petersen et al. (1999)[42]; ignition criterion: root of the tangent line at the first inflection point of the *Signal* profile							
x10004310	6	0.100	Ar	0.4	44.4 - 50.5	1203 - 1359	Table 2, Mixture 1, CH_4/O_2/Ar, dilution: 76.92%; *Signal*: pressure
x10004311	5	0.100	Ar	0.4	44.4 - 50.5	1203 - 1359	Table 2, Mixture 1, CH_4/O_2/Ar, dilution: 76.92%; *Signal*: [CHEX]
x10004312	8	0.100	Ar	0.4	94.5 - 100.9	1137 - 1361	Table 2, Mixture 1, CH_4/O_2/Ar, dilution: 76.92%; *Signal*: pressure
x10004313	5	0.100	Ar	0.4	94.5 - 100.0	1169 - 1361	Table 2, Mixture 1, CH_4/O_2/Ar, dilution: 76.92%; *Signal*: [CHEX]
x10004314	2	0.100	Ar	0.4	150.8 - 161.2	1198 - 1250	Table 2, Mixture 1, CH_4/O_2/Ar, dilution: 76.92%; *Signal*: pressure
x10004315	2	0.100	Ar	0.4	150.8 - 161.2	1198 - 1250	Table 2, Mixture 1, CH_4/O_2/Ar, dilution: 76.92%; *Signal*: [CHEX]
x10004316	5	0.236 - 0.255	N_2	3.0	34.5 - 47.5	1325 - 1536	Table 2, Mixture 2, $CH_4/O_2/N_2$, dilution: 66.67%; *Signal*: pressure
x10004317	6	0.131 - 0.167	N_2	3.0	77.7 - 92.9	1167 - 1418	Table 2, Mixture 2, $CH_4/O_2/N_2$, dilution: 66.67%; *Signal*: pressure

ID[.xml]	*Ni*	*σ*	Diluents	*φ*	*p* / atm	*T* / K	Comment
x10004318	3	0.100	N_2	3.0	77.7 - 91.0	1167 - 1206	Table 2, Mixture 2, $CH_4/O_2/N_2$, dilution: 66.67%; *Signal*: [CHEX]
x10004319	6	0.186 - 0.225	N_2	3.0	102.8 - 132.2	1156 - 1380	Table 2, Mixture 2, $CH_4/O_2/N_2$, dilution: 66.67%; *Signal*: pressure
x10004320	6	0.200 - 0.244	N_2	3.0	102.8 - 132.2	1156 - 1380	Table 2, Mixture 2, $CH_4/O_2/N_2$, dilution: 66.67%; *Signal*: [CHEX]
x10004321	3	0.100 - 0.141	N_2	3.0	163.0 - 178.4	1209 - 1372	Table 2, Mixture 2, $CH_4/O_2/N_2$, dilution: 66.67%; *Signal*: pressure
x10004322	3	0.102 - 0.182	N_2	3.0	256.2 - 263.6	1176 - 1301	Table 2, Mixture 2, $CH_4/O_2/N_2$, dilution: 66.67%; *Signal*: pressure
x10004323	10	0.149 - 0.175	Ar	3.0	36.7 - 48.2	1358 - 1511	Table 2, Mixture 3, CH_4/O_2/Ar, dilution: 66.67%; *Signal*: pressure
x10004324	5	0.100 - 0.137	Ar	3.0	72.1 - 76.5	1290 - 1466	Table 2, Mixture 3, CH_4/O_2/Ar, dilution: 66.67%; *Signal*: pressure
x10004325	3	0.100 - 0.135	Ar	3.0	72.1 - 76.5	1290 - 1466	Table 2, Mixture 3, CH_4/O_2/Ar, dilution: 66.67%; *Signal*: [CH_4]
x10004326	5	0.100 - 0.125	Ar	3.0	84.1 - 92.0	1227 - 1437	Table 2, Mixture 3, CH_4/O_2/Ar, dilution: 66.67%; *Signal*: pressure
x10004327	5	0.110 - 0.120	Ar	3.0	84.1 - 92.0	1227 - 1437	Table 2, Mixture 3, CH_4/O_2/Ar, dilution: 66.67%; *Signal*: [CHEX]
x10004328	4	0.100	Ar	3.0	103.1 - 117.4	1149 - 1323	Table 2, Mixture 3, CH_4/O_2/Ar, dilution: 66.67%; *Signal*: pressure
x10004329	1	0.100	Ar	3.0	113.0	1149	Table 2, Mixture 3, CH_4/O_2/Ar, dilution: 66.67%; *Signal*: [CHEX]
x10004330	4	0.100	Ar	3.0	134.9 - 148.2	1186 - 1317	Table 2, Mixture 3, CH_4/O_2/Ar, dilution: 66.67%; *Signal*: pressure
x10004331	3	0.100	N_2	3.0	44.9 - 51.5	1191 - 1362	Table 2, Mixture 4, $CH_4/O_2/N_2$, dilution: 54.55%; *Signal*: pressure
x10004332	3	0.100	N_2	3.0	44.9 - 51.5	1191 - 1362	Table 2, Mixture 4, $CH_4/O_2/N_2$, dilution: 54.55%; *Signal*: [CHEX]
x10004333	3	0.152 - 0.159	N_2	3.0	60.4 - 71.3	1215 - 1346	Table 2, Mixture 4, $CH_4/O_2/N_2$, dilution: 54.55%; *Signal*: pressure
x10004334	2	0.100	N_2	3.0	125.5 - 128.0	1089 - 1156	Table 2, Mixture 4, $CH_4/O_2/N_2$, dilution: 54.55%; *Signal*: pressure
x10004335	2	0.100	N_2	3.0	125.5 - 128.0	1089 - 1156	Table 2, Mixture 4, $CH_4/O_2/N_2$, dilution: 54.55%; *Signal*: [CHEX]
x10004336	3	0.100	Ar	3.0	54.4 - 59.6	1196 - 1371	Table 2, Mixture 5, CH_4/O_2/Ar, dilution: 54.55%; *Signal*: pressure
x10004337	2	0.100	Ar	3.0	54.4 - 55.3	1196 - 1258	Table 2, Mixture 5, CH_4/O_2/Ar, dilution: 54.55%; *Signal*: [CHEX]
x10004338	2	0.100	Ar	3.0	82.8 - 86.6	1242 - 1272	Table 2, Mixture 5, CH_4/O_2/Ar, dilution: 54.55%; *Signal*: pressure
x10004339	2	0.100	Ar	3.0	82.8 - 86.6	1242 - 1272	Table 2, Mixture 5, CH_4/O_2/Ar, dilution: 54.55%; *Signal*: [CH]
x10004340	7	0.119 - 0.170	Ar	3.0	122.8 - 139.9	1041 - 1327	Table 2, Mixture 5, CH_4/O_2/Ar, dilution: 54.55%; *Signal*: pressure
x10004341	1	0.100	Ar	3.0	138.5	1186	Table 2, Mixture 5, CH_4/O_2/Ar, dilution: 54.55%; *Signal*: [CHEX]
x10004342	4	0.100 - 0.149	Ar	3.0	169.7 - 194.0	1150 - 1268	Table 2, Mixture 5, CH_4/O_2/Ar, dilution: 54.55%; *Signal*: pressure
x10004343	1	0.100	Ar	3.0	176.6	1150	Table 2, Mixture 5, CH_4/O_2/Ar, dilution: 54.55%; *Signal*: [CH]
x10004344	6	0.100 - 0.104	He	6.0	12.0 - 20.3	1453 - 1607	Table 2, Mixture 6, CH_4/O_2/He, dilution: 33.33%; *Signal*: [soot]
x10004345	2	0.116 - 0.172	He	6.0	51.2 - 57.2	1456 - 1547	Table 2, Mixture 6, CH_4/O_2/He, dilution: 33.33%; *Signal*: pressure
x10004346	2	0.122 - 0.172	He	6.0	51.2 - 57.2	1456 - 1547	Table 2, Mixture 6, CH_4/O_2/He, dilution: 33.33%; *Signal*: [CHEX]
x10004347	3	0.100	He	6.0	68.4 - 79.0	1324 - 1395	Table 2, Mixture 6, CH_4/O_2/He, dilution: 33.33%; *Signal*: pressure
x10004348	3	0.127 - 0.146	He	6.0	68.4 - 79.0	1324 - 1395	Table 2, Mixture 6, CH_4/O_2/He, dilution: 33.33%; *Signal*: [CHEX]
x10004349	3	0.100	He	6.0	81.6 - 91.3	1128 - 1290	Table 2, Mixture 6, CH_4/O_2/He, dilution: 33.33%; *Signal*: pressure
x10004350	3	0.100	He	6.0	81.6 - 91.3	1128 - 1290	Table 2, Mixture 6, CH_4/O_2/He, dilution: 33.33%; *Signal*: [CHEX]

ID[.xml]	*Ni*	*σ*	Diluents	*φ*	*p* / atm	*T* / K	Comment
x10004351	4	0.100	He/N_2	3.0	27.0 - 35.5	1272 - 1458	Table 2, Mixture 7, $CH_4/O_2/He/N_2$, dilution: 70.57%; *Signal*: pressure
x10004352	3	0.100	He/N_2	3.0	27.0 - 29.5	1338 - 1458	Table 2, Mixture 7, $CH_4/O_2/He/N_2$, dilution: 70.57%; *Signal*: [CHEX]
x10004353	2	0.100	He/N_2	3.0	47.1 - 49.5	1342 - 1469	Table 2, Mixture 7, $CH_4/O_2/He/N_2$, dilution: 70.57%; *Signal*: pressure
x10004354	2	0.100	He/N_2	3.0	47.1 - 49.5	1342 - 1469	Table 2, Mixture 7, $CH_4/O_2/He/N_2$, dilution: 70.57%; *Signal*: [CHEX]
x10004355	3	0.100	He/N_2	3.0	57.2 - 61.5	1296 - 1391	Table 2, Mixture 7, $CH_4/O_2/He/N_2$, dilution: 70.57%; *Signal*: pressure
x10004356	3	0.100	He/N_2	3.0	57.2 - 61.5	1296 - 1391	Table 2, Mixture 7, $CH_4/O_2/He/N_2$, dilution: 70.57%; *Signal*: [CHEX]
x10004357	1	0.100	He/N_2	3.0	76.4	1347	Table 2, Mixture 7, $CH_4/O_2/He/N_2$, dilution: 70.57%; *Signal*: pressure
x10004358	1	0.100	He/N_2	3.0	76.4	1347	Table 2, Mixture 7, $CH_4/O_2/He/N_2$, dilution: 70.57%; *Signal*: [CHEX]
x10004359	2	0.100	He/N_2	3.0	92.5 - 106.6	1340 - 1358	Table 2, Mixture 7, $CH_4/O_2/He/N_2$, dilution: 70.57%; *Signal*: pressure
x10004360	2	0.100	He/N_2	3.0	92.5 - 106.6	1340 - 1358	Table 2, Mixture 7, $CH_4/O_2/He/N_2$, dilution: 70.57%; *Signal*: [CHEX]
Petersen et al. (1996)[43]; ignition criterion: root of the tangent line at the first inflection point of the *Signal* profile, unless otherwise noted							
x10004361	2	0.100	Ar	0.50	31.2 - 85.3	1680 - 1770	Table 2, Mixture 1, $CH_4/O_2/Ar$, dilution: 98.75%; *Signal*: [OH]
x10004362	2	0.100	Ar	0.50	31.2 - 85.3	1680 - 1770	Table 2, Mixture 1, $CH_4/O_2/Ar$, dilution: 98.75%; ignition criterion: time of maximum of [OH] profile
x10004363	1	0.100	Ar	0.50	84.4	1673	Table 2, Mixture 1, $CH_4/O_2/Ar$, dilution: 98.75%; *Signal*: [CH_4]
x10004364	4	0.223 - 0.273	Ar	2.00	10.2 - 60.3	1478 - 1635	Table 2, Mixture 10, $CH_4/O_2/Ar$, dilution: 90%; *Signal*: pressure
x10004365	4	0.215 - 0.263	Ar	2.00	10.2 - 60.3	1478 - 1635	Table 2, Mixture 10, $CH_4/O_2/Ar$, dilution: 90%; *Signal*: [CH_4]
x10004366	2	0.159 - 0.213	Ar	3.57	32.3 - 80.9	1706 - 1977	Table 2, Mixture 11, $CH_4/O_2/Ar$, dilution: 99.61%; *Signal*: [CH_4]
x10004367	1	0.100	Ar	4.00	85.7	1690	Table 2, Mixture 12, $CH_4/O_2/Ar$, dilution: 99.25%; *Signal*: [CH_4]
x10004368	5	0.413 - 0.433	Ar	0.50	10.5 - 80.9	1576 - 1853	Table 2, Mixture 2, $CH_4/O_2/Ar$, dilution: 97.5%; *Signal*: [OH]
x10004369	5	0.518 - 0.542	Ar	0.50	10.5 - 80.9	1576 - 1853	Table 2, Mixture 2, $CH_4/O_2/Ar$, dilution: 97.5%; *Signal*: pressure
x10004370	5	0.450 - 0.469	Ar	0.50	10.5 - 80.9	1576 - 1853	Table 2, Mixture 2, $CH_4/O_2/Ar$, dilution: 97.5%; ignition criterion: time of maximum of [OH] profile
x10004371	3	0.167 - 0.215	Ar	0.50	10.1 - 32.3	1532 - 1739	Table 2, Mixture 3, $CH_4/O_2/Ar$, dilution: 95%; *Signal*: [CH_4]
x10004372	3	0.166 - 0.214	Ar	0.50	10.1 - 32.3	1532 - 1739	Table 2, Mixture 3, $CH_4/O_2/Ar$, dilution: 95%; *Signal*: pressure
x10004373	1	0.100	Ar	1.00	83.9	1706	Table 2, Mixture 4, $CH_4/O_2/Ar$, dilution: 99.16%; *Signal*: pressure
x10004374	2	0.100	Ar	1.00	36.8 - 83.9	1706 - 1761	Table 2, Mixture 4, $CH_4/O_2/Ar$, dilution: 99.16%; ignition criterion: time of maximum of [OH] profile
x10004375	2	0.100	Ar	0.98	9.4 - 79.1	1778 - 2043	Table 2, Mixture 5, $CH_4/O_2/Ar$, dilution: 98.3%; *Signal*: [OH]
x10004376	1	0.100	Ar	0.98	79.1	1778	Table 2, Mixture 5, $CH_4/O_2/Ar$, dilution: 98.3%; *Signal*: pressure
x10004377	2	0.100	Ar	0.98	9.4 - 79.1	1778 - 2043	Table 2, Mixture 5, $CH_4/O_2/Ar$, dilution: 98.3%; ignition criterion: time of maximum of [OH] profile
x10004378	5	0.583 - 0.595	Ar	1.00	171.5 - 481.4	1481 - 1617	Table 2, Mixture 6, $CH_4/O_2/Ar$, dilution: 96.94%; *Signal*: pressure
x10004379	3	0.205 - 0.245	Ar	1.01	31.7 - 61.9	1496 - 1633	Table 2, Mixture 7, $CH_4/O_2/Ar$, dilution: 89.9%; *Signal*: pressure
x10004380	1	0.100	Ar	2.00	30.2	1988	Table 2, Mixture 8, $CH_4/O_2/Ar$, dilution: 99.5%; *Signal*: [CH_4]

ID[.xml]	*Ni*	*σ*	Diluents	*φ*	*p* / atm	*T* / K	Comment
x10004381	1	0.100	Ar	2.00	77.1	1896	Table 2, Mixture 9, $CH_4/O_2/Ar$, dilution: 99%; *Signal*: [CH_4]
x10004382	4	0.174 - 0.223	Ar	0.50	60	1542 - 1744	Fig 2, Mixture 2, $CH_4/O_2/Ar$, dilution: 97.5%; ignition criterion: time of maximum of [OH] profile
x10004383	6	0.175 - 0.215	N_2	0.50	60	1562 - 1738	Fig 2, Mixture 2N, $CH_4/O_2/N_2$, dilution: 97.5%; ignition criterion: time of maximum of [OH] profile
x10004384	4	0.161 - 0.184	Ar	0.50	18	1669 - 1788	Fig 2, Mixture 2, $CH_4/O_2/Ar$, dilution: 97.5%; ignition criterion: time of maximum of [OH] profile
x10004385	6	0.161 - 0.204	Ar	0.50	60	1506 - 1697	Fig 2, Mixture 2, $CH_4/O_2/Ar$, dilution: 97.5%; ignition criterion: time of maximum of [OH] profile
Grillo and Slack (1976)[44]; ignition criterion: time of maximum of d[OHEX]/d*t* profile							
x10004386	6	0.150 - 0.193	Ar	2	5	1672 - 2002	Fig 2, Mixture 1, $CH_4/O_2/Ar$, dilution: 96%
x10004387	10	0.140 - 0.192	Ar/N_2	2	5.76	1676 - 2066	Fig 2, Mixture 2, $CH_4/O_2/Ar/N_2$, dilution: 96.62%
x10004388	8	0.173 - 0.220	Ar	1	2.95	1651 - 1970	Fig 2, Mixture 3, $CH_4/O_2/Ar$, dilution: 94%
x10004389	4	0.108 - 0.175	Ar/N_2	1	2.95	1691 - 2152	Fig 2, Mixture 4, $CH_4/O_2/Ar/N_2$, dilution: 94.5%
x10004390	17	0.144 - 0.202	Ar/N_2	1	2.36	1635 - 2041	Fig 2, Mixture 5, $CH_4/O_2/Ar/N_2$, dilution: 94.93%
Huang and Bushe (2006)[45]; ignition criterion: root of the tangent line at the first inflection point of the [CH_3] profile							
x10004391	11	0.177 - 0.204	N_2	1	15.79	1037 - 1350	Fig 1a, $CH_4/O_2/N_2$, dilution: 71.49%
x10004392	13	0.142 - 0.176	N_2	1	39.48	1024 - 1298	Fig 1b, $CH_4/O_2/N_2$, dilution: 71.49%
Suzuki et al. (1991)[46]; ignition criterion: root of the tangent line at the first inflection point of the [OHEX] profile							
x10004393	11	0.140	Ar	1	2.9	1595 - 1993	Fig 2, Mixture 1, $CH_4/O_2/Ar$, dilution: 94%
Takahashi et al. (1988)[47]; ignition criterion: root of the tangent line at the first inflection point of the [OHEX] profile							
x10004394	13	0.100	Ar	1.00	2.9	1626 - 1993	Fig 1, Mixture 1, $CH_4/O_2/Ar$, dilution: 94%
x10004395	7	0.100	Ar	1.05	2.9	1638 - 1953	Fig 1, Mixture 2, $CH_4/O_2/Ar$, dilution: 93.9%
Walker (2000)[48]; ignition criterion: root of the tangent line at the first inflection point of the [OHEX] profile							
x10004396	7	0.156 - 0.169	Ar	0.50	1.03 - 1.21	1575 - 1873	Table 3, Mixture 16, $CH_4/O_2/Ar$, dilution: 75%
x10004397	8	0.106 - 0.124	Ar	1.01	1.13 - 1.27	1726 - 2248	Table 3, Mixture 4, $CH_4/O_2/Ar$, dilution: 98%
Huang et al. (2006)[49]; ignition criterion: root of the tangent line at the inflection point of *p*(t)							
x10004398	8	0.137 - 0.158	N_2	1.00	33.40 - 42.70	1028 - 1297	Table 3, Mixture 1, $CH_4/H_2/O_2/N_2$, dilution: 72.2%
x10004399	8	0.126 - 0.143	N_2	1.00	14.80 - 18.80	1096 - 1307	Table 3, Mixture 1, $CH_4/H_2/O_2/N_2$, dilution: 72.2%
x10004400	10	0.267 - 0.293	N_2	1.01	36.00 - 41.10	1035 - 1318	Table 3, Mixture 2, $CH_4/H_2/O_2/N_2$, dilution: 73.4%
x10004401	11	0.214 - 0.239	N_2	1.01	15.60 - 17.00	1019 - 1318	Table 3, Mixture 2, $CH_4/H_2/O_2/N_2$, dilution: 73.4%
Petersen et al. (2007)[50]; ignition criterion: root of the tangent line at the first inflection point of the [CHEX] profile							
x10004402	7	0.112	N_2	0.5	0.54 - 0.92	1431 - 2001	Table 2, Mixture 1, $CH_4/O_2/N_2$, dilution: 73.77%
x10004403	21	0.276	N_2	0.5	10.30 - 23.80	1243 - 1659	Table 2, Mixture 2, $CH_4/O_2/N_2$, dilution: 75%
x10004404	8	0.111	N_2	0.5	18.20 - 25.10	1141 - 1553	Table 2, Mixture 3, $CH_4/H_2/O_2/N_2$, dilution: 75.56%
x10004405	10	0.187	N_2	0.5	20.50 - 30.00	1132 - 1409	Table 2, Mixture 4, $CH_4/H_2/O_2/N_2$, dilution: 76.3%
Yu et al. (1995)[51]; ignition criterion: time of reaching $A\times$the maximum value in *Signal* profile							

ID[.xml]	*Ni*	*σ*	Diluents	*φ*	*p* / atm	*T* / K	Comment
x10004406	11	0.150 - 0.152	Ar	0.04	1.46 - 2.34	1651 - 2192	Table 3, Series A, $CH_4/O_2/Ar$, dilution: 79.6%; *A*: 0.25, *Signal*: [CO]
x10004407	11	0.147 - 0.148	Ar	0.04	1.46 - 2.34	1651 - 2192	Table 3, Series A, $CH_4/O_2/Ar$, dilution: 79.6%; *A*: 0.50, *Signal*: [CO]
x10004408	11	0.134 - 0.136	Ar	0.04	1.46 - 2.34	1651 - 2192	Table 3, Series A, $CH_4/O_2/Ar$, dilution: 79.6%; *A*: 0.75, *Signal*: [CO]
x10004409	11	0.145 - 0.147	Ar	0.04	1.46 - 2.34	1651 - 2192	Table 3, Series A, $CH_4/O_2/Ar$, dilution: 79.6%; *A*: 0.25, *Signal*: [OH]
x10004410	11	0.146 - 0.148	Ar	0.04	1.46 - 2.34	1651 - 2192	Table 3, Series A, $CH_4/O_2/Ar$, dilution: 79.6%; *A*: 0.50, *Signal*: [OH]
x10004411	11	0.215 - 0.216	Ar	0.04	1.46 - 2.34	1651 - 2192	Table 3, Series A, $CH_4/O_2/Ar$, dilution: 79.6%; *A*: 0.75, *Signal*: [OH]
x10004412	15	0.195 - 0.196	Ar	0.10	1.44 - 2.42	1538 - 1852	Table 3, Series B, $CH_4/O_2/Ar$, dilution: 89.51%; *A*: 0.25, *Signal*: [CO]
x10004413	15	0.191 - 0.192	Ar	0.10	1.44 - 2.42	1538 - 1852	Table 3, Series B, $CH_4/O_2/Ar$, dilution: 89.51%; *A*: 0.50, *Signal*: [CO]
x10004414	15	0.190 - 0.191	Ar	0.10	1.44 - 2.42	1538 - 1852	Table 3, Series B, $CH_4/O_2/Ar$, dilution: 89.51%; *A*: 0.75, *Signal*: [CO]
x10004415	15	0.187 - 0.189	Ar	0.10	1.44 - 2.42	1538 - 1852	Table 3, Series B, $CH_4/O_2/Ar$, dilution: 89.51%; *A*: 0.25, *Signal*: [OH]
x10004416	15	0.187 - 0.189	Ar	0.10	1.44 - 2.42	1538 - 1852	Table 3, Series B, $CH_4/O_2/Ar$, dilution: 89.51%; *A*: 0.50, *Signal*: [OH]
x10004417	15	0.180 - 0.182	Ar	0.10	1.44 - 2.42	1538 - 1852	Table 3, Series B, $CH_4/O_2/Ar$, dilution: 89.51%; *A*: 0.75, *Signal*: [OH]
x10004418	8	0.230 - 0.231	Ar	0.16	1.45 - 2.50	1687 - 2012	Table 3, Series C, $CH_4/O_2/Ar$, dilution: 94.6%; *A*: 0.25, *Signal*: [CO]
x10004419	8	0.235 - 0.236	Ar	0.16	1.45 - 2.50	1687 - 2012	Table 3, Series C, $CH_4/O_2/Ar$, dilution: 94.6%; *A*: 0.50, *Signal*: [CO]
x10004420	8	0.233 - 0.234	Ar	0.16	1.45 - 2.50	1687 - 2012	Table 3, Series C, $CH_4/O_2/Ar$, dilution: 94.6%; *A*: 0.75, *Signal*: [CO]
x10004421	8	0.209 - 0.210	Ar	0.16	1.45 - 2.50	1687 - 2012	Table 3, Series C, $CH_4/O_2/Ar$, dilution: 94.6%; *A*: 0.25, *Signal*: [OH]
x10004422	8	0.210 - 0.211	Ar	0.16	1.45 - 2.50	1687 - 2012	Table 3, Series C, $CH_4/O_2/Ar$, dilution: 94.6%; *A*: 0.50, *Signal*: [OH]
x10004423	8	0.216 - 0.217	Ar	0.16	1.45 - 2.50	1687 - 2012	Table 3, Series C, $CH_4/O_2/Ar$, dilution: 94.6%; *A*: 0.75, *Signal*: [OH]
x10004424	6	0.234 - 0.235	Ar	0.67	1.51 - 2.40	1680 - 1856	Table 3, Series D, $CH_4/O_2/Ar$, dilution: 96%; *A*: 0.25, *Signal*: [CO]
x10004425	6	0.216 - 0.217	Ar	0.67	1.51 - 2.40	1680 - 1856	Table 3, Series D, $CH_4/O_2/Ar$, dilution: 96%; *A*: 0.50, *Signal*: [CO]
x10004426	6	0.193 - 0.194	Ar	0.67	1.51 - 2.40	1680 - 1856	Table 3, Series D, $CH_4/O_2/Ar$, dilution: 96%; *A*: 0.75, *Signal*: [CO]
x10004427	6	0.186 - 0.188	Ar	0.67	1.51 - 2.40	1680 - 1856	Table 3, Series D, $CH_4/O_2/Ar$, dilution: 96%; *A*: 0.25, *Signal*: [OH]
x10004428	6	0.184 - 0.186	Ar	0.67	1.51 - 2.40	1680 - 1856	Table 3, Series D, $CH_4/O_2/Ar$, dilution: 96%; *A*: 0.50, *Signal*: [OH]
x10004429	6	0.184 - 0.185	Ar	0.67	1.51 - 2.40	1680 - 1856	Table 3, Series D, $CH_4/O_2/Ar$, dilution: 96%; *A*: 0.75, *Signal*: [OH]

ID[.xml]	*Ni*	*σ*	Diluents	*φ*	*p* / atm	*T* / K	Comment
Dean and Kistiakowsky (1971)[52]; ignition criterion: time of reaching [CO2] = 1.6E14 molecule/cm^3							
x10004430	16	0.100	Ar	1.01	0.12 - 0.18	1740 - 2571	Fig 3, Mixture 1, $CH_4/CO/O_2$/Ar, dilution: 97.88%
x10004431	19	0.100	Ar	1.06	0.12 - 0.18	1748 - 2579	Fig 3, Mixture 2, $CH_4/CO/O_2$/Ar, dilution: 97.82%
Chaumeix et al. (2007)[53]; ignition criterion: time of reaching 0.50×the maximum value in [OHEX] profile							
x10004432	6	0.210	Ar	0.4	1.88	1278 - 1658	Fig 9, Mixture S4, $CH_4/H_2/O_2$/Ar, dilution: 99%
x10004433	10	0.274	Ar	0.7	1.78	1442 - 2017	Fig 9, Mixture S5, $CH_4/H_2/O_2$/Ar, dilution: 99%
x10004434	5	0.164	Ar	1.0	1.84	1557 - 1896	Fig 9, Mixture S6, $CH_4/H_2/O_2$/Ar, dilution: 99%
x10004435	7	0.183	Ar	0.4	1.82	1461 - 1716	Fig 9, Mixture S7, $CH_4/H_2/O_2$/Ar, dilution: 99%
x10004436	6	0.301	Ar	1.0	1.9	1513 - 1930	Fig 9, Mixture S8, $CH_4/H_2/O_2$/Ar, dilution: 99%
x10004437	10	0.250	Ar	0.4	11.15	1617 - 1847	Fig 11, Mixture S4, $CH_4/H_2/O_2$/Ar, dilution: 99%
Heufer and Olivier (2010)[54]; ignition criterion: time of maximum of the d*p*/d*t* profile							
x10004438	7	0.264	N_2	1	22.7	1022 - 1726	Fig 10, $CH_4/O_2/N_2$, dilution: 72.11%
Seery and Bowman (1967)[55]; ignition criterion: time of maximum of the d*p*/d*t* profile							
x10004439	18	0.140	Ar	0.5	1.7	1426 - 1876	Fig 5, CH_4/O_2/Ar, dilution: 76%
x10004440	8	0.155	N_2	0.5	1.7	1458 - 1677	Fig 5, $CH_4/O_2/N_2$, dilution: 76%
x10004441	12	0.141	Ar	1.0	2	1429 - 1725	Fig 6, CH_4/O_2/Ar, dilution: 72.7%
x10004442	13	0.189	Ar	0.5	3.7	1349 - 1597	Fig 8, CH_4/O_2/Ar, dilution: 76%
x10004443	6	0.144	Ar	0.5	6	1410 - 1505	Fig 8, CH_4/O_2/Ar, dilution: 76%
Hidaka et al. (1978)[56]; ignition criterion: root of the tangent line at the inflection point of the [O2] profile							
x10004444	14	0.154	Ar	1.00	0.51 - 0.76	1860 - 2465	Table 1, Series A, CH_4/O_2/Ar, dilution: 97%
x10004445	8	0.151	Ar	0.67	0.55 - 0.69	1813 - 2285	Table 1, Series B, CH_4/O_2/Ar, dilution: 96%
x10004446	9	0.100	Ar	2.00	0.52 - 0.76	1862 - 2458	Table 1, Series C, CH_4/O_2/Ar, dilution: 96%
Skinner and Ruehrwein (1959)[57]; ignition criterion: time of maximum of the d*p*/d*t* profile							
x10004447	13	0.246	Ar	3.00	5	1387 - 1587	Table IV, CH_4/O_2/Ar, dilution: 90%
x10004448	8	0.253	Ar	3.00	10	1366 - 1543	Table IV, CH_4/O_2/Ar, dilution: 90%
x10004449	9	0.262	Ar	3.00	5	1299 - 1570	Table IV, CH_4/O_2/Ar, dilution: 80%
x10004450	10	0.346	Ar	3.00	3	1351 - 1529	Table IV, CH_4/O_2/Ar, dilution: 66.67%
x10004451	13	0.303	Ar	3.00	6	1152 - 1328	Table IV, CH_4/O_2/Ar, dilution: 0%
x10004452	19	0.276	Ar	4.67	10	1433 - 1706	Table IV, CH_4/O_2/Ar, dilution: 90%
x10004453	13	0.264	Ar	4.67	5	1385 - 1597	Table IV, CH_4/O_2/Ar, dilution: 80%
x10004454	6	0.226	Ar	4.67	3	1462 - 1567	Table IV, CH_4/O_2/Ar, dilution: 66.67%
x10004455	8	0.220	Ar	8.00	5	1484 - 1736	Table IV, CH_4/O_2/Ar, dilution: 80%
Gurentsov et al. (2002)[58]; ignition criterion: time of maximum of *Signal* profile							
x10004456	8	0.423	He	1	2.50 - 5.10	1346 - 1855	Table 2, Mixture C(He), CH_4/O_2/He, dilution: 72.73%; *Signal*: [H_2O]
x10004457	12	0.403	Ar	1	3.90 - 7.60	1453 - 1882	Table 2, Mixture C(Ar), CH_4/O_2/Ar, dilution: 72.73%; *Signal*: [H_2O]
x10004458	11	0.270	N_2	1	4.90 - 8.70	1342 - 1840	Table 2, Mixture C(N_2), $CH_4/O_2/N_2$, dilution: 72.73%; *Signal*: [OHEX]

ID[.xml]	*Ni*	σ	Diluents	φ	*p* / atm	*T* / K	Comment
x10004459	13	0.294	N_2/H_2O	1	4.70 - 9.10	1301 - 1757	Table 2, Mixture Z-0%(N_2), $CH_4/O_2/N_2/H_2O$, dilution: 75%; *Signal*: [OHEX]
x10004460	7	0.231	Ar/H_2O	1	3.30 - 5.80	1386 - 1885	Table 2, Mixture Z-0%(Ar), $CH_4/O_2/Ar/H_2O$, dilution: 75%; *Signal*: [OHEX]
x10004461	10	0.321	N_2/H_2O	1	3.30 - 7.00	1066 - 1417	Table 2, Mixture Z-50%(N_2), $CH_4/CO/H_2/O_2/N_2/H_2O$, dilution: 80.77%; *Signal*: [OHEX]
Koroglu et al. (2016)[59]; ignition criterion: root of the tangent line at the first inflection point of the [CHEX] profile							
x10004462	5	0.190	Ar	1.0	0.83 - 0.89	1577 - 2144	Table 2, $CH_4/O_2/Ar$, dilution: 89.5%
x10004463	6	0.188	Ar/CO_2	1.0	0.68 - 0.82	1737 - 2022	Table 2, $CH_4/O_2/Ar/CO_2$, dilution: 89.5%
x10004464	6	0.185	Ar/CO_2	1.0	3.54 - 4.04	1660 - 1904	Table 2, $CH_4/O_2/Ar/CO_2$, dilution: 89.5%
x10004465	6	0.226	Ar/CO_2	0.5	0.70 - 0.83	1714 - 2012	Table 2, $CH_4/O_2/Ar/CO_2$, dilution: 91.25%
x10004466	6	0.189	Ar/CO_2	0.5	3.56 - 4.41	1610 - 1881	Table 2, $CH_4/O_2/Ar/CO_2$, dilution: 91.25%
x10004467	7	0.196	Ar/CO_2	2.0	0.61 - 0.72	1736 - 1962	Table 2, $CH_4/O_2/Ar/CO_2$, dilution: 86%
x10004468	8	0.194	Ar/CO_2	2.0	3.29 - 3.90	1632 - 1896	Table 2, $CH_4/O_2/Ar/CO_2$, dilution: 86%
x10004469	5	0.198	Ar/CO_2	1.0	0.53 - 0.70	1799 - 2114	Table 2, $CH_4/O_2/Ar/CO_2$, dilution: 89.5%
Zeng et al. (2015)[60] - with PRR; ignition criterion: root of the tangent line at the first inflection point of the [CHEX] profile							
x10004470	11	0.111	N_2	0.5	0.99	1491 - 1897	Fig 2b(a), $CH_4/O_2/N_2$, dilution: 75.06%
x10004471	10	0.167	N_2	0.5	2.96	1385 - 1752	Fig 2b(a), $CH_4/O_2/N_2$, dilution: 75.06%
x10004472	8	0.120	N_2	0.5	4.93	1407 - 1823	Fig 2b(a), $CH_4/O_2/N_2$, dilution: 75.06%
x10004473	7	0.151	N_2	0.5	9.87	1335 - 1663	Fig 2b(a), $CH_4/O_2/N_2$, dilution: 75.06%
x10004474	22	0.153	N_2	1.0	0.99	1481 - 1925	Fig 2b(b), $CH_4/O_2/N_2$, dilution: 71.5%
x10004475	9	0.109	N_2	1.0	2.96	1461 - 1821	Fig 2b(b), $CH_4/O_2/N_2$, dilution: 71.5%
x10004476	8	0.111	N_2	1.0	4.93	1444 - 1758	Fig 2b(b), $CH_4/O_2/N_2$, dilution: 71.5%
x10004477	8	0.118	N_2	1.0	9.87	1352 - 1718	Fig 2b(b), $CH_4/O_2/N_2$, dilution: 71.5%
x10004478	9	0.115	N_2	2.0	0.99	1556 - 1830	Fig 2b(c), $CH_4/O_2/N_2$, dilution: 65.31%
x10004479	7	0.126	N_2	2.0	2.96	1460 - 1729	Fig 2b(c), $CH_4/O_2/N_2$, dilution: 65.31%
x10004480	8	0.143	N_2	2.0	4.93	1413 - 1767	Fig 2b(c), $CH_4/O_2/N_2$, dilution: 65.31%
x10004481	7	0.114	N_2	2.0	9.87	1326 - 1661	Fig 2b(c), $CH_4/O_2/N_2$, dilution: 65.31%
x10004482	7	0.138	N_2	0.5	0.99	1512 - 1819	Fig 3b(a), $CH_4/O_2/N_2$, dilution: 80.05%
x10004483	6	0.123	N_2	0.5	9.87	1377 - 1659	Fig 3b(b), $CH_4/O_2/N_2$, dilution: 80.05%
x10004484	10	0.128	N_2	1.0	0.99	1588 - 2014	Fig 3b(c), $CH_4/O_2/N_2$, dilution: 77.2%
x10004485	6	0.146	N_2	1.0	9.87	1386 - 1624	Fig 3b(d), $CH_4/O_2/N_2$, dilution: 77.2%
x10004486	10	0.142	N_2	2.0	0.99	1580 - 1997	Fig 7a(d), $CH_4/O_2/N_2$, dilution: 72.22%
x10004487	9	0.144	N_2	0.5	0.99	1509 - 1967	Fig 3b(a), $CH_4/O_2/N_2$, dilution: 87.53%
x10004488	7	0.125	N_2	0.5	9.87	1415 - 1738	Fig 3b(b), $CH_4/O_2/N_2$, dilution: 87.53%

ID[.xml]	*Ni*	σ	Diluents	φ	*p* / atm	*T* / K	Comment
x10004489	15	0.130	N_2	1.0	0.99	1587 - 2027	Fig 3b(c), $CH_4/O_2/N_2$, dilution: 85.75%
x10004490	7	0.144	N_2	1.0	9.87	1423 - 1733	Fig 3b(d), $CH_4/O_2/N_2$, dilution: 85.75%
x10004491	11	0.120	N_2	2.0	0.99	1646 - 2088	Fig 7a(d), $CH_4/O_2/N_2$, dilution: 82.64%
x10004492	6	0.113	N_2/CO_2	0.5	0.99	1568 - 1917	Fig 4b(a), $CH_4/O_2/N_2/CO_2$, dilution: 80.05%
x10004493	7	0.148	N_2/CO_2	0.5	9.87	1348 - 1703	Fig 4b(b), $CH_4/O_2/N_2/CO_2$, dilution: 80.05%
x10004494	10	0.124	N_2/CO_2	1.0	0.99	1584 - 1918	Fig 4b(c), $CH_4/O_2/N_2/CO_2$, dilution: 77.2%
x10004495	6	0.126	N_2/CO_2	1.0	9.87	1438 - 1713	Fig 4b(d), $CH_4/O_2/N_2/CO_2$, dilution: 77.2%
x10004496	8	0.112	N_2/CO_2	2.0	0.99	1622 - 1988	Fig 7b(d), $CH_4/O_2/N_2/CO_2$, dilution: 72.22%
x10004497	9	0.115	N_2/CO_2	0.5	0.99	1668 - 2071	Fig 4b(a), $CH_4/O_2/N_2/CO_2$, dilution: 87.53%
x10004498	6	0.108	N_2/CO_2	0.5	9.87	1456 - 1726	Fig 4b(b), $CH_4/O_2/N_2/CO_2$, dilution: 87.53%
x10004499	10	0.133	N_2/CO_2	1.0	0.99	1687 - 1985	Fig 4b(c), $CH_4/O_2/N_2/CO_2$, dilution: 85.75%
x10004500	6	0.185	N_2/CO_2	1.0	9.87	1492 - 1798	Fig 4b(d), $CH_4/O_2/N_2/CO_2$, dilution: 85.75%
x10004501	6	0.103	N_2/CO_2	2.0	0.99	1702 - 1984	Fig 7b(d), $CH_4/O_2/N_2/CO_2$, dilution: 82.64%
Chang (1995)[61]; ignition criterion: time of reaching A×the maximum value in *Signal* profile							
x10004502	4	0.121	Ar	0.99	0.40 - 0.54	2164 - 2470	Methane Table 1, $CH_4/O_2/Ar$, dilution: 99.09%; *A*: 0.25, *Signal*: [CO_2]
x10004503	4	0.208	Ar	0.50	0.37 - 0.62	2140 - 2408	Methane Table 1, $CH_4/O_2/Ar$, dilution: 98.49%; *A*: 0.25, *Signal*: [CO_2]
x10004504	4	0.100	Ar	4.02	0.94 - 1.07	1951 - 2401	Methane Table 2, $CH_4/O_2/Ar$, dilution: 99.7%; *A*: 1.00, *Signal*: [CH_3]
x10004505	3	0.100	Ar	0.99	0.92 - 1.09	1942 - 2503	Methane Table 2, $CH_4/O_2/Ar$, dilution: 99.7%; *A*: 1.00, *Signal*: [CH_3]
x10004506	5	0.274	Ar	0.98	1.02 - 1.22	1989 - 2338	Methane Table 2, $CH_4/O_2/Ar$, dilution: 99.7%; *A*: 1.00, *Signal*: [CH_3]
x10004507	3	0.100	Ar	0.50	0.91 - 1.10	1933 - 2460	Methane Table 2, $CH_4/O_2/Ar$, dilution: 99.5%; *A*: 1.00, *Signal*: [CH_3]
x10004508	2	0.100	Ar	1.00	1.04 - 1.13	2056 - 2190	Methane Table 3, $CH_4/O_2/Ar$, dilution: 99.7%; *A*: 0.50, *Signal*: [OH]
x10004509	3	0.100	Ar	1.00	1.06 - 1.10	2145 - 2216	Methane Table 3, $CH_4/O_2/Ar$, dilution: 99.7%; *A*: 0.50, *Signal*: [OH]
x10004510	5	0.398	Ar	1.00	0.35 - 0.50	2169 - 2623	Methane Table 3, $CH_4/O_2/Ar$, dilution: 99.7%; *A*: 0.50, *Signal*: [OH]
Merhubi et al. (2016)[62] - with PRR; ignition criterion: time of maximum of the d*p*/d*t* profile							
x10004511	17	0.215	Ar	0.5	9.5 - 10.9	1451 - 1950	Fig 4, $CH_4/O_2/Ar$, dilution: 95%
x10004512	14	0.168	Ar	0.5	17.8 - 20.5	1428 - 1706	Fig 4, $CH_4/O_2/Ar$, dilution: 95%
x10004513	8	0.103	Ar	0.5	38.5 - 40.4	1412 - 1592	Fig 4, $CH_4/O_2/Ar$, dilution: 95%
x10004514	28	0.162	Ar	1.0	9.4 - 10.6	1471 - 1839	Fig 5, $CH_4/O_2/Ar$, dilution: 94%
x10004515	12	0.155	Ar	1.0	19 - 20.7	1418 - 1656	Fig 5, $CH_4/O_2/Ar$, dilution: 94%
x10004516	11	0.134	Ar	1.0	37.6 - 40.6	1456 - 1721	Fig 5, $CH_4/O_2/Ar$, dilution: 94%

ID[.xml]	*Ni*	*σ*	Diluents	*φ*	*p* / atm	*T* / K	Comment
x10004517	6	0.216	Ar	2.0	9.8 - 10.3	1565 - 1753	Fig 6, CH_4/O_2/Ar, dilution: 92%
x10004518	9	0.168	Ar	2.0	18.3 - 21.4	1501 - 1690	Fig 6, CH_4/O_2/Ar, dilution: 92%
x10004519	8	0.134	Ar	2.0	38.9 - 39.9	1445 - 1556	Fig 6, CH_4/O_2/Ar, dilution: 92%
Leschevich et al. (2016)[63]; ignition criterion: time of reaching 0.05×the maximum value in *Signal* profile							
x10004520	7	0.241	N_2	1.0	6.28 - 8.01	1123 - 1479	Table 2, $CH_4/O_2/N_2$, dilution: 71.49%; *Signal*: [CHEX]
x10004521	7	0.111	N_2	1.0	6.28 - 8.01	1123 - 1479	Table 2, $CH_4/O_2/N_2$, dilution: 71.49%; *Signal*: [OHEX]
x10004522	3	0.100	N_2	1.0	7.36 - 8.01	1312 - 1479	Table 2, $CH_4/O_2/N_2$, dilution: 71.49%; *Signal*: [C_2]
x10004523	7	0.185	N_2	1.0	6.28 - 8.01	1123 - 1479	Table 2, $CH_4/O_2/N_2$, dilution: 71.49%; *Signal*: pressure
x10004524	7	0.100	N_2	1.0	13.03 - 15.20	1130 - 1372	Table 2, $CH_4/O_2/N_2$, dilution: 71.49%; *Signal*: [CHEX]
x10004525	7	0.100	N_2	1.0	13.03 - 15.20	1130 - 1372	Table 2, $CH_4/O_2/N_2$, dilution: 71.49%; *Signal*: [OHEX]
x10004526	7	0.134	N_2	1.0	13.03 - 15.20	1130 - 1372	Table 2, $CH_4/O_2/N_2$, dilution: 71.49%; *Signal*: [C_2]
x10004527	7	0.100	N_2	1.0	13.03 - 15.20	1130 - 1372	Table 2, $CH_4/O_2/N_2$, dilution: 71.49%; *Signal*: pressure
x10004528	7	0.100	N_2	0.5	6.71 - 8.24	1168 - 1430	Table 2, $CH_4/O_2/N_2$, dilution: 75.06%; *Signal*: [CHEX]
x10004529	5	0.100	N_2	0.5	6.71 - 7.90	1168 - 1376	Table 2, $CH_4/O_2/N_2$, dilution: 75.06%; *Signal*: [OHEX]
x10004530	7	0.132	N_2	0.5	6.71 - 8.24	1168 - 1430	Table 2, $CH_4/O_2/N_2$, dilution: 75.06%; *Signal*: [C_2]
x10004531	7	0.108	N_2	0.5	6.71 - 8.24	1168 - 1430	Table 2, $CH_4/O_2/N_2$, dilution: 75.06%; *Signal*: pressure
x10004532	7	0.100	N_2	0.5	13.42 - 15.50	1149 - 1385	Table 2, $CH_4/O_2/N_2$, dilution: 75.06%; *Signal*: [CHEX]
x10004533	7	0.101	N_2	0.5	13.42 - 15.50	1149 - 1385	Table 2, $CH_4/O_2/N_2$, dilution: 75.06%; *Signal*: [OHEX]
x10004534	7	0.134	N_2	0.5	13.42 - 15.50	1149 - 1385	Table 2, $CH_4/O_2/N_2$, dilution: 75.06%; *Signal*: [C_2]
x10004535	7	0.216	N_2	0.5	13.42 - 15.50	1149 - 1385	Table 2, $CH_4/O_2/N_2$, dilution: 75.06%; *Signal*: pressure
x10004536	7	0.100	N_2	2.0	6.67 - 8.09	1166 - 1519	Table 2, $CH_4/O_2/N_2$, dilution: 65.29%; *Signal*: [CHEX]
x10004537	7	0.121	N_2	2.0	6.67 - 8.09	1166 - 1519	Table 2, $CH_4/O_2/N_2$, dilution: 65.29%; *Signal*: [OHEX]
x10004538	7	0.104	N_2	2.0	6.67 - 8.09	1166 - 1519	Table 2, $CH_4/O_2/N_2$, dilution: 65.29%; *Signal*: [C_2]
x10004539	7	0.105	N_2	2.0	6.67 - 8.09	1166 - 1519	Table 2, $CH_4/O_2/N_2$, dilution: 65.29%; *Signal*: pressure
x10004540	7	0.100	N_2	2.0	12.73 - 16.48	1120 - 1460	Table 2, $CH_4/O_2/N_2$, dilution: 65.29%; *Signal*: [CHEX]
x10004541	7	0.100	N_2	2.0	12.73 - 16.48	1120 - 1460	Table 2, $CH_4/O_2/N_2$, dilution: 65.29%; *Signal*: [OHEX]
x10004542	7	0.100	N_2	2.0	12.73 - 16.48	1120 - 1460	Table 2, $CH_4/O_2/N_2$, dilution: 65.29%; *Signal*: [C_2]
x10004543	7	0.100	N_2	2.0	12.73 - 16.48	1120 - 1460	Table 2, $CH_4/O_2/N_2$, dilution: 65.29%; *Signal*: pressure
Deng et al. (2016)[64] - with PRR; ignition criterion: root of the tangent line at the first inflection point of the [OHEX] profile							
x10004544	7	0.236	Ar	0.50	1 - 1.4	1600 - 2150	Suppl. Table S1, CH_4/O_2/Ar, dilution: 94.31%
x10004545	6	0.248	Ar	0.50	4.1 - 4.7	1430 - 1874	Suppl. Table S1, CH_4/O_2/Ar, dilution: 94.31%
x10004546	7	0.205	Ar	0.50	9.9 - 12.5	1374 - 1751	Suppl. Table S1, CH_4/O_2/Ar, dilution: 94.31%
x10004547	8	0.212	Ar	0.99	1.1 - 1.3	1567 - 2047	Suppl. Table S1, CH_4/O_2/Ar, dilution: 94.27%
x10004548	7	0.249	Ar	0.99	4.2 - 4.5	1502 - 1890	Suppl. Table S1, CH_4/O_2/Ar, dilution: 94.27%

ID[.xml]	*Ni*	σ	Diluents	φ	*p* / atm	*T* / K	Comment
x10004549	7	0.225	Ar	0.99	10.1 - 11	1410 - 1812	Suppl. Table S1, CH_4/O_2/Ar, dilution: 94.27%
x10004550	11	0.254	Ar	2.00	1.1 - 1.4	1563 - 2118	Suppl. Table S1, CH_4/O_2/Ar, dilution: 94.25%
x10004551	10	0.217	Ar	2.00	4 - 4.7	1462 - 2045	Suppl. Table S1, CH_4/O_2/Ar, dilution: 94.25%
x10004552	8	0.213	Ar	2.00	10.3 - 11.4	1421 - 1905	Suppl. Table S1, CH_4/O_2/Ar, dilution: 94.25%
Deng et al. (2016)[65] - with PRR; ignition criterion: root of the tangent line at the first inflection point of the [OHEX] profile							
x10004553	8	0.212	Ar	1	1.2	1567 - 2047	Suppl. Table S1, CH_4/O_2/Ar, dilution: 94.29%
x10004554	7	0.250	Ar	1	4	1502 - 1890	Suppl. Table S1, CH_4/O_2/Ar, dilution: 94.29%
x10004555	7	0.225	Ar	1	10	1410 - 1812	Suppl. Table S1, CH_4/O_2/Ar, dilution: 94.29%
Mathieu et al. (2013)[66]; ignition criterion: root of the tangent line at the first inflection point of the [OHEX] profile							
x10004556	12	0.137	Ar	0.5	1.50 - 2.00	1012 - 1921	Suppl. Table S5, $CH_4/CO/H_2/O_2$/Ar, dilution: 98.81%
x10004557	10	0.162	Ar	0.5	11.50 - 12.70	1148 - 1407	Suppl. Table S5, $CH_4/CO/H_2/O_2$/Ar, dilution: 98.81%
x10004558	6	0.224	Ar	0.5	29.90 - 32.30	1155 - 1321	Suppl. Table S5, $CH_4/CO/H_2/O_2$/Ar, dilution: 98.81%
x10004559	14	0.144	Ar/CO_2/H_2O	0.5	1.50 - 2.00	1051 - 2031	Suppl. Table S7, $CH_4/CO/H_2/O_2/Ar/CO_2/H_2O$, dilution: 98.96%
x10004560	11	0.134	Ar/CO_2/H_2O	0.5	11.10 - 13.50	1163 - 1449	Suppl. Table S7, $CH_4/CO/H_2/O_2/Ar/CO_2/H_2O$, dilution: 98.96%
x10004561	8	0.254	Ar/CO_2/H_2O	0.5	30.40 - 32.60	1185 - 1303	Suppl. Table S7, $CH_4/CO/H_2/O_2/Ar/CO_2/H_2O$, dilution: 98.96%
Pryor et al. (2017)[67]; ignition criterion: root of the tangent line at the first inflection point of the *Signal* profile, unless otherwise noted							
x10004562	4	0.200	Ar	1	0.6 - 0.8	1672 - 1770	Table 2, CH_4/O_2/Ar, dilution: 89.5%; ignition criterion: time of maximum of [OHEX] profile
x10004563	4	0.200	Ar	1	0.6 - 0.8	1672 - 1770	Table 2, CH_4/O_2/Ar, dilution: 89.5%; ignition criterion: time of reaching 0.50×the maximum value in [OHEX] profile
x10004564	4	0.200	Ar	1	0.6 - 0.8	1672 - 1770	Table 2, CH_4/O_2/Ar, dilution: 89.5%; *Signal*: [OHEX]
x10004565	4	0.200	Ar	1	0.6 - 0.8	1672 - 1770	Table 2, CH_4/O_2/Ar, dilution: 89.5%; *Signal*: [CH_4]
x10004566	4	0.200	Ar	1	0.6 - 0.8	1672 - 1770	Table 2, CH_4/O_2/Ar, dilution: 89.5%; *Signal*: pressure
x10004567	3	0.242	CO_2/Ar	1	0.8 - 0.9	1750 - 1920	Table 2, $CH_4/O_2/Ar/CO_2$, dilution: 89.5%; ignition criterion: time of maximum of [OHEX] profile
x10004568	3	0.267	CO_2/Ar	1	0.8 - 0.9	1750 - 1920	Table 2, $CH_4/O_2/Ar/CO_2$, dilution: 89.5%; ignition criterion: time of reaching 0.50×the maximum value in [OHEX] profile
x10004569	3	0.328	CO_2/Ar	1	0.8 - 0.9	1750 - 1920	Table 2, $CH_4/O_2/Ar/CO_2$, dilution: 89.5%; *Signal*: [OHEX]
x10004570	3	0.200	CO_2/Ar	1	0.8 - 0.9	1750 - 1920	Table 2, $CH_4/O_2/Ar/CO_2$, dilution: 89.5%; *Signal*: [CH_4]
x10004571	1	0.200	CO_2	1	0.6	2038 - 2038	Table 2, $CH_4/O_2/CO_2$, dilution: 89.5%; ignition criterion: time of maximum of [OHEX] profile
x10004572	1	0.200	CO_2	1	0.6	2038 - 2038	Table 2, $CH_4/O_2/CO_2$, dilution: 89.5%; ignition criterion: time of reaching 0.50×the maximum value in [OHEX] profile
x10004573	1	0.200	CO_2	1	0.6	2038 - 2038	Table 2, $CH_4/O_2/CO_2$, dilution: 89.5%; *Signal*: [OHEX]

ID[.xml]	*Ni*	*σ*	Diluents	*φ*	*p* / atm	*T* / K	Comment
x10004574	1	0.200	CO_2	1	0.6	2038 - 2038	Table 2, $CH_4/O_2/CO_2$, dilution: 89.5%; *Signal*: [CH_4]
x10004575	5	0.227	CO_2	1	0.9 - 1.1	1724 - 1951	Table 2, $CH_4/O_2/CO_2$, dilution: 85%; ignition criterion: time of maximum of [OHEX] profile
x10004576	5	0.223	CO_2	1	0.9 - 1.1	1724 - 1951	Table 2, $CH_4/O_2/CO_2$, dilution: 85%; ignition criterion: time of reaching 0.50×the maximum value in [OHEX] profile
x10004577	5	0.229	CO_2	1	0.9 - 1.1	1724 - 1951	Table 2, $CH_4/O_2/CO_2$, dilution: 85%; *Signal*: [OHEX]
x10004578	5	0.237	CO_2	1	0.9 - 1.1	1724 - 1951	Table 2, $CH_4/O_2/CO_2$, dilution: 85%; *Signal*: [CH_4]
Liu et al. (2018)[68]; ignition criterion: root of the tangent line at the first inflection point of the [OHEX] profile							
x10004579	15	0.235	N_2	0.5	0.7 - 0.8	1501 - 1847	Suppl. Table S1, Mixture 1,$CH_4/O_2/N_2$, dilution: 75%
x10004580	11	0.255	CO_2	0.5	0.7 - 1	1533 - 1776	Suppl. Table S1, Mixture 2,$CH_4/O_2/CO_2$, dilution: 75%
x10004581	10	0.251	CO_2	0.5	1.6 - 2	1503 - 1785	Suppl. Table S1, Mixture 2,$CH_4/O_2/CO_2$, dilution: 75%
Shao et al. (2018)[69]; ignition criterion: root of the tangent line at the first inflection point of the *Signal* profile							
x10004582	13	0.119	Ar	1.00	13.5 - 15.5	1420 - 1752	Appendix A, Mixture 1, $CH_4/O_2/Ar$, dilution: 94.12%, *Signal*: pressure
x10004583	13	0.119	Ar	1.00	13.5 - 15.5	1420 - 1752	Appendix A, Mixture 1, $CH_4/O_2/Ar$, dilution: 94.12%, *Signal*: [OHEX]
x10004584	8	0.107	Ar	1.00	51.1 - 58.3	1437 - 1663	Appendix A, Mixture 1, $CH_4/O_2/Ar$, dilution: 94.12%, *Signal*: pressure
x10004585	8	0.107	Ar	1.00	51.1 - 58.3	1437 - 1663	Appendix A, Mixture 1, $CH_4/O_2/Ar$, dilution: 94.12%, *Signal*: [OHEX]
x10004586	14	0.107	Ar	2.00	13.3 - 14.8	1464 - 1782	Appendix A, Mixture 2, $CH_4/O_2/Ar$, dilution: 92.30%, *Signal*: pressure
x10004587	14	0.107	Ar	2.00	13.3 - 14.8	1464 - 1782	Appendix A, Mixture 2, $CH_4/O_2/Ar$, dilution: 92.30%, *Signal*: [OHEX]
Mathieu et al. (2015)[40]; ignition criterion: root of the tangent line at the inflection point of p(t)							
x10004588	3	0.100	N_2	1.01	41.4 - 44.2	1308 - 1348	Appendix A, Table S1, Mixture 14, $CH_4/O_2/N_2$, dilution: 71.58%
x10004589	5	0.219	N_2	2.00	1.77 - 2.08	1544 - 1785	Appendix A, Table S1, Mixture 16, $CH_4/O_2/N_2$, dilution: 65.30%
x10004590	5	0.114	N_2	2.00	12.8 - 15.3	1338 - 1533	Appendix A, Table S1, Mixture 16, $CH_4/O_2/N_2$, dilution: 65.30%
x10004591	4	0.141	N_2	0.5	15.8 - 21.3	1263 - 1539	Appendix A, Table S1, Mixture 12, $CH_4/O_2/N_2$, dilution: 75.00%
x10004592	4	0.141	N_2	0.5	42.0 - 48.2	1238 - 1425	Appendix A, Table S1, Mixture 12, $CH_4/O_2/N_2$, dilution: 75.00%

Table B. Ignition delay time measurements of methane combustion in rapid compression machines

ID[.xml]	***Ni***	***σ***	**Dil-uents**	***φ***	***p* / atm**	***T* / K**	**Comment**
Yu (2012)[70]; ignition criterion: time of maximum of the d*p*/d*t* profile							
x40004001	57	0.100	Ar	0.7	10.82 - 22.38	980 - 994	Chapter IV, Figure 23, $CH_4/O_2/Ar$, dilution: 73.59%
x40004002	16	0.100	Ar/N_2	0.7	16.36 - 22.04	969 - 974	Chapter IV, Figure 1, $CH_4/O_2/Ar/N_2$, dilution: 73.59%
x40004003	16	0.100	Ar/N_2	0.7	16.09 - 21.58	945 - 950	Chapter IV, Figure 1, $CH_4/O_2/Ar/N_2$, dilution: 73.59%
x40004004	24	0.118	Ar/N_2	0.7	15.78 - 21.25	919 - 924	Chapter IV, Figure 1, $CH_4/O_2/Ar/N_2$, dilution: 73.59%
x40004005	5	0.125	Ar/N_2	0.7	20.82 - 20.85	894 - 897	Chapter IV, Figure 1, $CH_4/O_2/Ar/N_2$, dilution: 73.59%
x40004006	36	0.100	Ar	1.0	13.32 - 21.23	950 - 953	Chapter IV, Figure 23, $CH_4/O_2/Ar$, dilution: 71.50%
x40004007	15	0.100	Ar/N_2	1.0	15.69 - 21.01	932 - 934	Chapter IV, Figure 1, $CH_4/O_2/Ar/N_2$, dilution: 71.50%
x40004008	11	0.100	Ar/N_2	1.0	15.41 - 20.67	911 - 914	Chapter IV, Figure 1, $CH_4/O_2/Ar/N_2$, dilution: 71.58%
x40004009	15	0.110	Ar/N_2	1.0	20.16 - 20.26	887 - 891	Chapter IV, Figure 1, $CH_4/O_2/Ar/N_2$, dilution: 71.53%
Ramalingam et al. (2017)[71]; ignition criterion: time of maximum of the d*p*/d*t* profile							
x40004010	3	0.100	Ar/N_2	0.527	104.12 - 104.32	894 - 896	Table S1, Mixture 1, $CH_4/O_2/Ar/N_2$, dilution: 77.27%
x40004011	2	0.100	Ar/N_2	0.527	104.32	919	Table S1, Mixture 1, $CH_4/O_2/Ar/N_2$, dilution: 77.27%
x40004012	2	0.100	Ar/N_2	0.527	104.12 - 104.22	936 - 938	Table S1, Mixture 1, $CH_4/O_2/Ar/N_2$, dilution: 77.27%
x40004013	3	0.100	Ar/N_2	0.527	103.23 - 104.22	906 - 907	Table S1, Mixture 1, $CH_4/O_2/Ar/N_2$, dilution: 77.27%
x40004014	3	0.114	Ar/N_2	0.527	123.96 - 124.35	906 - 908	Table S2, Mixture 2, $CH_4/O_2/Ar/N_2$, dilution: 77.27%
x40004015	2	0.114	Ar/N_2	0.527	124.45 - 124.45	895 - 896	Table S2, Mixture 2, $CH_4/O_2/Ar/N_2$, dilution: 77.27%
x40004016	2	0.114	Ar/N_2	0.527	124.35 - 124.35	922	Table S2, Mixture 2, $CH_4/O_2/Ar/N_2$, dilution: 77.27%
x40004017	3	0.114	Ar/N_2	0.527	123.66 - 124.65	935 - 937	Table S2, Mixture 2, $CH_4/O_2/Ar/N_2$, dilution: 77.27%
x40004018	2	0.100	Ar/N_2	0.527	145.87 - 145.87	909	Table S3, Mixture 3, $CH_4/O_2/Ar/N_2$, dilution: 77.27%
x40004019	2	0.100	Ar/N_2	0.527	145.97 - 146.06	887	Table S3, Mixture 3, $CH_4/O_2/Ar/N_2$, dilution: 77.27%
x40004020	2	0.100	Ar/N_2	0.527	145.97 - 145.97	898 - 899	Table S3, Mixture 3, $CH_4/O_2/Ar/N_2$, dilution: 77.27%
x40004021	1	0.100	Ar/N_2	0.527	145.18	922	Table S3, Mixture 3, $CH_4/O_2/Ar/N_2$, dilution: 77.25%
x40004022	1	0.109	Ar/N_2	0.526	124.15	896	Table S4, Mixture 4, $CH_4/O_2/Ar/N_2$, dilution: 74.86%
x004023	2	0.109	Ar/N_2	0.526	123.66 - 124.06	886 - 887	Table S4, Mixture 4, $CH_4/O_2/Ar/N_2$, dilution: 74.86%
x40004024	1	0.109	Ar/N_2	0.526	124.85	933	Table S4, Mixture 4, $CH_4/O_2/Ar/N_2$, dilution: 74.86%
x40004025	2	0.109	Ar/N_2	0.526	121.39 - 124.25	915 - 918	Table S4, Mixture 4, $CH_4/O_2/Ar/N_2$, dilution: 74.86%
x40004026	2	0.109	Ar/N_2	0.526	124.55 - 126.42	902	Table S4, Mixture 4, $CH_4/O_2/Ar/N_2$, dilution: 74.86%
x40004027	1	0.109	Ar/N_2	0.526	123.56	928	Table S4, Mixture 4, $CH_4/O_2/Ar/N_2$, dilution: 74.86%
x40004028	2	0.100	Ar/N_2	0.997	156.23 - 156.33	913 - 914	Table S6, Mixture 6, $CH_4/O_2/Ar/N_2$, dilution: 80.06%
x40004029	2	0.100	Ar/N_2	0.997	155.93 - 155.93	900	Table S6, Mixture 6, $CH_4/O_2/Ar/N_2$, dilution: 80.06%
x40004030	2	0.100	Ar/N_2	0.997	156.23 - 156.62	926	Table S6, Mixture 6, $CH_4/O_2/Ar/N_2$, dilution: 80.06%

ID[.xml]	*Ni*	*σ*	Dil-uents	*φ*	*p* / atm	*T* / K	Comment
x40004031	2	0.100	Ar/N_2	0.997	156.43 - 156.43	893	Table S6, Mixture 6, $CH_4/O_2/Ar/N_2$, dilution: 80.06%
x40004032	2	0.100	Ar/N_2	0.417	124.45 - 124.45	936	Table S7, Mixture 7, $CH_4/O_2/Ar/N_2$, dilution: 75.68%
x40004033	2	0.100	Ar/N_2	0.417	125.14 - 125.24	920	Table S7, Mixture 7, $CH_4/O_2/Ar/N_2$, dilution: 75.68%
x40004034	2	0.100	Ar/N_2	0.417	124.85 - 124.94	905	Table S7, Mixture 7, $CH_4/O_2/Ar/N_2$, dilution: 75.69%
x40004035	2	0.100	Ar/N_2	0.417	125.44 - 125.73	888 - 889	Table S7, Mixture 7, $CH_4/O_2/Ar/N_2$, dilution: 75.69%
Burke et al. (2015)[35]; ignition criterion: time of maximum of the d*p*/d*t* profile							
x40004036	7	0.252	Ar	0.3	9.87 - 9.87	1087 - 1178	Fig 5(a), $CH_4/O_2/Ar$, dilution: 76.58%
x40004037	7	0.237	Ar	0.3	22.42 - 22.42	1057 - 1147	Fig 5(a), $CH_4/O_2/Ar$, dilution: 76.58%
x40004038	12	0.236	Ar	0.5	10.61 - 10.61	1036 - 1164	Fig 5(b), $CH_4/O_2/Ar$, dilution: 75.06%
x40004039	11	0.204	Ar	0.5	24.68 - 24.68	993 - 1112	Fig 5(b), $CH_4/O_2/Ar$, dilution: 75.06%
x40004040	11	0.209	Ar	1.0	10.71 - 10.71	987 - 1098	Fig 5(c), $CH_4/O_2/Ar$, dilution: 71.48%
x40004041	16	0.206	Ar	1.0	24.44 - 24.44	922 - 1085	Fig 5(c), $CH_4/O_2/Ar$, dilution: 71.48%
x40004042	8	0.245	Ar	2.0	10.55 - 10.55	970 - 1007	Fig 5(d), $CH_4/O_2/Ar$, dilution: 65.28%
x40004043	11	0.211	Ar	2.0	24.05 - 24.05	870 - 986	Fig 5(d), $CH_4/O_2/Ar$, dilution: 65.28%
Hashemi et al. (2016)[72]; ignition criterion: time of maximum of the d*p*/d*t* profile							
x40004044	23	0.100	Ar	0.5	14.66 - 15.08	1002 - 1200	Table S8, Mixture D, $CH_4/H_2/Ar$, dilution: 76.19%
x40004045	8	0.100	Ar	0.5	29.47 - 30.79	954 - 1174	Table S9, Mixture D, $CH_4/H_2/Ar$, dilution: 76.19%
x40004046	11	0.100	Ar/N_2	0.5	48.84 - 49.78	960 - 1110	Table S10, Mixture C, $CH_4/H_2/Ar/N_2$, dilution: 76.19%
x40004047	7	0.100	Ar/N_2	0.5	39.55 - 78.66	967 - 971	Table S12, Mixture C, $CH_4/H_2/Ar/N_2$, dilution: 76.19%
x40004048	7	0.156	Ar/N_2	0.5	29.49 - 78.90	1008 - 1011	Table S11, Mixture C, $CH_4/H_2/Ar/N_2$, dilution: 76.19%
x40004049	13	0.107	Ar	1.0	14.59 - 15.09	1002 - 1175	Table S5, Mixture B, $CH_4/H_2/Ar$, dilution: 72.73%
x40004050	13	0.100	Ar/N_2	1.0	39.19 - 39.78	908 - 1041	Table S6, Mixture A, $CH_4/H_2/Ar/N_2$, dilution: 72.73%
x40004051	7	0.100	Ar/N_2	1.0	24.62 - 49.45	993 - 996	Table S7, Mixture A, $CH_4/H_2/Ar/N_2$, dilution: 72.73%
Gersen et al. (2012)[73]; ignition criterion: time of maximum of the d*p*/d*t* profile							
x40004052	12	0.100	Ar/N_2	1.000	39.18 - 39.77	908 - 1041	Fig 2, $CH_4/O_2/Ar/N_2$, dilution: 72.7%
x40004053	7	0.100	Ar/N_2	1.003	39.34 - 39.75	941 - 1047	Fig 2, $CH_4/CO/H_2/O_2/Ar/N_2$, dilution: 69.0%
x40004054	8	0.131	Ar/N_2	1.000	39.28 - 39.87	939 - 1049	Fig 2, $CH_4/H_2/O_2/Ar/N_2$, dilution: 70.9%
x40004055	6	0.100	Ar/N_2	0.997	39.26 - 39.47	950 - 1050	Fig 2, $CH_4/CO/O_2/Ar/N_2$, dilution: 71.6%
x40004056	12	0.100	Ar/N_2	0.505	48.85 - 49.74	960 - 1110	Fig 3, $CH_4/O_2/Ar/N_2$, dilution: 76.2%
x40004057	9	0.100	Ar/N_2	0.500	48.95 - 49.84	960 - 1070	Fig 3, $CH_4/CO/H_2/O_2/Ar/N_2$, dilution: 74.1%
x40004058	8	0.100	Ar/N_2	0.495	49.05 - 49.74	961 - 1070	Fig 3, $CH_4/H_2/O_2/Ar/N_2$, dilution: 75.2%
x40004059	7	0.137	Ar/N_2	0.505	29.49 - 78.90	1008 - 1011	Fig 4, $CH_4/O_2/Ar/N_2$, dilution: 76.2%
x40004060	8	0.100	Ar/N_2	0.500	19.74 - 74.51	1007 - 1012	Fig 4, $CH_4/CO/H_2/O_2/Ar/N_2$, dilution: 74.1%
x40004061	7	0.100	Ar/N_2	0.495	19.89 - 69.08	1008 - 1011	Fig 4, $CH_4/H_2/O_2/Ar/N_2$, dilution: 75.2%
Liu et al. (2018)[74]; ignition criterion: time of maximum of the d*p*/d*t* profile							
x40004062	10	0.100 - 0.122	Ar	1.0	19.59 - 21.60	895 - 1082	Table S1, $CH_4/O_2/Ar$, dilution: 71.48%
x40004063	10	0.100 - 0.289	Ar	1.0	19.02 - 21.35	889 - 1056	Table S1, $CH_4/H_2/O_2/Ar$, dilution: 70.30%

ID[.xml]	*Ni*	σ	Dil-uents	φ	*p* / atm	*T* / K	Comment
x40004064	10	0.100 - 0.130	Ar	1.0	18.95 - 20.71	893 - 1078	Table S1, $CH_4/CO/O_2/Ar$, dilution: 70.30%
x40004065	7	0.100	Ar	1.5	19.63 - 20.50	872 - 1003	Table S1, $CH_4/O_2/Ar$, dilution: 68.24%
Donohoe et al. (2014)[17]; ignition criterion: time of maximum of the d*p*/d*t* profile							
x40004066	10	0.159	Ar/N_2	0.500	10.10 - 10.17	1016 - 1065	Appendix, Table Mix 2, $CH_4/H_2/O_2/Ar/N_2$, dilution: 90.00%
x40004067	11	0.236	Ar/N_2	0.499	9.95 - 10.03	969 - 1013	Appendix, Table Mix 2b, $CH_4/H_2/O_2/Ar/N_2$, dilution: 72.12%
x40004068	11	0.191	Ar/N_2	1.000	29.23 - 29.71	928 - 1052	Appendix, Table Mix 3, $CH_4/H_2/O_2/Ar/N_2$, dilution: 90.00%
x40004069	10	0.171	Ar/N_2	1.000	29.83 - 30.32	884 - 973	Appendix, Table Mix 3b, $CH_4/H_2/O_2/Ar/N_2$, dilution: 62.58%

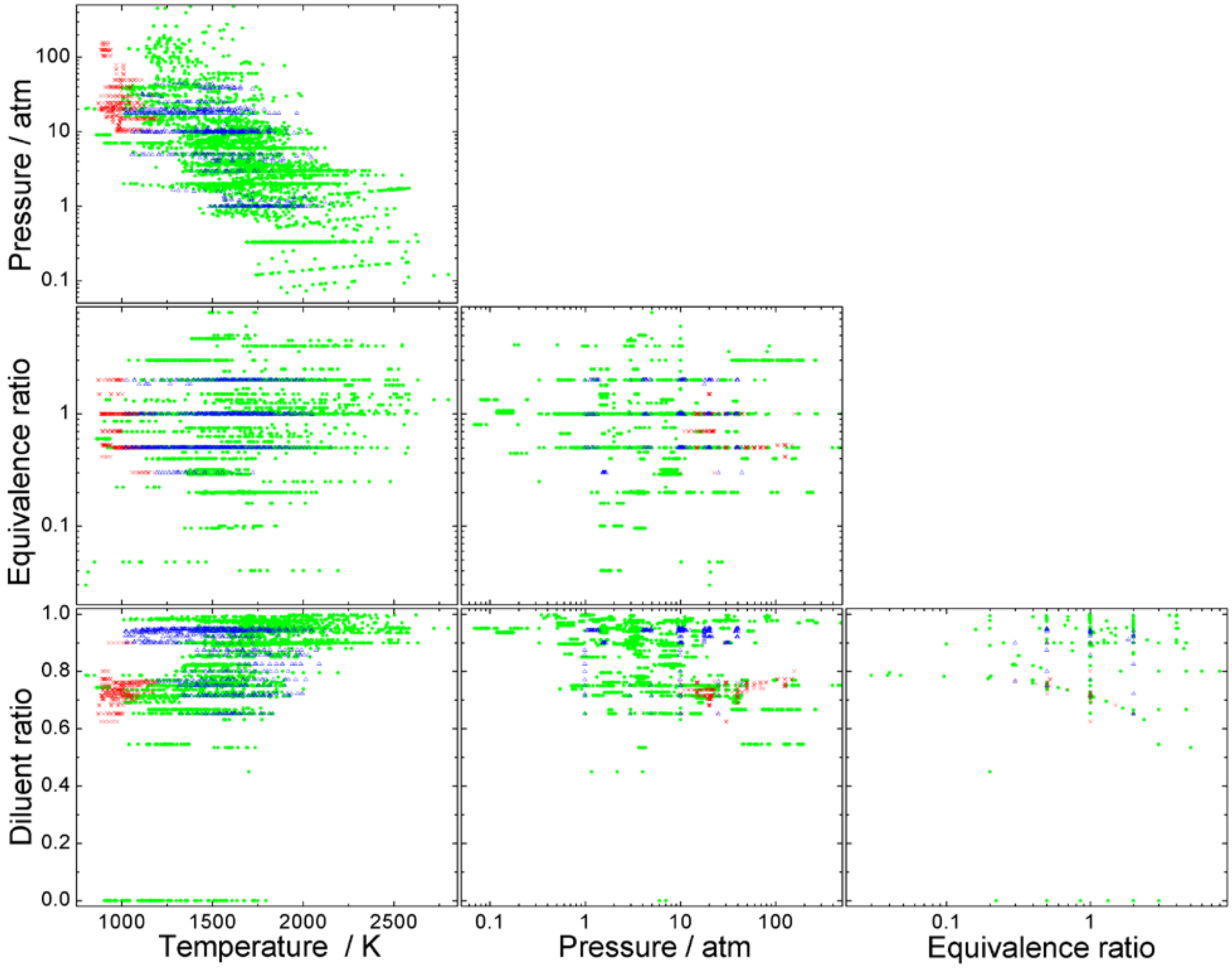

Fig. S1. Distribution of the conditions of the collected experimental data with respect to temperature, pressure, equivalence ratio and diluent ratio. Green circle: ST experimental point, blue triangle: ST experimental point with PRR, red cross: RCM experimental point.

Part 2: Calculation of the uncertainties of measured ignition delay times from the uncertainties of pressure and initial temperature

The uncertainty of IDT measurements can be estimated from the reported uncertainty of initial composition, pressure, and temperature. The following derivation is a continuation of the work of Zhang et al. [75]. Usually the uncertainty of the initial composition is small in the IDT measurements and does not influence significantly the measured ignition delay. Therefore, in the following, the uncertainty of ignition delays is deduced from the uncertainty of temperature and pressure. First, let us assume the following empirical relation between the IDT and the pressure and initial temperature:

$$\tau = Ap^{a}e^{\frac{b}{T}} \tag{S1}$$

Using the principle of Gaussian error propagation yields:

$$d\tau = \sqrt{\left(Ae^{\frac{b}{T}}ap^{a-1}\,dp\right)^2 + \left(\frac{Ae^{\frac{b}{T}}p^{a}b\,dT}{T^2}\right)^2} \tag{S2}$$

Further,

$$\frac{d\tau}{\tau} = \sqrt{\left(\frac{a}{p}dp\right)^2 + \left(\frac{b}{T^2}dT\right)^2} \tag{S3}$$

where dT and dP are the uncertainty of temperature and pressure, respectively.

Based on Equation S1, the following equation is valid for ln τ:

$$\ln\tau = a\ln p + b\frac{1}{T} + \ln A \tag{S4}$$

The three parameters *a*, *b*, *A* of equation S4 can be determined for each dataset based on a least-square-fitting. The residual error between the fitted and measured ignition delays for the *i*-th dataset having *n* data points can be calculated as follows:

$$M_i = \sum_{j=1}^{n}\left(\ln\tau_{ij} - \left(a_i\ln p_{ij} + b_i\frac{1}{T_{ij}} + \ln A_i\right)\right)^2 \tag{S5}$$

M_i has a minimum if the three partial derivatives of M_i are zero:

$$\frac{\partial M_i}{\partial a_i} = 0 \tag{S6}$$

$$\frac{\partial M_i}{\partial b_i} = 0 \tag{S7}$$

$$\frac{\partial M_i}{\partial (\ln A_i)} = 0 \tag{S8}$$

Calculating the partial derivatives of M_i , we obtain that

$$a_i \sum_{j=1}^{n} (\ln p_{ij})^2 + b_i \sum_{j=1}^{n} \frac{1}{T_{ij}} \ln p_{ij} + \ln A_i \sum_{j=1}^{n} \ln p_{ij} = \sum_{j=1}^{n} \ln p_{ij} \ln \tau_{ij} \tag{S9}$$

$$a_i \sum_{j=1}^{n} \frac{1}{T_{ij}} \ln p_{ij} + b_i \sum_{j=1}^{n} \frac{1}{T_{ij}^2} + \ln A_i \sum_{j=1}^{n} \frac{1}{T_{ij}} = \sum_{j=1}^{n} \frac{1}{T_{ij}} \ln \tau_{ij} \tag{S10}$$

$$a_i \sum_{j=1}^{n} \ln p_{ij} + b_i \sum_{j=1}^{n} \frac{1}{T_{ij}} + \ln A_i \sum_{j=1}^{n} 1 = \sum_{j=1}^{n} \ln \tau_{ij} \tag{S11}$$

Equations S9, S10, and S11, can be summarized in the following matrix equation:

$$\begin{pmatrix} \sum_{j=1}^{n} (\ln p_{ij})^2 & \sum_{j=1}^{n} \frac{1}{T_{ij}} \ln p_{ij} & \sum_{j=1}^{n} \ln p_{ij} \\ \sum_{j=1}^{n} \frac{1}{T_{ij}} \ln p_{ij} & \sum_{j=1}^{n} \frac{1}{T_{ij}^2} & \sum_{j=1}^{n} \frac{1}{T_{ij}} \\ \sum_{j=1}^{n} \ln p_{ij} & \sum_{j=1}^{n} \frac{1}{T_{ij}} & n \end{pmatrix} \begin{pmatrix} a_i \\ b_i \\ \ln A_i \end{pmatrix} = \begin{pmatrix} \sum_{j=1}^{n} \ln p_{ij} \ln \tau_{ij} \\ \sum_{j=1}^{n} \frac{1}{T_{ij}} \ln \tau_{ij} \\ \sum_{j=1}^{n} \ln \tau_{ij} \end{pmatrix} \tag{S12}$$

Solution of matrix equation S12 provides the estimated values of the three parameters. As a result, we may get the uncertainty of ignition delay of each data points using equations S2 or S3. When either the pressure or the temperature values within one dataset are identical, then the other, changing variable (T or p) is used for the calculation of the uncertainty of the IDT only.

Part 3: Comparison of OHEX sub-mechanisms

In Table A, 1251 experimental ignition delays of 141 datasets were determined based on measured excited OH radical (OHEX) concentration profiles. In the simulations, we always calculated the ignition delays in an identical way to the experimental definition. However, only four of the investigated mechanisms (FFCM1-2016, Aramco-II-2016, Konnov-2017, and Glarborg-2018) included OHEX sub-mechanisms. Using the ground-state OH concentration profile may yield different IDT values, therefore OHEX chemistry had to be added to the other mechanisms.

Table C. Reactions and parameters of the four OHEX sub-mechanisms, units are cm^3, mole, s, cal, K.

No	Reactions	FFCM1-2016			Aramco-II-2016			Konnov-2017			Glarborg-2018		
		A	*n*	E_a	*A*	*n*	E_a	*A*	*n*	E_a	*A*	*n*	E_a
1a	OHEX = OH				1.45E+06	0	0	1.40E+06	0	0	1.00E+06	0	0
1b	OHEX => OH	1.45E+06	0	0									
2	OHEX + H = OH + H				1.31E+12	0.5	-167	1.50E+12	0.5	0	1.50E+12	0.5	0
3	OHEX + H_2 = OH + H_2	2.95E+12	0.5	-444	2.95E+12	0.5	-444	3.54E+11	0.5	-444	3.00E+12	0.5	-444
4	OHEX + H_2 = H_2O + H							2.60E+12	0.5	-444			
5	OHEX + O = OH + O							1.50E+12	0.5	0	1.50E+12	0.5	0
6	OHEX + O_2 = OH + O_2	2.10E+12	0.5	-482	2.10E+12	0.5	-478	8.40E+11	0.5	-482	2.10E+12	0.5	-482
7	OHEX + O_2 = O_3 + H							2.52E+11	0.5	-482			
8	OHEX + O_2 = HO_2 + O							1.01E+12	0.5	-482			
9	OHEX + OH = OH + OH				6.01E+12	0.5	-764	1.50E+12	0.5	0	1.50E+12	0.5	0
10	OHEX + H_2O = OH + H_2O	5.92E+12	0.5	-861	5.93E+12	0.5	-860	2.96E+12	0.5	-861	5.90E+12	0.5	-861
11	OHEX + H_2O = H_2O_2 + H							2.96E+12	0.5	-861			
12	OHEX + CO = OH + CO	3.23E+12	0.5	-787	3.23E+12	0.5	-787						
13	OHEX + CO_2 = OH + CO_2	2.75E+12	0.5	-968	2.75E+12	0.5	-968						
14	OHEX + CH_4 = OH + CH_4	3.36E+12	0.5	-635	3.36E+12	0.5	-635						
15	OHEX + N_2 = OH + N_2	1.08E+11	0.5	-1238	1.08E+11	0.5	-1242	1.08E+11	0.5	-1238			
16	OHEX + Ar = OH + Ar	1.25E+10	0.5	0	1.69E+12	0	4135	2.17E+10	0.5	2060			
17	OHEX + He = OH + He	1.95E+09	0.5	0									
18	2OH + H => OHEX + H_2O	1.45E+15	0	0									
19	N_2O + H = N_2 + OHEX										1.60E+14	0	50300
20	CH + O_2 = CO + OHEX	1.80E+11	0	0	4.04E+13	0	0	3.24E+14	-0.4	4150			
21a	H + O + M = OHEX + M				1.50E+13	0	5975	1.50E+13	0	5970	3.10E+14	0	10000
					(H_2 / 1.00 / H_2O / 6.50 / O_2 / 0.40 / N_2 / 0.40 / Ar / 0.35 /)			(Ar / 0.35 / H_2O / 6.5 / O_2 / 0.4 / N_2 / 0.4 /)			(H_2 / 1.00 / H_2O / 6.50 / O_2 / 0.40 / N_2 / 0.40 / Ar / 0.35 /)		
21b	H + O + M => OHEX + M	5.45E+12	0	0									
		(H_2 / 1.00 / H_2O / 6.50 / O_2 / 0.40 / N_2 / 0.40 / Ar / 0.35 /)											
22	OHEX + M = OH + M										2.20E+10	0.5	2060
											(H_2 / 1.00 / H_2O / 6.50 / O_2 / 0.40 / N_2 / 0.40 / Ar / 0.35 /)		

Reaction steps with their Arrhenius parameters of the four OHEX sub-mechanisms are compared in Table C. A blank cell means that the step is missing in the sub-mechanism. Coupling each of these sub-mechanisms to the other nine mechanisms yields 36 mechanisms to be investigated. Error function values *E* were calculated considering the OHEX experiments only. The calculated *E* values are given in Table D, and a visible comparison is shown in Fig. S2.

Table D. The error function values of coupled mechanisms

Main Mech / OHEX Sub-mech	GRI30-1999	Leeds-2001	USC-II-2007	Konnov-2009	GDFkin-2012	SanDiego-2014	CRECK-2014	Caltech-2015	SanDiego-2016	Average
FFCM1-2016	4.338	5.352	3.956	11.240	6.261	4.774	21.797	3.000	4.985	7.300
Aramco_II-2016	4.235	4.923	3.736	11.326	6.270	3.373	20.291	2.862	3.523	6.727
Konnov-2017	4.234	4.467	3.627	11.351	6.206	3.306	21.211	2.779	3.447	6.736
Glarborg-2018	4.370	4.700	4.112	10.531	6.445	5.236	17.189	3.187	5.401	6.797

For mechanisms USC-II-2007, SanDiego-2014, Caltech-2015 and SanDiego-2016, the calculated error function values using the OHEX sub-mechanisms of Aramco-II-2016 and Konnov-2017 are lower than using those of the other two sub-mechanisms. For CRECK-2014, the OHEX sub-mechanism of Glarborg-2018 has the best performance. For the other 5 mechanisms, there is no significant difference among the calculated *E* error values for the four OHEX sub-mechanisms. The lowest error values are highlighted.

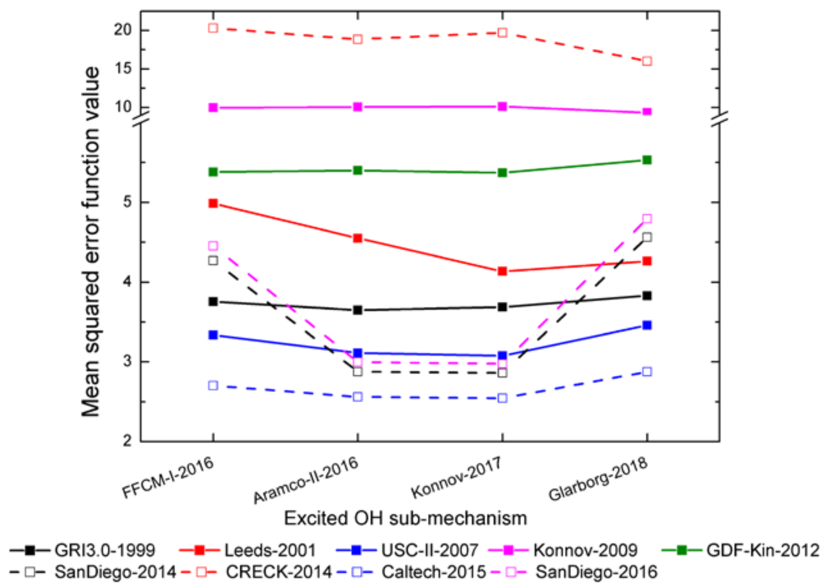

Fig. S2. Error function values *E* of nine mechanisms related to the OHEX IDT measurements, if they are coupled with the OHEX chemistry mechanism of four mechanisms (FFCM1-2016, Aramco-II-2016, Konnov-2017, and Glarborg-2018).

Except for coupling with SanDiego-2014 and SanDiego-2016, the performance of the four OHEX sub-mechanisms are not very different from each other. Based on the average error function values of the coupled mechanisms in Table D, we decided to use the one from Aramco-II-2016 as an extension to the nine mechanisms without OHEX sub-mechanism for the simulation.

Part 4: Comparison of the performance of the mechanisms at low temperatures and at IDTs of various orders of magnitude

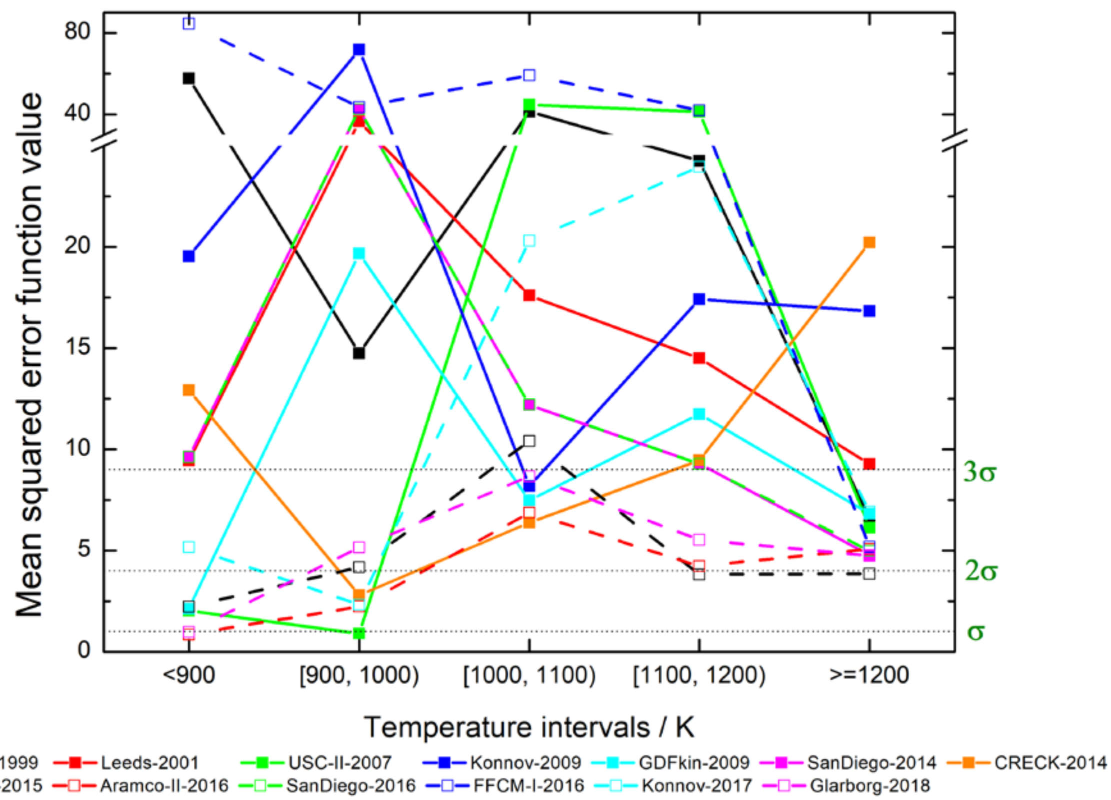

Fig. S3. Error function values *E* of the mechanisms at low temperatures

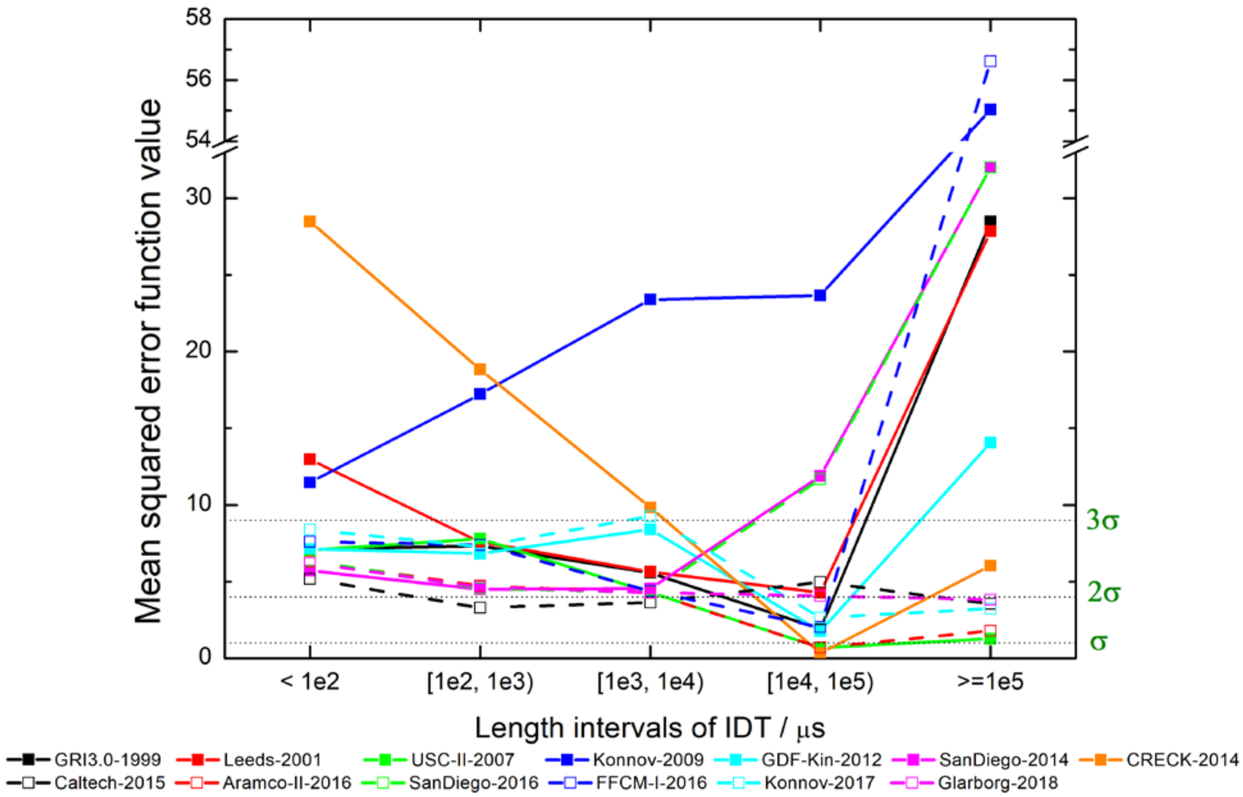

Fig. S4. Dependence of error function values *E* of the mechanisms on the lengths of the experimental IDT.

Fig. S3 shows that the reproducing ability of the mechanisms does not decrease monotonically with decreasing temperature except for FFCM1-2016, GRI3.0-1999 and Konnov-2009, and. Fig. S4 presents that almost half of the mechanisms can reproduce even long ignition delays with low error.

Part 5: Comparison of the mean signed deviations

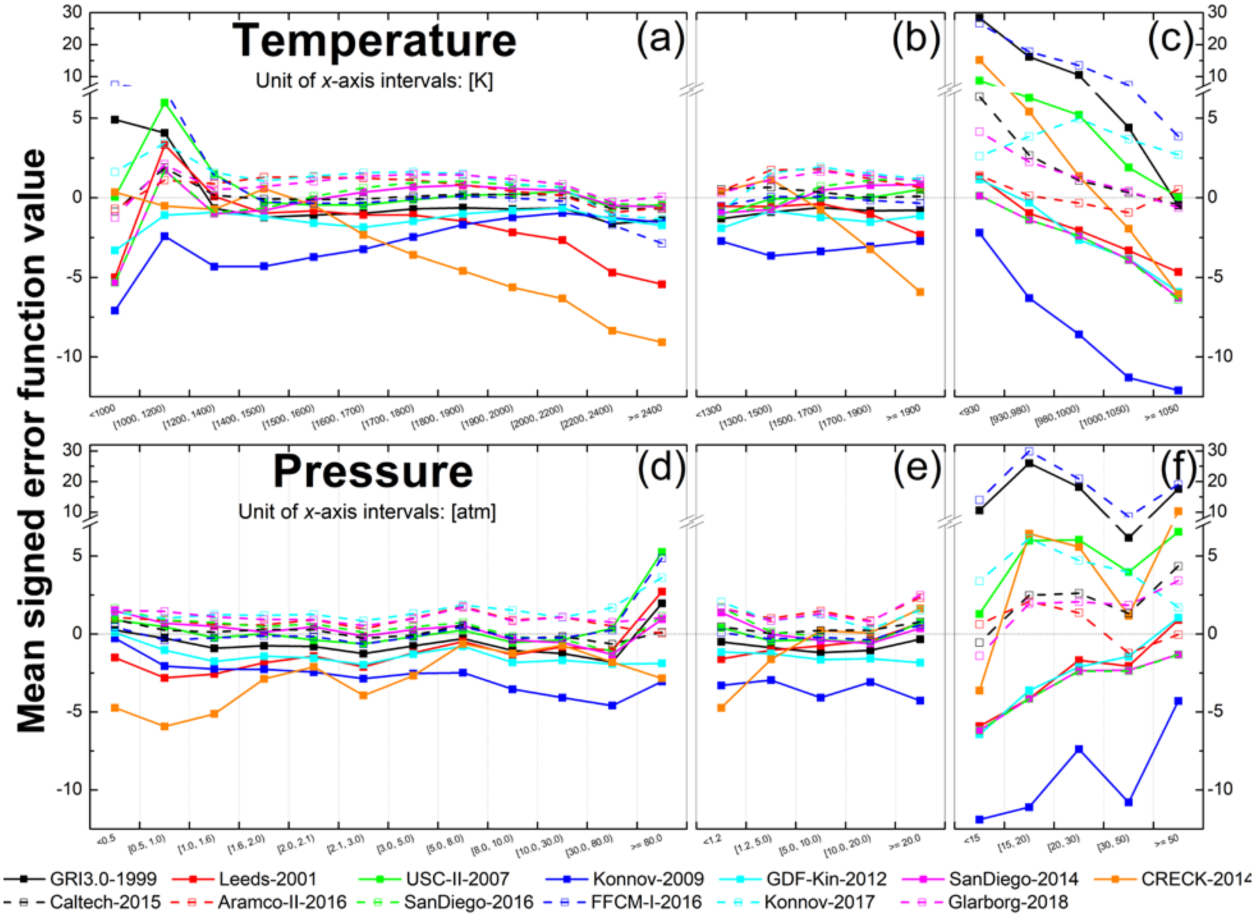

Fig. S5. Mean signed deviations of the mechanisms for ranges of temperature and pressure. Panels (a) and (d) are for shock tubes without PRR, (b) and (e) are for shock tubes with PRR, (c) and (f) are for RCM experiments.

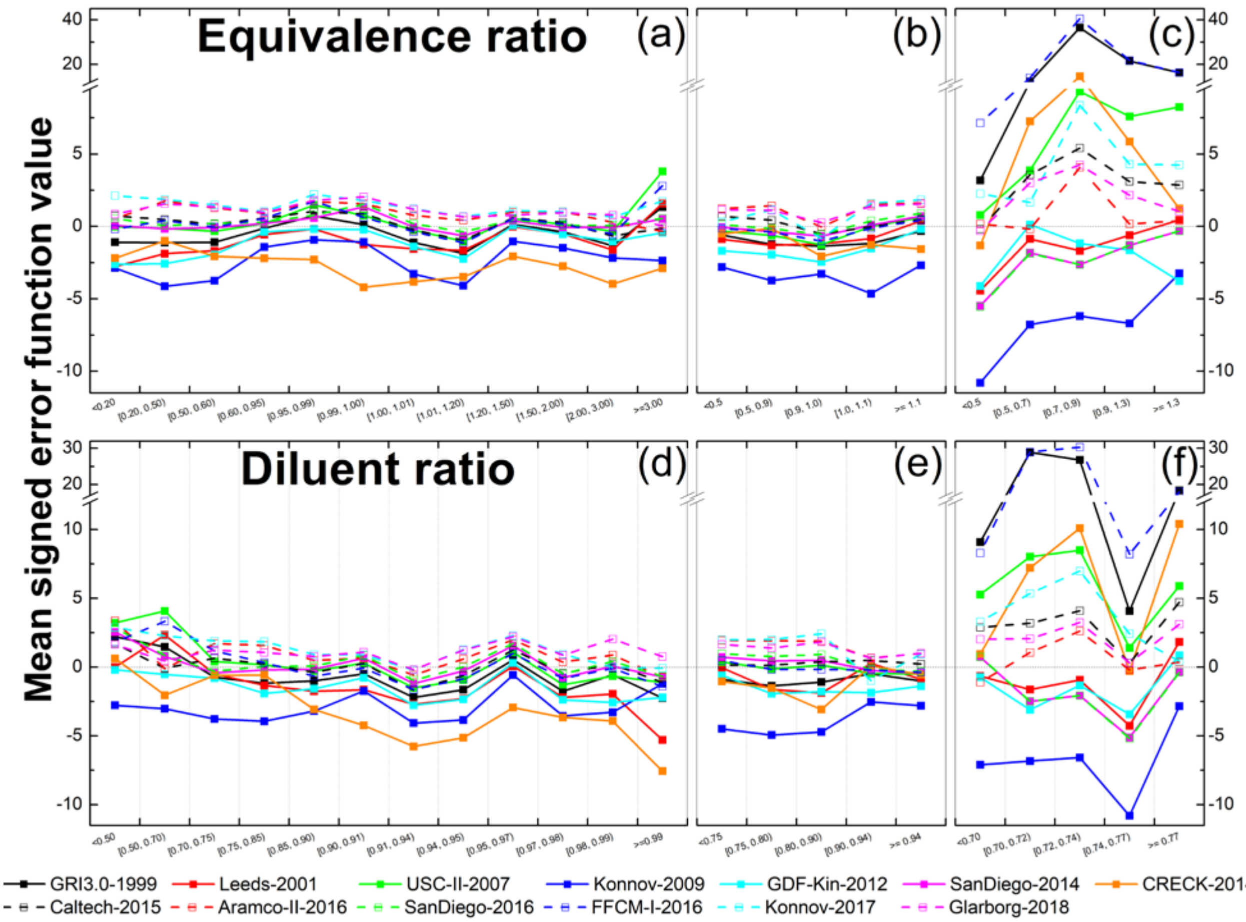

Fig. S6. Mean signed deviations of the mechanisms for ranges of equivalence ratio and diluent ratio. Panels (a) and (d) are for shock tubes without PRR, (b) and (e) are for shock tubes with PRR, (c) and (f) are for RCM experiments.

Part 6: Highly sensitive reactions of four selected mechanisms

Table E: The Arrhenius parameters of reaction R2: CH3 + O2 = CH2O + OH as used in the various mechanisms and their origin. The units of the Arrhenius parameters are expressed in cm, mol, s.

No.	Mech ID	A	n	Ea	Origin
1	GRI3.0-1999	2.31E+12	0	20315	Optimized value. The *A* factor of the Arrhenius expression of Yu et al. [51] was multiplied by 1.25
2	Leeds-2001	3.31E+11	0	8944	Taken from Baulch et al. [76 77]. The rate parameters of Baulch et al. were based on the measurements of Saito et al [78] and the unpublished data of Frank et al.
3	USC-II-2007	3.60E+10	0	8940	Taken from the GRI-1.2 mechanism, which used the rate parameters from the Thesis of W. Fraatz (Universität Göttingen, 1992) without any modification.
4	Konnov-2009	3.40E+11	0	8940	Taken from an earlier Konnov mechanism [79], which was based on the Baulch et al.recommendation [76 77]
5	GDF-Kin-2012	4.38E+11	0	14656	fitted value
6	SanDiego-2014	3.30E+11	0	8941	see the comment at the Leeds-2001 mech
7	CRECK-2014	this reaction is not included			
8	Caltech-2015	5.87E+11	0	13841	from Petersen et al. [80] , who derived the expression from the studies of Srinivasan et al. [81] and Herbon et al. [82]
9	Aramco-II-2016	2.64E+00	3.28	8105	based on a personal communication with Steven Klippenstein, as commented in Aramco v1.3 [83].
10	SanDiego-2016	3.30E+11	0	8941	see the comment at the Leeds-2001 mech
11	FFCM-I-2016	9.98E+01	2.86	9768	optimized values, starting from the Arrhenius expression of Herbon et al. [82]
12	Konnov-2017	6.39E+11	0	13515	from Christensen et al [84], who took it from Srinivasen et al. [85]
13	Glarborg-2018	1.90E+11	0	9842	from Srinivasan et al. [81]

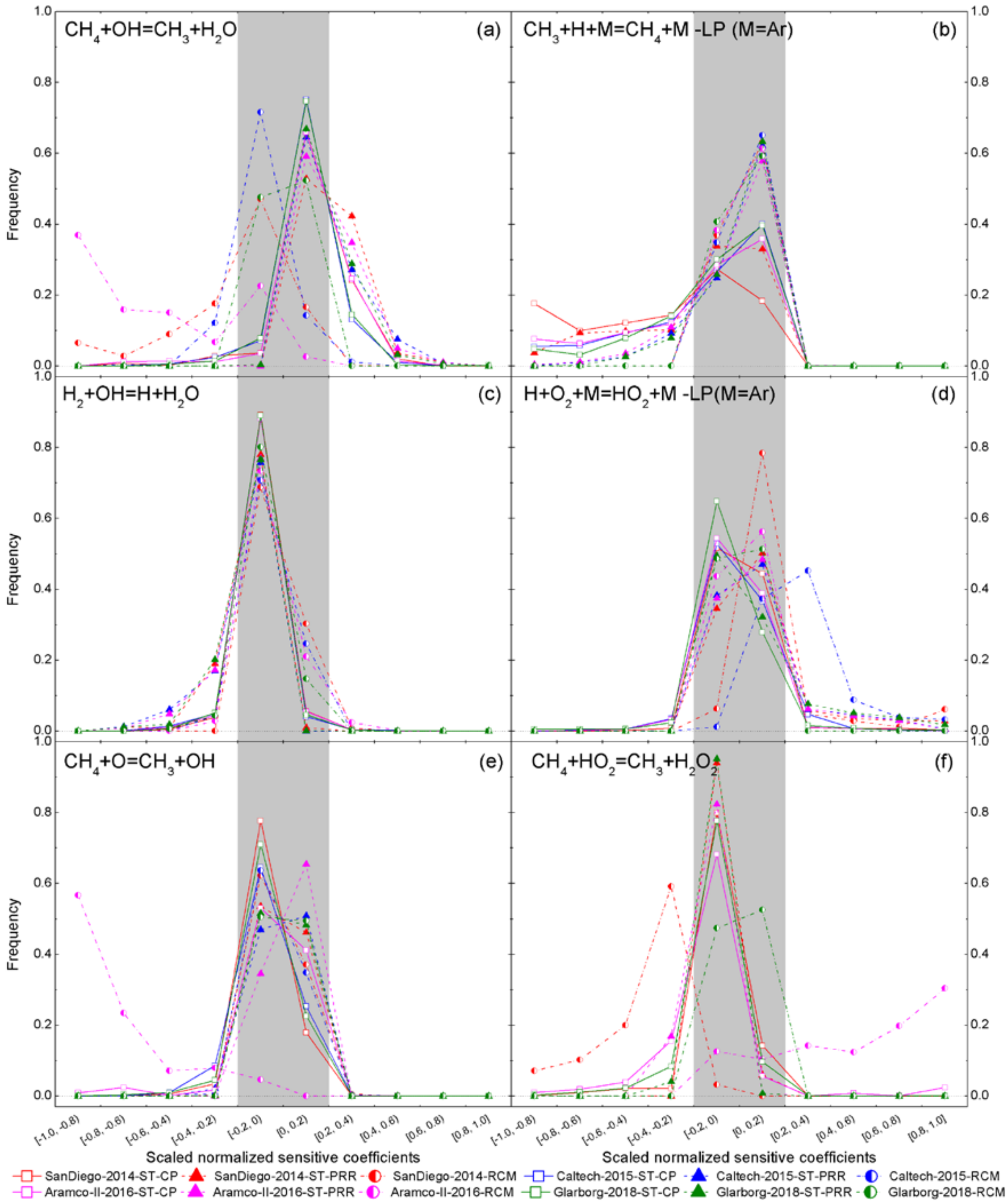

Fig. S7. Frequencies of the sensitivity coefficients of R7: $CH_4 + OH = CH_3 + H_2O$ (a), R8: $CH_3 + H + M = CH_4 + M$ (LP) (b), R9: $OH + H_2 = H + H_2O$ (c), R10: $H + O_2 + M = HO_2 + M$ (LP) (d), R11: $CH_4 + O = CH_3 + OH$ (e), R12: $CH_4 + HO_2 = CH_3 + H_2O_2$ (f) , for the three types of measurements (ST-CP, ST-PRR, RCM). The sensitivity analyses were based on mechanisms SanDiego-2014, Caltech-2015, Aramco-II-2016 and Glarborg-2018. The experimental conditions are given for each type of measurement. The grey shaded rectangle indicates the interval of low sensitivity.

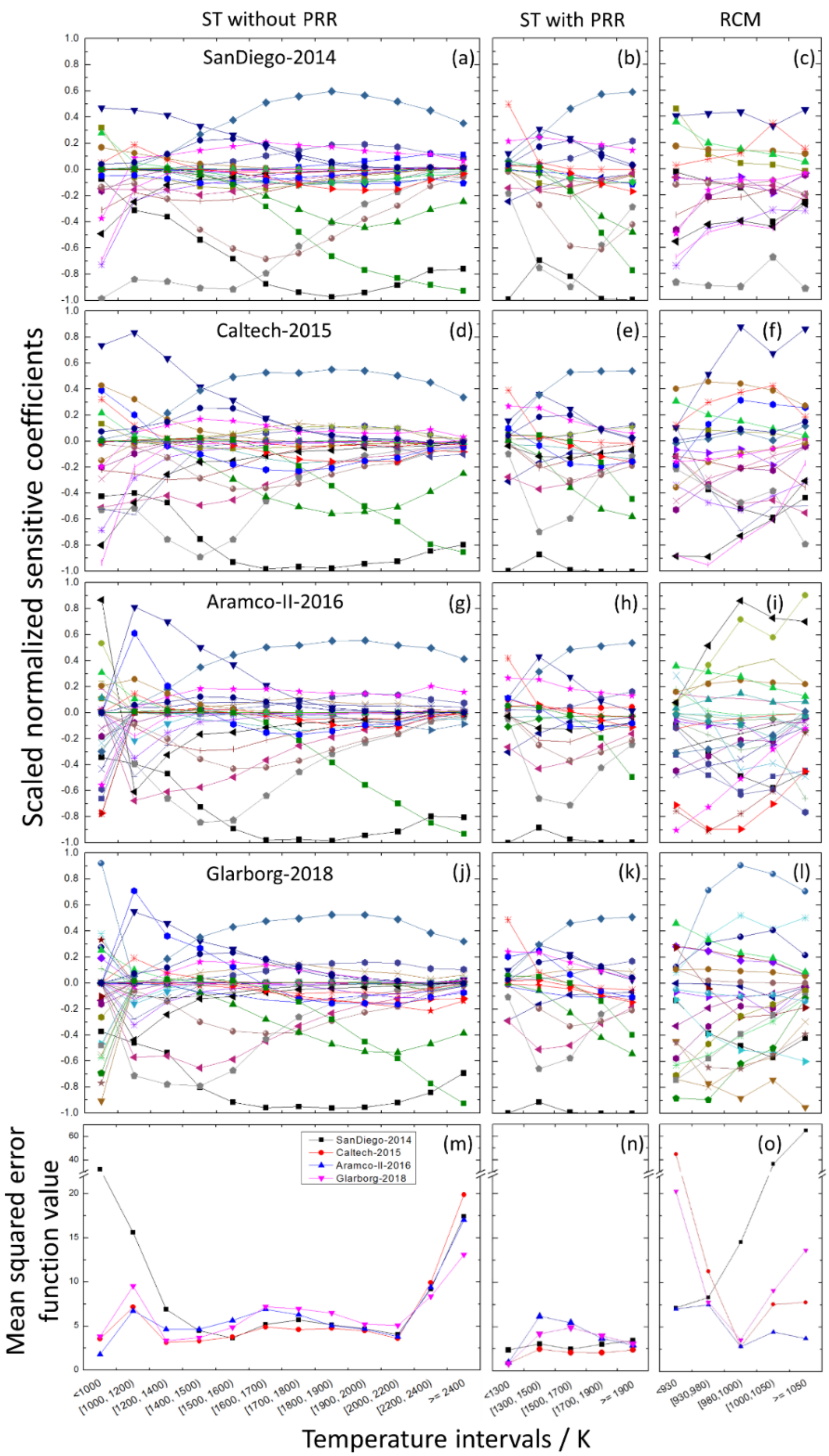

Fig. S8. Performance of the four best mechanisms and the scaled normalized sensitive coefficients in various intervals of temperature with respect to IDT.

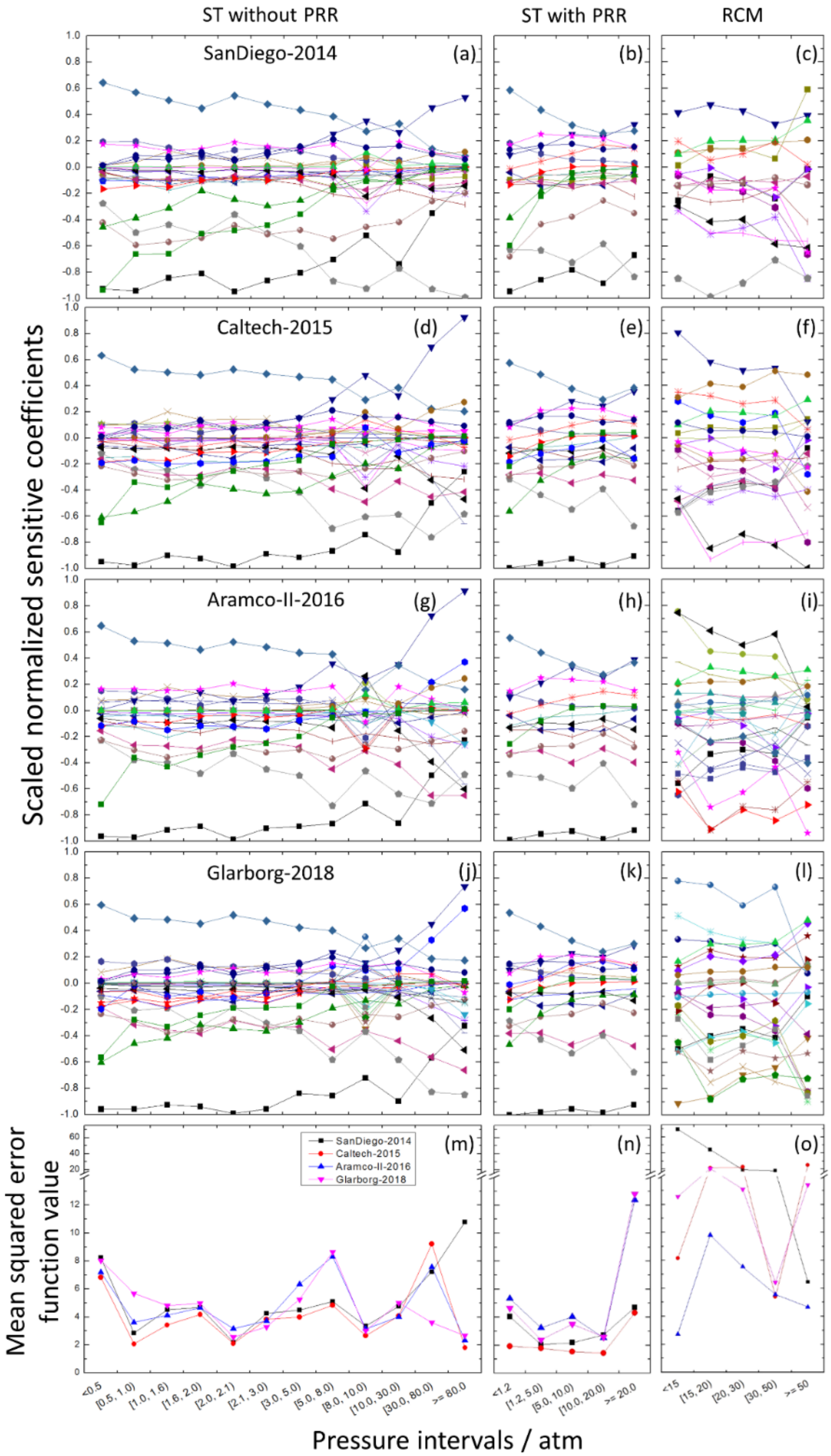

Fig. S9. Performance of the four best mechanisms and the scaled normalized sensitive coefficients in various intervals of pressure with respect to IDT.

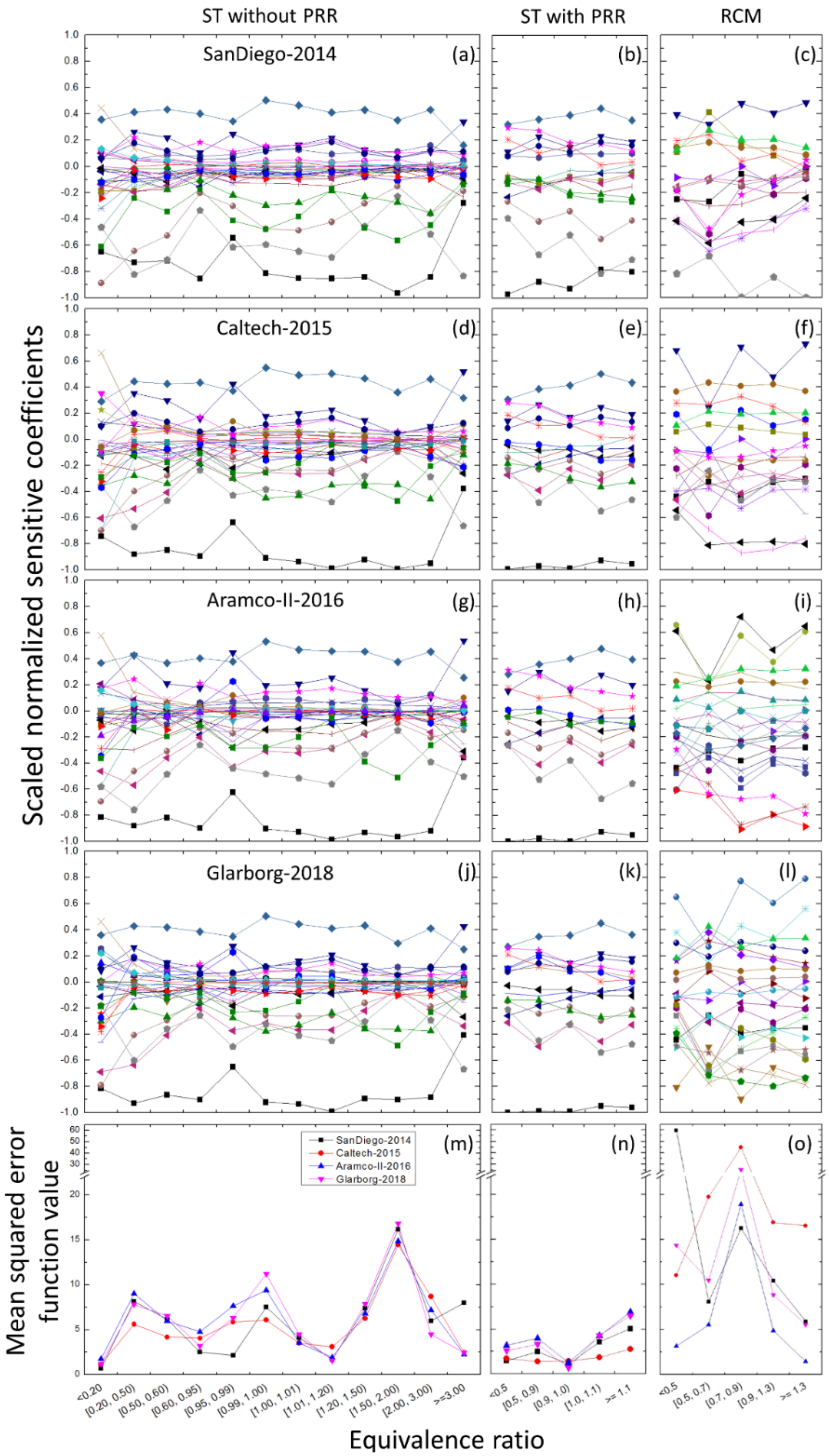

Fig S10. Performance of the four best mechanisms and the scaled normalized sensitive coefficients in various intervals of equivalence ratio with respect to IDT.

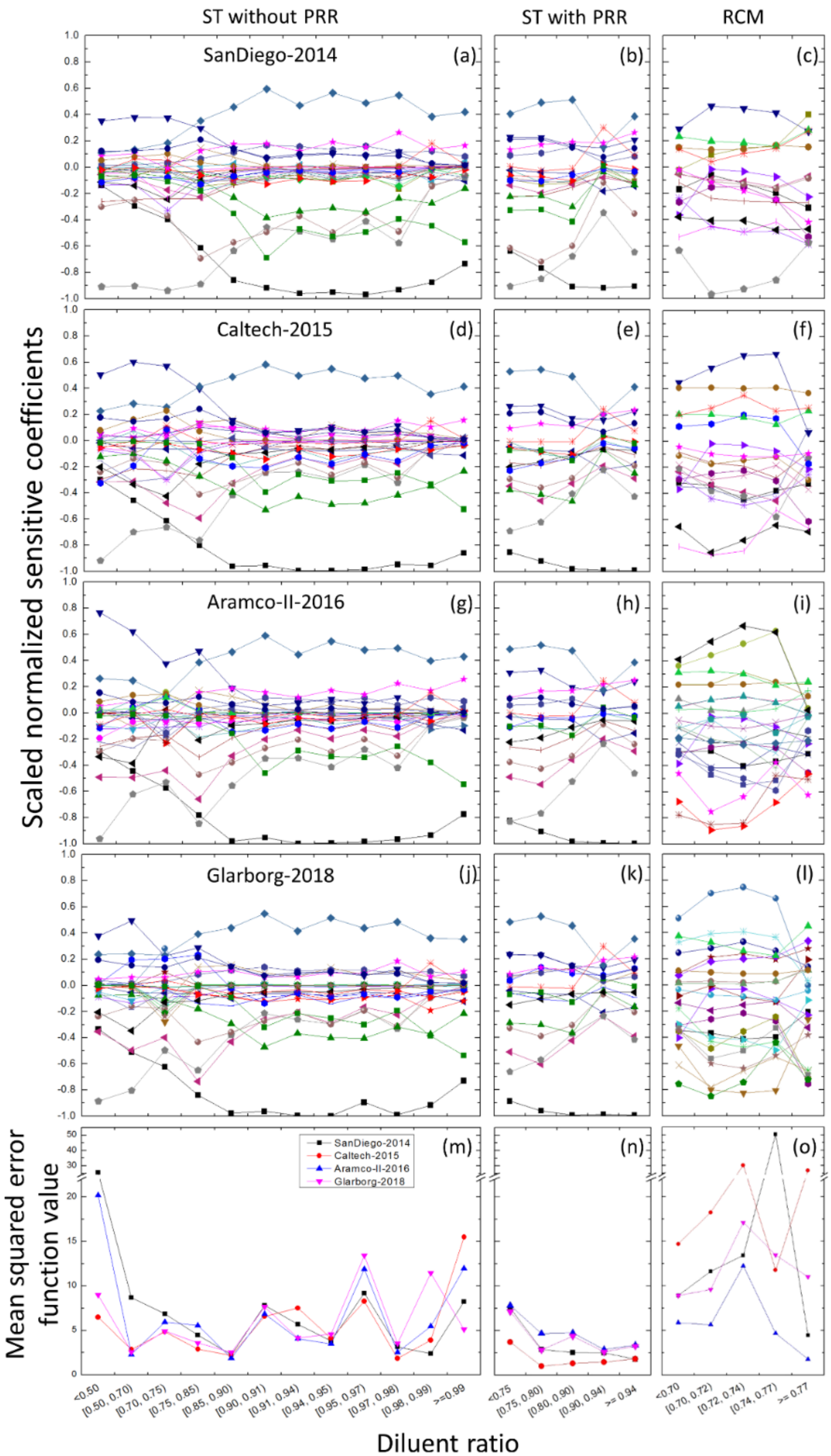

Fig. S11. Performance of the four best mechanisms and the scaled normalized sensitive coefficients in various intervals of diluent ratio with respect to IDT.

Common legend to Figs. S10 – S13

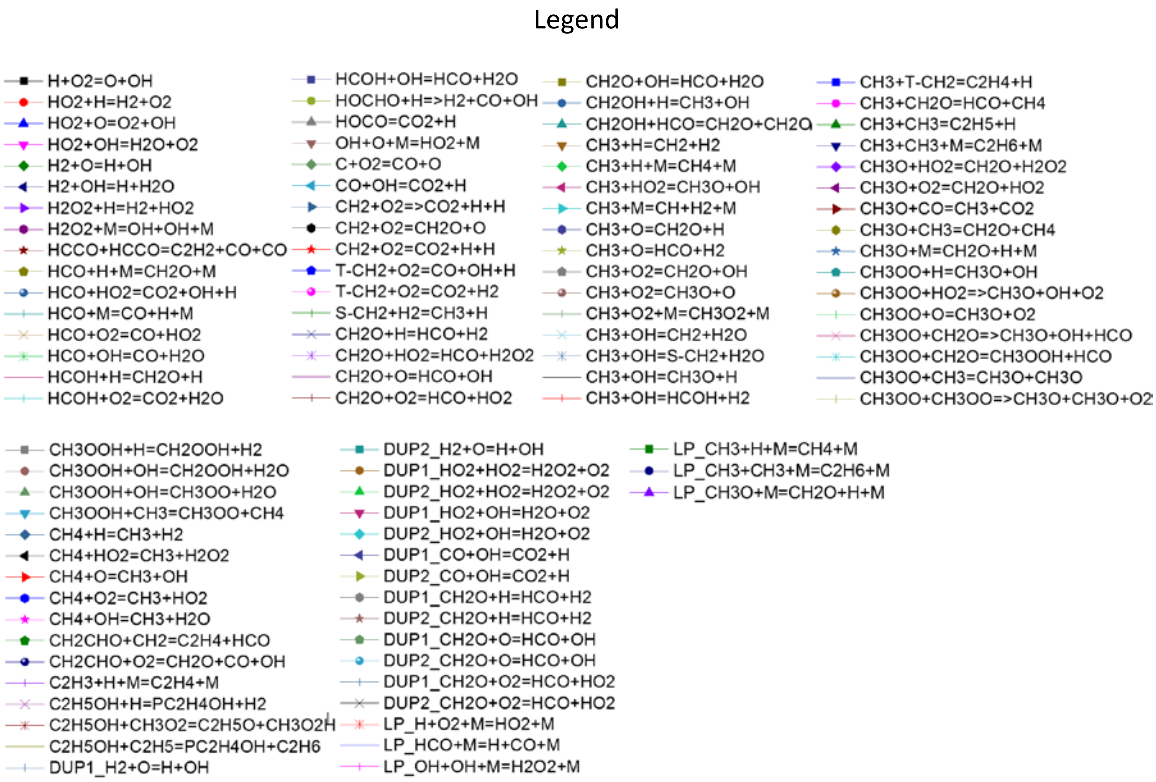

References

(1) ReSpecTh Information System, (http://respecth.hu/).

(2) Seery, D. J.; Bowman, C. T. An Experimental and Analytical Study of Methane Oxidation behind Shock Waves. *Combust Flame* **1970**, *14*, 34–47. https://doi.org/10.1016/s0010-2180(70)80008-6.

(3) Spadaccini, L. J.; Colket, M. B. Ignition Delay Characteristics of Methane Fuels. *Prog Energy Combust Sci* **1994**, *20* (5), 431–460. https://doi.org/10.1016/0360-1285(94)90011-6.

(4) Brabbs, T. A.; Robertson, T. F. Methane Oxidation behind Reflected Shock Waves -- Ignition Delay Times Measured by Pressure and Flame Band Emission. *Cent. States Meet. Combust. Inst.* **1986**.

(5) Lamoureux, N.; Paillard, C. E.; Vaslier, V. Low Hydrocarbon Mixtures Ignition Delay Times Investigation behind Reflected Shock Waves. *Shock Waves* **2002**, *11*, 309–322. https://doi.org/10.1007/s001930100108.

(6) Beerer, D. J.; McDonell, V. G. An Experimental and Kinetic Study of Alkane Autoignition at High Pressures and Intermediate Temperatures. *Proc Combust Inst* **2011**, *33*, 301–307. https://doi.org/10.1016/j.proci.2010.05.015.

(7) Aul, C. J.; Metcalfe, W. K.; Burke, S. M.; Curran, H. J.; Petersen, E. L. Ignition and Kinetic Modeling of Methane and Ethane Fuel Blends with Oxygen: A Design of Experiments Approach. *Combust Flame* **2013**, *160*, 1153–1167. https://doi.org/10.1016/j.combustflame.2013.01.019.

(8) Zhang, Y.; Huang, Z.; Wei, L.; Niu, S. Experimental and Kinetic Study on Ignition Delay Times of Methane/Hydrogen/Oxygen/Nitrogen Mixtures by Shock Tube. *Chinese Sci. Bull.* **2011**, *56* (26), 2853–2861. https://doi.org/10.1007/s11434-011-4635-4.

(9) Zhang, Y.; Huang, Z.; Wei, L.; Zhang, J.; Law, C. K. Experimental and Modeling Study on Ignition Delays of Lean Mixtures of Methane, Hydrogen, Oxygen, and Argon at Elevated Pressures. *Combust Flame* **2012**, *159* (3), 918–931. https://doi.org/10.1016/j.combustflame.2011.09.010.

(10) Krishnan, S.; Ravikumar, R. Ignition Delay of Methane in Reflected Shock Waves. *Combust. Sci. Technol.* **1980**, *24*, 239–245. https://doi.org/10.1080/00102208008952443.

(11) Asaba, T.; Yoneda, K.; Kakihara, N.; Hikita, T. A Shock Tube Study of Ignition of Methane-Oxygen Mixtures. *Symp Combust* **1963**, *9*, 193–200. https://doi.org/10.1016/b978-1-4832-2759-7.50028-5.

(12) Burcat, A.; Scheller, K.; Lifshitz, A. Shock-Tube Investigation of Comparative Ignition Delay Times for C1-C5 Alkanes. *Combust. Flame* **1971**, *16*, 29–33.

(13) Cooke, D. F.; Williams, A. Shock-Tube Studies of the Ignition and Combustion of Ethane and Slightly Rich Methane Mixtures with Oxygen. *Symp Combust* **1971**, *13*, 757–766. https://doi.org/10.1016/s0082-0784(71)80078-4.

(14) Cooke, D. F.; Williams, A. Shock Tube Studies of Methane and Ethane Oxidation. *Combust Flame* **1975**, *24*, 245–256. https://doi.org/10.1016/0010-2180(75)90154-6.

(15) Dabora, E. K. Effect of NO_2 on the Ignition Delay of CH_4-Air Mixtures. *Combust Flame* **1975**, *24*, 181–184. https://doi.org/10.1016/0010-2180(75)90146-7.

(16) de Vries, J.; Petersen, E. L. Autoignition of Methane-Based Fuel Blends under Gas Turbine Conditions. *Proc Combust Inst* **2007**, *31*, 3163–3171. https://doi.org/10.1016/j.proci.2006.07.206.

(17) Donohoe, N.; Heufer, A.; Metcalfe, W. K.; Curran, H. J.; Davis, M. L.; Mathieu, O.; Plichta, D.; Morones, A.; Petersen, E. L.; Güthe, F. Ignition Delay Times, Laminar Flame Speeds, and Mechanism Validation for Natural Gas/Hydrogen Blends at Elevated Pressures. *Combust Flame* **2014**, *161*, 1432–1443. https://doi.org/10.1016/j.combustflame.2013.12.005.

(18) Eubank, C. S.; Rabinowitz, M. J.; Gardiner Jr, W. C.; Zellner, R. E. Shock-Initiated Ignition of Natural Gas-Air Mixtures. *Symp Combust* **1981**, *18*, 1767–1774. https://doi.org/10.1016/s0082-0784(81)80181-6.

(19) Frenklach, M.; Bornside, D. E. Shock-Initiated Ignition in Methane-Propane Mixtures. *Combust Flame* **1984**, *56*, 1–27. https://doi.org/10.1016/0010-2180(84)90002-6.

(20) Higgin, R. M. R.; Williams, A. A Shock-Tube Investigation of the Ignition of Lean Methane and n-Butane Mixtures with Oxygen. *Symp Combust* **1969**, *12*, 579–590. https://doi.org/10.1016/s0082-0784(69)80439-x.

(21) Huang, J.; Hill, P. G.; Bushe, W. K.; Munshi, S. R. Shock-Tube Study of Methane Ignition under Engine-Relevant Conditions: Experiments and Modeling. *Combust Flame* **2004**, *136*, 25–42. https://doi.org/10.1016/j.combustflame.2003.09.002.

(22) Krishnan, K. S.; Ravikumar, R.; Bhaskaran, K. A. Experimental and Analytical Studies on the Ignition of Methane-Acetylene Mixtures. *Combust Flame* **1983**, *49*, 41–50. https://doi.org/10.1016/0010-2180(83)90149-9.

(23) Lifshitz, A.; Scheller, K.; Burcat, A.; Skinner, G. B. Shock-Tube Investigation of Ignition in Methane-Oxygen-Argon Mixtures. *Combust Flame* **1971**, *16*, 311–321. https://doi.org/10.1016/s0010-2180(71)80102-5.

(24) Slack, M. W.; Grillo, A. R. Shock Tube Investigation of Methane-Oxygen Ignition Sensitized by NO_2. *Combust Flame* **1981**, *40*, 155–172. https://doi.org/10.1016/0010-2180(81)90120-6.

(25) Tang, C.; Wei, L.; Zhang, J.; Man, X.; Huang, Z. Shock Tube Measurements and Kinetic Investigation on the Ignition Delay Times of Methane/Dimethyl Ether Mixtures. *Energy Fuels* **2012**, *26*, 6720–6728. https://doi.org/10.1021/ef301339m.

(26) Tsuboi, T.; Wagner, H. G. Homogeneous Thermal Oxidation of Methane in Reflected Shock Waves. *Symp Combust* **1974**, *15*, 883–890. https://doi.org/10.1016/s0082-0784(75)80355-9.

(27) Tsuboi, T.; Katoh, M. On Induction Periods of Shock-Heated Methane-Oxygen-Argon-Mixtures. *Jpn. J. Appl. Phys.* **1985**, *24* (12), 1697–1702. https://doi.org/10.1143/jjap.24.1697.

(28) Zhang, Y.; Jiang, X.; Wei, L.; Zhang, J.; Tang, C.; Huang, Z. Experimental and Modeling Study on Auto-Ignition Characteristics of Methane/Hydrogen Blends under Engine Relevant Pressure. *Int J Hydrog. Energy* **2012**, *37*, 19168–19176. https://doi.org/10.1016/j.ijhydene.2012.09.056.

(29) Zhukov, V. P.; Sechenov, V. A.; Starikovskii, A. Y. Spontaneous Ignition of Methane-Air Mixtures in a Wide Range of Pressures. *Combust Explos Shock Waves* **2003**, *39*, 487–495. https://doi.org/10.1023/A:1026186231905.

(30) Bowman, C. T. Non-Equilibrium Radical Concentrations in Shock-Initiated Methane Oxidation. *Symp Combust* **1975**, *15* (1), 869–882. https://doi.org/10.1016/S0082-0784(75)80354-7.

(31) Cheng, R. K.; Oppenheim, A. K. Autoignition in Methane-Hydrogen Mixtures. *Combust Flame* **1984**, *58*, 125–139. https://doi.org/10.1016/0010-2180(84)90088-9.

(32) Hidaka, Y.; Sato, K.; Henmi, Y.; Tanaka, H.; Inami, K. Shock-Tube and Modeling Study of Methane Pyrolysis and Oxidation. *Combust Flame* **1999**, *118*, 340–358. https://doi.org/10.1016/s0010-2180(99)00010-3.

(33) Bowman, C. T. An Experimental and Analytical Investigation of the High Temperature Exidation Mechanisms of Hydrocarbon Fuels. *Combust. Sci. Technol.* **1970**, *2*, 161–172.

(34) Bozhenkov, S. A.; Starikovskaia, S. M.; Starikovskii, A. Y. Nanosecond Gas Discharge Ignition of H2 and CH4-Containing Mixtures. *Combust Flame* **2003**, *133*, 133–146.

(35) Burke, U.; Somers, K. P.; O'Toole, P.; Zinner, C. M.; Marquet, N.; Bourque, G.; Petersen, E. L.; Metcalfe, W. K.; Serinyel, Z.; Curran, H. J. An Ignition Delay and Kinetic Modeling Study of Methane, Dimethyl Ether, and Their Mixtures at High Pressures. *Combust Flame* **2015**, *162*, 315–330. https://doi.org/10.1016/j.combustflame.2014.08.014.

(36) Hu, E.; Li, X.; Meng, X.; Chen, Y.; Cheng, Y.; Xie, Y.; Huang, Z. Laminar Flame Speeds and Ignition Delay Times of Methane–Air Mixtures at Elevated Temperatures and Pressures. *Fuel* **2015**, *158*, 1–10. https://doi.org/10.1016/j.fuel.2015.05.010.

(37) Jachimowski, C. J. Kinetics of Oxygen Atom Formation during the Oxidation of Methane behind Shock Waves. *Combust Flame* **1974**, *23*, 233–248. https://doi.org/10.1016/0010-2180(74)90061-3.

(38) Kistiakowsky, G. B.; Willard Richards, L. Emission of Vacuum Ultraviolet Radiation from the Acetylene-Oxygen and the Methane-Oxygen Reactions in Shock Waves. *J Chem Phys* **1962**, *36* (7), 1707–1714. https://doi.org/10.1063/1.1701256.

(39) Levy, Y.; Olchanski, E.; Sherbaum, V.; Erenburg, V.; Burcat, A. Shock-Tube Ignition Study of Methane in Air and Recirculating Gases Mixtures. *J Propul Power* **2006**, *22* (3), 669–676. https://doi.org/10.2514/1.12511.

(40) Mathieu, O.; Pemelton, J. M.; Bourque, G.; Petersen, E. L. Shock-Induced Ignition of Methane Sensitized by NO_2 and N_2O. *Combust Flame* **2015**, *162*, 3053–3070. https://doi.org/10.1016/j.combustflame.2015.03.024.

(41) Petersen, E. L.; Davidson, D. F.; Hanson, R. K. Kinetics Modeling of Shock-Induced Ignition in Low-Dilution CH4/O2 Mixtures at High Pressures and Intermediate Temperatures. *Combust. Flame* **1999**, *117* (1–2), 272–290.

(42) Petersen, E. L.; Davidson, D. F.; Hanson, R. K. Ignition Delay Times of Ram Accelerator CH4/O2/Diluent Mixtures. *J. Propuls. Power* **1999**, *15*, 82–91.

(43) Petersen, E. L.; Röhrig, M.; Davidson, D. F.; Hanson, R. K.; Bowman, C. T. High-Pressure Methane Oxidation behind Reflected Shock Waves. *Proc. Combust. Inst.* **1996**, *26*, 799–806. https://doi.org/10.1016/s0082-0784(96)80289-x.

(44) Grillo, A.; Slack, M. W. Shock Tube Study of Ignition Delay Times in Methane - Oxygen - Nitrogen - Argon Mixtures. *Combust. Flame* **1976**, *27*, 377–381.

(45) Huang, J.; Bushe, W. K. Experimental and Kinetic Study of Autoignition in Methane/Ethane/Air and Methane/Propane/Air Mixtures under Engine-Relevant Conditions. *Combust Flame* **2006**, *144*, 74–88. https://doi.org/10.1016/j.combustflame.2005.06.013.

(46) Suzuki, A.; Inomata, T.; Jinno, H.; Moriwaki, T. Effect of Bromotrifluoromethane on the Ignition in Methane and Ethane-Oxygen-Argon Mixtures behind Shock Waves. *Bull Chem Soc Jpn* **1991**, *64*, 3345–3354. https://doi.org/10.1246/bcsj.64.3345.

(47) Takahashi, K.; Inomata, T.; Moriwaki, T.; Okazaki, S. The Addition Effect of CH_3Br and CH_3Cl on Ignition of CH_4 by Shock Wave. *Bull Chem Soc Jpn* **1988**, *61*, 3307–3313. https://doi.org/10.1246/bcsj.61.3307.

(48) Walker, B. C. Shock-Tube Investigation of Ignition Delay Times of Blends of Methane and Ethane with Oxygen, B.S. University of Tennessee, 2000.

(49) Huang, J.; Bushe, W. K.; Hill, P. G.; Munshi, S. R. Experimental and Kinetic Study of Shock Initiated Ignition in Homogeneous Methane-Hydrogen-Air Mixtures at Engine-Relevant Conditions. *Int J Chem Kinet* **2006**, *38*, 221–233. https://doi.org/10.1002/kin.20157.

(50) Petersen, E. L.; Hall, J. M.; Smith, S. D.; de Vries, J.; Amadio, A. R.; Crofton, M. W. Ignition of Lean Methane-Based Fuel Blends at Gas Turbine Pressures. *J Eng Gas Turbines Power* **2007**, *129*, 937–944. https://doi.org/10.1115/1.2720543.

(51) Yu, C. L.; Wang, C.; Frenklach, M. Chemical Kinetics of Methyl Oxidation by Molecular Oxygen. *J Phys Chem* **1995**, *99*, 14377–14387. https://doi.org/10.1021/j100039a027.

(52) Dean, A. M.; Kistiakowsky, G. B. Oxidation of Carbon Monoxide/Methane Mixtures in Shock Waves. *J Chem Phys* **1971**, *54* (4), 1718–1725. https://doi.org/:10.1063/1.1675077.

(53) Chaumeix, N.; Pichon, S.; Lafosse, F.; Paillard, C. E. Role of Chemical Kinetics on the Detonation Properties of Hydrogen /Natural Gas/Air Mixtures. *Int J Hydrog. Energy* **2007**, *32* (13), 2216–2226. https://doi.org/10.1016/j.ijhydene.2007.04.008.

(54) Heufer, K. A.; Olivier, H. Determination of Ignition Delay Times of Different Hydrocarbons in a New High Pressure Shock Tube. *Shock Waves* **2010**, *20*, 307–316. https://doi.org/10.1007/s00193-010-0262-2.

(55) Seery, D. J.; Bowman, C. T. A Shock Tube Study of Methane Oxidation. *Div Fuel Chem* **1967**, *11* (4), 82–95.

(56) Hidaka, Y.; Nagayama, M.; Suga, M. The Application of a Quadrupole Mass Spectrometer to a Study of Methane Oxidation in Shock Waves. *Bull Chem Soc Jpn* **1978**, *51* (6), 1644–1659. https://doi.org/10.1246/bcsj.51.1659.

(57) Skinner, G. B.; Ruehrwein, R. A. Shock Tube Studies on the Pyrolysis and Oxidation of Methane. *J Phys Chem* **1959**, *63*, 1736–1742. https://doi.org/10.1021/j150580a040.

(58) Gurentsov, E. V; Divakov, O. G.; Eremin, A. V. Ignition of Multicomponent Hydrocarbon/Air Mixtures behind Shock Waves. *High Temp.* **2002**, *40*, 379–386. https://doi.org/10.1023/A:1016012007493.

(59) Koroglu, B.; Pryor, O. M.; Lopez, J.; Nash, L.; Vasu, S. S. Shock Tube Ignition Delay Times and Methane Time-Histories Measurements during Excess CO_2 Diluted Oxy-Methane Combustion. *Combust Flame* **2016**, *164*, 152–163. https://doi.org/10.1016/j.combustflame.2015.11.011.

(60) Zeng, W.; Ma, H.; Liang, Y.; Hu, E. Experimental and Modeling Study on Effects of N_2 and CO_2 on Ignition Characteristics of Methane/Air Mixture. *J. Adv. Res.* **2015**, *6*, 189–201. https://doi.org/10.1016/j.jare.2014.01.003.

(61) Chang, E. J. Shock Tube Experiments for the Development and Validation of Models of Hydrocarbon Combustion, Stanford University, 1995.

(62) Merhubi, H. El; Kéromnès, A.; Catalano, G.; Lefort, B.; Moyne, L. Le. A High Pressure Experimental and Numerical Study of Methane Ignition. *Fuel* **2016**, *177*, 164–172. https://doi.org/https://doi.org/10.1016/j.fuel.2016.03.016.

(63) Leschevich, V. V; Martynenko, V. V; Penyazkov, O. G.; Sevrouk, K. L.; Shabunya, S. I. Auto-Ignitions of a Methane/Air Mixture at High and Intermediate Temperatures. *Shock Waves* **2016**, *26*, 657–672. https://doi.org/10.1007/s00193-016-0665-9.

(64) Deng, F.; Yang, F.; Zhang, P.; Pan, Y.; Zhang, Y.; Huang, Z. Ignition Delay Time and Chemical Kinetic Study of Methane and Nitrous Oxide Mixtures at High Temperatures. *Energy Fuels* **2016**, *30*, 1415–1427. https://doi.org/10.1021/acs.energyfuels.5b02581.

(65) Deng, F.; Yang, F.; Zhang, P.; Pan, Y.; Bugler, J.; Curran, H. J.; Zhang, Y.; Huang, Z. Towards a Kinetic Understanding of the NO_x Promoting-Effect on Ignition of Coalbed Methane: A Case Study of Methane/Nitrogen Dioxide Mixtures. *Fuel* **2016**, *181*, 188–198. https://doi.org/https://doi.org/10.1016/j.fuel.2016.04.090.

(66) Mathieu, O.; Kopp, M. M.; Petersen, E. L. Shock-Tube Study of the Ignition of Multi-Component Syngas Mixtures with and without Ammonia Impurities. *Proc Combust Inst* **2013**, *34*, 3211–3218. https://doi.org/10.1016/j.proci.2012.05.008.

(67) Pryor, O.; Barak, S.; Koroglu, B.; Ninnemann, E.; Vasu, S. S. Measurements and Interpretation of Shock Tube Ignition Delay Times in Highly CO_2 Diluted Mixtures Using Multiple Diagnostics. *Combust. Flame* **2017**, *180*, 63–76. https://doi.org/10.1016/j.combustflame.2017.02.020.

(68) Liu, Y.; Zou, C.; Cheng, J.; Jia, H.; Zheng, C. Experimental and Numerical Study of the Effect of CO_2 on the Ignition Delay Times of Methane under Different Pressures and Temperatures. *Energy & Fuels* **2018**, *32* (10), 10999–11009. https://doi.org/10.1021/acs.energyfuels.8b02443.

(69) Shao, J.; Davidson, D. F.; Hanson, R. K. A Shock Tube Study of Ignition Delay Times in Diluted Methane, Ethylene, Propene and Their Blends at Elevated Pressures. *Fuel* **2018**, *225*, 370–380. https://doi.org/https://doi.org/10.1016/j.fuel.2018.03.146.

(70) Yu, Y. Cinétique d'auto-Inflammation de Carburants Gazeux a Haute Pression: Etude Experimentale et de Modelisation, L'Universite des Sciences et Technologies de Lille, 2012.

(71) Ramalingam, A.; Zhang, K.; Dhongde, A.; Virnich, L.; Sankhla, H.; Curran, H.; Heufer, A. An RCM Experimental and Modeling Study on CH_4 and CH_4/C_2H_6 Oxidation at Pressures up to 160 Bar. *Fuel* **2017**, *206*, 325–333. https://doi.org/10.1016/j.fuel.2017.06.005.

(72) Hashemi, H.; Christensen, J. M.; Gersen, S.; Levinsky, H.; Klippenstein, S. J.; Glarborg, P. High-Pressure Oxidation of Methane. *Combust Flame* **2016**, *172*, 349–364. https://doi.org/10.1016/j.combustflame.2016.07.016.

(73) Gersen, S.; Darmeveil, H.; Levinsky, H. The Effects of CO Addition on the Autoignition of H_2, CH_4 and CH_4/H_2 Fuels at High Pressure in an RCM. *Combust Flame* **2012**, *159*, 3472–3475. https://doi.org/10.1016/j.combustflame.2012.06.021.

(74) Liu, C.; Song, H.; Zhang, P.; Wang, Z.; Wooldridge, M. S.; He, X.; Suo, G. A Rapid Compression Machine Study of Autoignition, Spark-Ignition and Flame Propagation Characteristics of H_2/CH_4/CO/Air Mixtures. *Combust. Flame* **2018**, *188*, 150–161. https://doi.org/10.1016/j.combustflame.2017.09.031.

(75) Zhang, Z.; Hu, E.; Pan, L.; Chen, Y.; Gong, J.; Huang, Z. Shock-Tube Measurements and Kinetic Modeling Study of Methyl Propanoate Ignition. *Energy & Fuels* **2014**, *28* (11), 7194–7202. https://doi.org/10.1021/ef501527z.

(76) Baulch, D. L.; Cobos, C. J.; Cox, R. A.; Frank, J. H.; Hayman, G.; Just, \relax Th; Kerr, J. A.; Murrels, T.; Pilling, M. J.; Troe, J.; Walker, B. F.; Warnatz, J. Summary Table of Evaluated Kinetic Data for Combustion Modeling: Supplement 1. *Combust Flame* **1994**, *98*, 59–79. https://doi.org/10.1016/0010-2180(94)90198-8.

(77) Baulch, D. L.; Cobos, C. J.; Cox, R. A.; Esser, C.; Frank, P.; Just, \relax Th; Kerr, J. A.; Pilling, M. J.; Troe, J.; Walker, R. W.; Warnatz, J. Evaluated Kinetic Data for Combustion Modelling. *J Phys Chem Ref Data* **1992**, *21*, 411. https://doi.org/10.1063/1.555908.

(78) Saito, K.; Ito, R.; Kakumoto, T.; Imamura, A. The Initial Process of the Oxidation of the Methyl Radical in Reflected Shock Waves. *J. Phys. Chem.* **1986**, *90* (7), 1422–1427. https://doi.org/10.1021/j100398a042.

(79) Coppens, F. H. V; De Ruyck, J.; Konnov, A. A. The Effects of Composition on Burning Velocity and Nitric Oxide Formation in Laminar Premixed Flames of CH_4 + H_2 + O_2 + N_2. *Combust. Flame* **2007**, *149* (4), 409–417. https://doi.org/https://doi.org/10.1016/j.combustflame.2007.02.004.

(80) Petersen, E. L.; Kalitan, D. M.; Simmons, S.; Bourque, G.; Curran, H. J.; Simmie, J. M. Methane/Propane Oxidation at High Pressures: Experimental and Detailed Chemical Kinetic Modeling. *Proc Combust Inst* **2007**, *31*, 447–454. https://doi.org/10.1016/j.proci.2006.08.034.

(81) Srinivasan, N. K.; Su, M. C.; Sutherland, J. W.; Michael, J. V. Reflected Shock Tube Studies of High-Temperature Rate Constants for CH_3 + O_2, H_2CO + O_2, and OH + O_2. *J Phys Chem A* **2005**, *109* (35), 7902–7914. https://doi.org/10.1021/jp0581330.

(82) Herbon, J. T.; Hanson, R. K.; Bowman, C. T.; Golden, D. M. The Reaction of CH3+O2: Experimental Determination of the Rate Coefficients for the Product Channels at High Temperatures. *Proc. Combust. Inst.* **2005**, *30* (1), 955–963. https://doi.org/https://doi.org/10.1016/j.proci.2004.08.094.

(83) Metcalfe, W. K.; Burke, S. M.; Ahmed, S. S.; Curran, H. J. A Hierarchical and Comparative Kinetic Modeling Study of C1-C2 Hydrocarbon and Oxygenated Fuels. *Int J Chem Kinet* **2013**, *45* (10), 638–675. https://doi.org/10.1002/kin.20802.

(84) Christensen, M.; Nilsson, E. J. K.; Konnov, A. A. A Systematically Updated Detailed Kinetic Model for CH2O and CH3OH Combustion. *Energy & Fuels* **2016**, *30* (8), 6709–6726. https://doi.org/10.1021/acs.energyfuels.6b00049.

(85) Srinivasan, N. K.; Su, M.-C.; Michael, J. V. CH_3 + O_2 → H_2CO + OH Revisited. *J. Phys. Chem. A* **2007**, *111* (45), 11589–11591. https://doi.org/10.1021/jp0757210.